National Library of Canada
Acquisitions and Bibliographic Services Branch
395 Wellington Street
Ottawa, Ontario
K1A 0N4

Bibliothèque nationale du Canada
Direction des acquisitions et des services bibliographiques
395, rue Wellington
Ottawa (Ontario)
K1A 0N4

Your file Votre référence

Our file Notre référence

NOTICE

The quality of this microform is heavily dependent upon the quality of the original thesis submitted for microfilming. Every effort has been made to ensure the highest quality of reproduction possible.

If pages are missing, contact the university which granted the degree.

Some pages may have indistinct print especially if the original pages were typed with a poor typewriter ribbon or if the university sent us an inferior photocopy.

Reproduction in full or in part of this microform is governed by the Canadian Copyright Act, R.S.C. 1970, c. C-30, and subsequent amendments.

AVIS

La qualité de cette microforme dépend grandement de la qualité de la thèse soumise au microfilmage. Nous avons tout fait pour assurer une qualité supérieure de reproduction.

S'il manque des pages, veuillez communiquer avec l'université qui a conféré le grade.

La qualité d'impression de certaines pages peut laisser à désirer, surtout si les pages originales ont été dactylographiées à l'aide d'un ruban usé ou si l'université nous a fait parvenir une photocopie de qualité inférieure.

La reproduction, même partielle, de cette microforme est soumise à la Loi canadienne sur le droit d'auteur, SRC 1970, c. C-30, et ses amendements subséquents.

Canada

University of Alberta

Stereochemistry and Redox Cofactor of the Copper Amine Oxidases

by

Gordon Robert Alton

A thesis submitted to the Faculty of Graduate Studies and Research
in partial fulfillment of the requirements for the degree of

Doctor of Philosophy

in

Food Chemistry

Department of Food Science and Nutrition

Edmonton, Alberta

Spring 1996

National Library
of Canada

Acquisitions and
Bibliographic Services Branch

395 Wellington Street
Ottawa, Ontario
K1A 0N4

Bibliothèque nationale
du Canada

Direction des acquisitions et
des services bibliographiques

395, rue Wellington
Ottawa (Ontario)
K1A 0N4

Your file - Votre référence

Our file - Notre référence

The author has granted an irrevocable non-exclusive licence allowing the National Library of Canada to reproduce, loan, distribute or sell copies of his/her thesis by any means and in any form or format, making this thesis available to interested persons.

L'auteur a accordé une licence irrévocable et non exclusive permettant à la Bibliothèque nationale du Canada de reproduire, prêter, distribuer ou vendre des copies de sa thèse de quelque manière et sous quelque forme que ce soit pour mettre des exemplaires de cette thèse à la disposition des personnes intéressées.

The author retains ownership of the copyright in his/her thesis. Neither the thesis nor substantial extracts from it may be printed or otherwise reproduced without his/her permission.

L'auteur conserve la propriété du droit d'auteur qui protège sa thèse. Ni la thèse ni des extraits substantiels de celle-ci ne doivent être imprimés ou autrement reproduits sans son autorisation.

ISBN 0-612-10565-2

Canada

University of Alberta
Edmonton
Canada T6G 2G2

Department of Chemistry
Faculty of Science
E3-44 Chemistry Bldg., Tel. (403) 492-3254 Fax (403) 492-8231

March 20, 1996

To whom it may concern,

I hereby grant permission to Gordon Alton to include the previously published research from the Archives of Biochemistry and Biophysics, volume 316(1), pages 353-361, 1995 in his doctoral thesis.

Monica Palcic

Dr. Monica Palcic
Professor of Chemistry

University of Alberta

Library Release Form

Name of Author:	**Gordon Robert Alton**
Title of Thesis:	**Stereochemistry and Redox Cofactor of the Copper Amine Oxidases**
Degree:	**Doctor of Philosophy**
Year this Degree Granted:	**1996**

Permission is hereby granted to the University of Alberta Library to reproduce single copies of this thesis and to lend or sell such copies for private, scholarly, or scientific research purposes only.

The author reserves all other publication and other rights in association with the copyright in the thesis, and except as hereinbefore provided, neither the thesis nor any substantial portion thereof may be printed or otherwise reproduced in any material form whatever without the author's prior written permission.

Gordon Alton

54053 Range Road 215, Ardrossan,
Alberta, T8E 2B7

Date: March 21, 1996

University of Alberta

Faculty of Graduate Studies and Research

The undersigned certify that they have read, and recommend to the Faculty of Graduate Studies and Research, for acceptance, a thesis entitled

Stereochemistry and Redox Cofactor of the Copper Amine Oxidases

submitted by **Gordon Robert Alton**

in partial fulfillment of the requirements for the

degree of **Doctor of Philosophy**

in **Food Chemistry**

Monica Palcic

M.M. Palcic, Supervisor

Michael E. Stiles

M.E. Stiles

Peter Sporns

P. Sporns

G. Ben Armstrong

G. Armstrong

Robert L. Phillips

R. Phillips (External Examiner)

Date: March 18, 1996

Dedication

"Chance favors only the prepared mind"

Louis Pasteur

I wish to dedicate this work to **my family**,
who have supported and encouraged me....

and especially to **Jeannie,**
who provided the necessary Life Support!

Abstract

Copper amine oxidases (EC 1.4.3.6) oxidatively deaminate a variety of aryl and alkyl amines. The enzymic reaction products are ammonia, hydrogen peroxide, and aryl or alkyl aldehyde, respectively. Enzymes isolated from different sources have previously been shown to catalyze the deamination of tyramine and dopamine with abstraction either of the *pro*-R hydrogen at C-1, the *pro*-S hydrogen, or with net non-stereospecific proton abstraction.

To probe enzyme stereochemistry further, R-deutero and S-deuterobenzylamines were prepared by a combined chemical-enzymatic method. The product benzaldehydes from the amine oxidase reactions were reduced *in situ* by alcohol dehydrogenase and NADH, providing benzyl alcohols which were analyzed by ^{1}H NMR spectroscopy. Ten amine oxidases derived from plant, animal, and bacterial sources all reacted with abstraction of the *pro*-S hydrogen of benzylamine, irrespective of the stereochemical course for the oxidation of tyramine or dopamine.

The copper amine oxidases contain topaquinone (TPQ) as an organic cofactor which directly mediates substrate deamination via Schiff's base formation at the active site. Bovine and porcine aortic amine oxidases, known as tissue-bound semicarbazide-sensitive amine oxidases (SSAO), were derivatized with *p*-nitrophenylhydrazine. These displayed similar absorbance spectra as authentic TPQ enzymes. However, some differences were observed with the phenylhydrazine derivatized SSAO enzymes.

To determine unambiguously TPQ as the redox cofactor in these enzymes, these SSAOs were derivatized with *p*-nitrophenylhydrazine and proteolyzed with pronase. The liberated peptides were purified by reverse-phase HPLC and the

major peak had a retention time which correlated with topaquinone-*p*-nitrophenylhydrazone aspartate dipeptide derived from the known TPQ enzyme, porcine kidney diamine oxidase. Subsequent mass spectrometric analysis of this major peak revealed a mass spectrum consistent with TPQ.

Resonance Raman spectra of *p*-nitrophenylhydrazine derivatized bovine and porcine SSAO were compared with a spectrum from the known TPQ enzyme from pea seedling. These spectra confirmed the presence of TPQ in the SSAO enzymes.

Acknowledgments

"The best way to have a good idea is to have lots of ideas."
Linus Pauling

I am very grateful to my supervisor and friend, Monica Palcic, whose guidance, advice, and wisdom have been very important to me both personally and professionally. My experiences and training in your laboratory have laid a foundation on which to build my career further .

There have been many individuals who have contributed, in varying degrees, to my research and to my development as a scientist. I thank them all, and in particular, the following.

I am indebted to Suzanne Crawley, Todd Lowary, Luis Quadri, and Michael Arlt who provided many hours of much needed advice and encouragement. I am also appreciative of May, Taha, and Richard who proved to be invaluable and reliable summer students. Also Hong, Chris, Sylvie, Nora, York and especially Cathy helped me in innumerable ways and made working in "the lab" an enjoyable experience.

I am grateful to Glen Loppnow, Andy Holt, Chris Scaman and Dale Cameron who have directly contributed to the amine oxidase cofactor studies. Many thanks to Mike Stiles, Luis Quadri, Randy Wrobo, Linda Saucier and the rest of the "food micro crew" who instructed me in molecular biology protocols.

Andy *"The Goods"* Holt deserves special mention for he provided valuable papers and even more valuable ideas from across his desk. In addition to illuminating discussions concerning the physiological role of SSAO (amongst other things) he proved to be an exceptional HPLC chromatographer who provided the "first glimpse" of TPQ in our lab.

I am grateful to the Alberta Heritage Foundation for Medical Research, who provided financial support for my final two years of graduate studies.

Finally, I wish to thank Ole Hindsgaul, my mentor, who took a chance and thus made my scientific research career a reality. Thank you.

CONTENTS

CHAPTER ONE

General Introduction to the Amine Oxidases 1

1.1 Amine Oxidase Classification 1

1.2 Copper Amine Oxidases 4

1.2.1 Function and Physiology 4

1.2.2 Amino Acid Homology and Three Dimensional Structure 8

1.2.3 Determination of Topaquinone as the Redox Cofactor 10

1.2.4 Enzymatic Reaction Mechanism 14

1.2.5 Enzyme Stereochemistry 15

References 23

CHAPTER TWO

Stereochemistry of Benzylamine Oxidation by Copper Amine Oxidases 30

2.1 Introduction 30

2.2 Experimental Procedures 31

2.3 Results and Discussion 36

References 53

CHAPTER THREE

Stereochemistry of Bacterial Copper Amine Oxidase Reactions 56

3.1 Introduction 56

3.2 Experimental Procedures 58

3.3 Results and Discussion 61

References 71

CHAPTER FOUR

Identification of Topaquinone as the Redox Cofactor in Tissue-Bound Semicarbazide-Sensitive Amine Oxidases **73**

4.1 Introduction 73

4.2 Experimental Procedures 77

4.3 Results and Discussion 83

References 104

CHAPTER FIVE

General Conclusions and Discussion **108**

5.1 Literature Relevance and Research Objectives 108

5.2 Research Results 110

5.3 Future Research 112

Appendix I **114**

Visible absorbance spectrum of pNPHZ-derivatized rabbit plasma amine oxidase.

Appendix II 115

Partial 500 MHz ^{1}H NMR spectra of benzyl alcohols derived from coupled incubations of bovine, porcine and horse plasma amine oxidases.

Appendix III 116

Partial 500 MHz ^{1}H NMR spectra of benzyl alcohols derived from coupled incubations of bacterial amine oxidases and R-[*methylene*-^{2}H] benzylamine.

Appendix IV 117

Partial 500 MHz ^{1}H NMR spectra of benzyl alcohols derived from coupled incubations of bacterial amine oxidases and S-[*methylene*-^{2}H] benzylamine.

Appendix V 118

Partial 500 MHz ^{1}H NMR spectra of the *p*-hydroxyphenethyl alcohols derived from coupled incubations of [1(R)-^{2}H]tyramine and [1(S)-^{2}H]tyramine with bacterial amine oxidases.

Appendix VI 119

Partial 500 MHz ^{1}H NMR spectra of the *p*-hydroxyphenethyl alcohols derived from coupled incubations of tyramine and [2,2-^{2}H]tyramine with bacterial amine oxidases.

List of Tables

Table		Page
1.1	Structure and physical constants for amine oxidase substrates and inhibitors	5
1.2	Summary of the stereochemistry of proton abstraction and solvent exchange with tyramine, dopamine or phenethylamine substrates by amine oxidases	18
4.1	Benzylamine affinity and semicarbazide sensitivity of the amine oxidases	74

List of Figures

Figure		Page
1.1	Molecular structure of oxidized flavin adenine dinucleotide	2
1.2	Formation of cross-linked collagen by lysyl oxidase (LO)	3
1.3	Amine oxidase reaction products	7
1.4	Molecular structure of topaquinone	10
1.5	Topaquinone hydantoin phenylhydrazone (azo tautomer)	11
1.6	Topaquinone *p*-nitrophenylhydrazone C-terminal aspartate dipeptide	12
1.7	Topaquinone-hydrazine adducts display pH-dependent optical properties	13
1.8	Mechanism of the copper amine oxidases	16
1.9	Stereochemical and configurational assignment of phenethylamine, tyramine and dopamine	17
1.10	Reversible tautomerization of the phenethylamine-TPQ pre-hydrolysis complex	20
2.1	Absorbance spectra of *p*-nitrophenylhydrazine-derivatized horse plasma amine oxidase	37
2.2	Partial 500 MHz ^{1}H NMR spectra of R- and S-[*methylene*-^{2}H] benzylamine	40
2.3	Partial 500 MHz ^{1}H NMR spectra of products from the camphanic acid chloride derivatization of benzylamine, R-[*methylene*-^{2}H] benzylamine and S-[*methylene*-^{2}H]benzylamine	42
2.4	Partial 500 MHz ^{1}H NMR spectra of benzyl alcohols derived from coupled incubations of pea seedling amine oxidase with S-[*methylene*-^{2}H] benzylamine and R-[*methylene*-^{2}H]benzylamine	44
2.5	Overall reaction for S-[*methylene*-^{2}H]benzylamine producing diprotonated benzyl alcohol, and R-[*methylene*-^{2}H]benzylamine producing monodeuterated benzyl alcohol	46
2.6	Side view and a top view of the partial structure of a topaquinone-benzylamine adduct	48
2.7	Side view and a top view of the partial structure of a topaquinone-tyramine adduct	49

2.8 Top view of the partial structure of a topaquinone-tyramine adduct drawn in a conformation that presents the *pro*-R hydrogen for abstraction..... 51

3.1 Stereochemical and configurational nomenclature for tyramine..... 57
3.2 Molecular structure of S-[*methylene*-^{2}H]benzylamine and [1(R)-^{2}H]tyramine..... 57
3.3 Partial 500 MHz ^{1}H NMR spectra of benzyl alcohols derived from coupled incubations of *A. globiformis* phenethylamine oxidase with R-[*methylene*-^{2}H]benzylamine and S-[*methylene*-^{2}H]benzylamine..... 64
3.4 Overall reaction for R-[*methylene*-^{2}H]benzylamine producing monodeuterated benzyl alcohol and S-[*methylene*-^{2}H]benzylamine producing diprotonated benzyl alcohol.....65
3.5 Partial 500 MHz ^{1}H NMR spectra of [1(R)-^{2}H]tyramine, [1(S)-^{2}H]tyramine and the *p*-hydroxyphenethyl alcohols derived from coupled incubations of the deuterated amines with *A. globiformis* phenethylamine oxidase.....67
3.6 Partial 500 MHz ^{1}H NMR spectra of [2,2-^{2}H]tyramine, tyramine and the *p*-hydroxyphenethyl alcohols derived from their coupled incubations with *A. globiformis* phenethylamine oxidase.....69

4.1 Topaquinone, the redox active cofactor of the copper amine oxidases.. 75
4.2 pH-Dependent spectral properties of topaquinone..... 85
4.3 Absorbance spectra of phenylhydrazine-derivatized bovine aorta SSAO. Absorbance spectra of *p*-nitrophenylhydrazine-derivatized bovine aorta SSAO and PSAO.....87
4.4 Absorbance spectra of *p*-nitrophenylhydrazine-derivatized porcine aorta SSAO. Absorbance spectra of the isolated peptide released from *p*-nitrophenylhydrazine-derivatized porcine SSAO with pronase..89
4.5 Resonance Raman spectra of the *p*-nitrophenylhydrazine derivatives of PSAO, bovine SSAO and porcine SSAO.....92
4.6 The azo tautomer of *p*-nitrophenylhydrazone-topaquinone aspartate.... 95
4.7 The HPLC chromtograms of the chromophoric peptides derived from the tryptic digestion of *p*-nitrophenylhydrazine-derivatized bovine SSAO.....97

4.8 HPLC chromatogram (A_{400} nm) of the chromophoric peptides derived from the thermolytic digestion of *p*-nitrophenylhydrazine-derivatized bovine SSAO..... 98
4.9 HPLC purification of cofactor-containing peptides released by pronase digestion of pNPHZ-derivatized enzymes.....100
4.10 The MALDI-TOF mass spectrum of the major pNPHZ-derivatized peptide isolated from pronase digestion of bovine SSAO.....103

List of Schemes

Scheme Page

2.1 Synthesis of S-[*methylene*-^{2}H]benzylamine.....39

3.1 Reversible tautomerization of the tyramine-TPQ pre-hydrolysis complex..... 58

3.2 *Pro*-S specific oxidative deamination of R-[*methylene*-^{2}H]benzylamine coupled to alcohol dehydrogenase (ADH)..... 62

List of Abbreviations

Å	Angström
ADH	horse liver alcohol dehydrogenase
BSAO	bovine serum amine oxidase
C18	octyldecylsilane
cDNA	complementary deoxyribonucleic acid
cm	centimeter
CuAO	copper amine oxidase
Da	Dalton (g/mole)
DAO	diamine oxidase
DBU	1,8-diazabicyclo-[5.4.0]undecene-7
DCC	N,N'-dicyclohexylcarbodiimide
DMF	dimethylformamide
DNA	deoxyribonucleic acid
E.C.	Enzyme Commission
FAD	flavin adenine dinucleotide, oxidized form
FPLC	fast protein liquid chromatography
HPLC	high performance liquid chromatography
Hz	hertz (cycles/sec)
k_{cat}	turnover number
kDa	kiloDalton
K_m	Michaelis constant
KOH	potassium hydroxide
LO	lysyl oxidase
MALDI-TOF	matrix-assisted laser desorption and ionization time-of-flight
MAO	monoamine oxidase
MHz	megahertz
MS	mass spectrometry
NAD	β-nicotinamide adenine dinucleotide, oxidized form
NADH	β-nicotinamide adenine dinucleotide, reduced form
NMR	nuclear magnetic resonance
PAGE	polyacrylamide gel electrophoresis
PHZ	phenylhydrazine
pNPHZ	*p*-nitrophenylhydrazine
ppm	part per million

psi	pounds per square inch
SDS	sodium dodecyl sulfate
SSAO	semicarbazide-sensitive amine oxidase
TFA	trifluoroacetic acid
TMS	tetramethylsilane
TPQ	topaquinone
U	international units of enzyme activity (micromole/min)

Chapter One

General Introduction to the Amine Oxidases

1.1 Amine Oxidase Classification

Amine oxidases are a large and diverse family of enzymes that oxidatively deaminate alkyl and aryl amines to yield ammonia, hydrogen peroxide and an alkyl or aryl aldehyde, respectively (Equation 1.1)[1].

$$RCH_2NH_2 + H_2O + O_2 \rightarrow RCHO + NH_3 + H_2O_2 \qquad (1.1)$$

There are three different classes of amine oxidases. They are the monoamine oxidases (MAO), lysyl oxidase (LO) and the copper amine oxidases (CuAO). The MAOs and CuAOs catabolize biogenic amines produced by animals, plants, and microorganisms. Lysyl oxidase is responsible for cross-linking of collagen and elastin.

Monoamine oxidases [amine: oxygen oxidoreductase (deaminating) (flavin containing); EC 1.4.3.4] contain flavin adenine dinucleotide (FAD) as the prosthetic redox cofactor (Figure 1.1)[2]. The first report of such an enzyme was in 1928 by M.L.C. Hare, who demonstrated enzyme activity in rabbit liver[3]. The subcellular location of MAO is in the outer mitochondrial membrane of many different tissue types[4]. These FAD-containing amine oxidases do not require copper and are rarely inhibited by carbonyl reactive reagents[5]. All known MAOs catalyze the deamination of primary, secondary and tertiary amines[6]. Only the *pro*-R C1 hydrogen is abstracted from all known substrates[7].

The MAOs are important for the regulation of neurotransmitters such as dopamine, noradrenaline and serotonin[8]. Inhibitors of MAOs are pharmacologically

significant as this inhibition alleviates the symptoms of Parkinson's disease (e.g., deprenyl) and depression (e.g., tranylcypromine)[9,10].

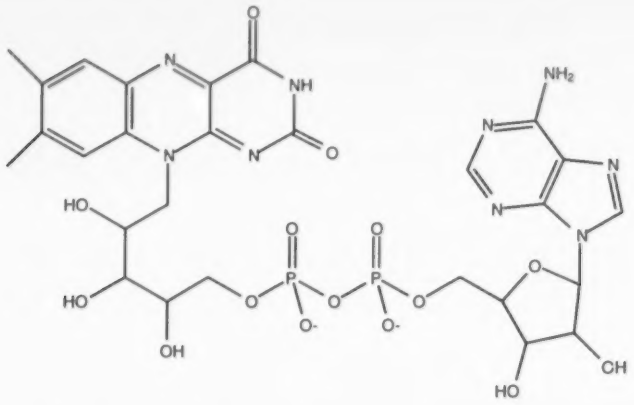

Figure 1.1 Molecular structure of oxidized flavin adenine dinucleotide (FAD).

Lysyl oxidase (LO) [protein-lysine 6-oxidase; EC 1.4.3.13] is found in the extracellular matrix and is physiologically important for proper connective tissue development[11]. Lysine or hydroxylysine residues in tropocollagen, or tropoelastin, are oxidatively deaminated at the ε-amino group to yield α-aminoadipic-δ-semialdehydes[12]. Lysines, on separate tropocollagen molecules, cross-link with the aldehydes through Schiff's base formation[13]. Subsequent reduction of the Schiff's base provides the high tensile strength of native collagen (Figure 1.2)[14]. Both fibroblasts and smooth muscle cells secrete LO. Thus, the enzyme is important for wound healing and proper maintenance of vasculature[15].

The LO enzyme is similar to the CuAOs in that it contains copper but has a smaller molecular weight of 29 kDa[16,17]. The nature of the redox cofactor has not been precisely established, but is believed to be a carbonyl-containing molecule based on inhibitor studies[18,19]. Resonance Raman studies of phenylhydrazine-

derivatized enzyme indicate that the cofactor is not the same as the copper amine oxidase cofactor, topaquinone (see section 1.2.3)[20]. Also, the reported cDNA sequence of mammalian LO does not have the consensus sequence associated with topaquinone-containing copper amine oxidases[17].

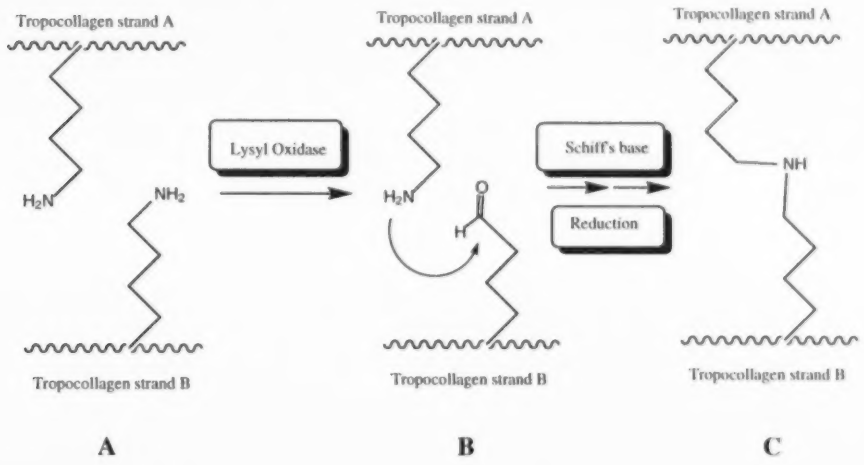

Figure 1.2 Formation of cross-linked collagen by lysyl oxidase (LO). Native tropocollagen (A) is oxidatively deaminated by LO. Nucleophilic attack by a neighbouring amine on the product aldehyde (B) results in Schiff's base formation. Reduction of the Schiff's base yields a lysinonorleucine crosslink (C).

The copper amine oxidases [amine: oxygen oxidoreductase (deaminating) (copper containing); EC 1.4.3.6] have been discovered in fungi, yeast, bacteria, insects, plants, and animals[1,21-23]. A recent review (1993) by Davidson reports that over 100 CuAO enzymes have been characterized in many different organisms[23]. The CuAOs have several designations in the literature based on substrate specificity and sensitivity to inhibitors. The term diamine oxidase (DAO) is used for those CuAOs with preference for primary diamine substrates. Putrescine, spermine and spermidine are physiologically important diamines and the heterocyclic amine,

histamine is also an important substrate (Table 1.1)[24]. Since most of the CuAOs metabolize benzylamine (Table 1.1) efficiently they are sometimes referred to as benzylamine oxidases[25]. The CuAOs are sensitive to inhibition by carbonyl reagents such as hydrazines and semicarbazide (Table 1.1)[26]. Therefore, they have also been called semicarbazide-sensitive amine oxidases (SSAO), particularly in the pharmacological literature[27]. Enzymologists typically reserve the SSAO term for the tissue-bound enzymes.

1.2 Copper Amine Oxidases

1.2.1 Function and Physiology

The CuAO enzymes oxidize an extensive variety of amines and many enzymes are active towards several different amine substrates[28]. In bacteria, yeast and fungi, CuAOs provide carbon and/or nitrogen necessary for growth of the organism by oxidative deamination of amines. Tyramine and phenethylamine (Table 1.1), derived from the amino acids, tyrosine and phenylalanine, are usually the preferred substrates[29]. The bacterial enzymes oxidize benzylamine with a rate that is less than 1% of the rate for tyramine, whereas these rates are comparable for most other copper amine oxidases[30].

Plant amine oxidases have several different physiological roles. A potential role is the oxidation of polyamines. Polyamines are known to control DNA transcription which affects cell division and differentiation[31]. During seedling development, amine oxidase synthesis peaks when seedlings are growing most rapidly[32]. Amine oxidases are detected histochemically at the cell wall where hydrogen peroxide is required for lignin biosynthesis (Figure 1.3 A)[33]. Alkaloid biosynthesis in some plants requires amine oxidases[34].

Table 1.1 Structure and physical constants for amine oxidase substrates and inhibitors.

NAME	STRUCTURE	M.W.	pKa (20°C)
AMINES			
methylamine		31.1	10.6
allylamine	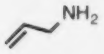	57.1	
propylamine	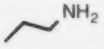	59.1	10.6
aminoacetone	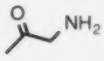	73.1	
3-methylbutylamine	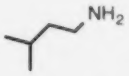	87.1	10.6
putrescine		88.2	9.4
spermidine	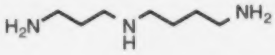	145.2	
spermine	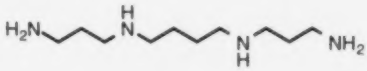	202.3	
benzylamine	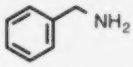	107.2	9.3
p-hydroxybenzylamine	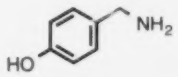	123.2	
p-methoxybenzylamine	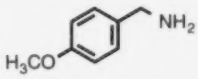	137.2	
phenethylamine	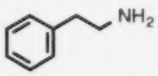	121.2	
tyramine	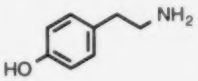	137.2	9.7

Table 1.1 CONTINUED

NAME	STRUCTURE	M.W.	pKa (20°C)
AMINES			
histamine	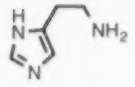	111.2	9.8
tryptamine	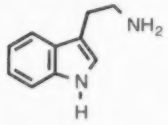	160.2	10.2
5-hydroxytryptamine (serotonin)	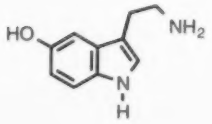	176.2	9.8
dopamine	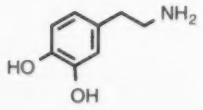	153.2	10.6
noradrenaline	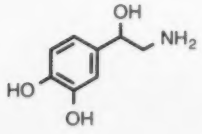	169.2	8.6
adrenaline	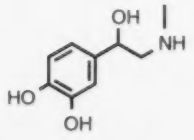	183.2	8.7
INHIBITORS			
semicarbazide	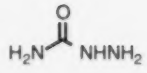	75.1	
phenylhydrazine	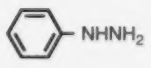	107.2	
p-nitrophenylhydrazine	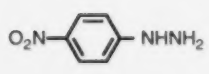	153.1	

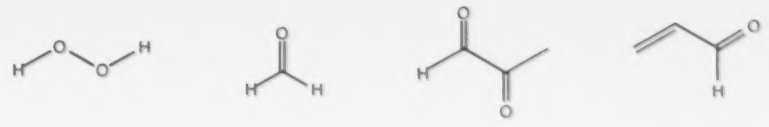

A B C D

Figure 1.3 Amine oxidase reaction products: hydrogen peroxide (A), formaldehyde (B), methylglyoxal (C) and acrolein (D).

In mammals the CuAOs (or SSAOs) are found in a variety of tissues including plasma, adipose tissue, vascular smooth muscle, heart, lung, intestine, kidney, liver, spermatozoa, placenta and semen[1,19,35,36]. Despite their widespread distribution it has proved difficult to determine the physiological roles for the CuAO enzymes[25]. Benzylamine is a preferred substrate but is probably not an endogenous mammalian substrate[37,38].

Methylamine (Table 1.1) is a good substrate for both the soluble plasma enzyme and the tissue-bound aorta smooth muscle cell enzyme[39-41]. It is produced endogenously through gut microfloral metabolism of creatinine, lecithin, and choline and intracellularly through MAO metabolism of adrenaline (Table 1.1)[40,41]. Formaldehyde (Figure 1.3 B) is the cytotoxic product of methylamine deamination[42]. The cardiovascular damage that is observed in diabetics may be due to the elevated levels of methylamine and increased SSAO activity[37].

Aminoacetone (Table 1.1), another endogenous amine, is deaminated to produce methylglyoxal (Figure 1.3 C). This has been shown to have *in vitro* cytotoxic effects[25]. Methylglyoxal dehydrogenase converts methylglyoxal to pyruvate. This potentially alleviates *in vivo* cytotoxicity under normal physiological conditions[25].

The plasma enzymes from ruminants deaminate polyamines. Putrescine, spermine and spermidine are thus good substrates. This was first discovered in

bovine plasma by Hirsch in 1953 and he called the enzyme "spermine oxidase"[43]. Amine oxidases may thus regulate circulating levels of the polyamines, which are known to control cell growth and differentiation[44]. Since oncogenic transformation involves uncontrolled cellular growth, the CuAOs may have an important role in cancer[45]. During pregnancy (in several species) the level of circulating maternal plasma amine oxidase increases approximately 1000-fold[24]! This may not be surprising since the fetus releases large amounts of spermine and spermidine. In non-ruminants, diamines are poorly metabolized but benzylamine, tyramine, tryptamine, serotonin and histamine (Table 1.1) are better substrates[46].

Vascular smooth muscle cells, particularly from the aorta, contain large amounts of amine oxidase activity[19]. This tissue-bound SSAO is a glycoprotein located at the cell surface with the active site facing outwards[47]. The oxidative deamination of allylamine (Table 1.1), an industrially important chemical, by aorta SSAO yields acrolein (Figure1.3 D). This is an extremely cytotoxic compound that has been shown to induce atherosclerotic-like lesions in the aorta[48]. While the "genuine" physiological roles of the CuAOs remain obscure, it is certain that they are important in human pathophysiology. This is especially true with regard to the toxicology of xenobiotic amines[25].

1.2.2 Amino Acid Homology and Three Dimensional Structure

The CuAOs are homodimeric glycoproteins with a monomer molecular weight of 70-97 kDa. Each monomer may contain as much as 5-7% N-linked glycans and has a redox active cofactor that is covalently linked to the alpha-carbon backbone of the protein[49]. There is little primary amino acid sequence identity between the amine oxidases from different organisms[50]. However, within species the identity is higher[51,52]. A pairwise identity comparison between *Arthrobacter*

globiformis histamine oxidase and *A. globiformis* phenethylamine oxidase reveals 58% identity, whereas comparison with bovine serum amine oxidase reveals only 25% identity[51]. There are 33 completely conserved amino acids seen in all reported sequences with very high homology near the C-terminus[21,52,53]. The C-terminal region of the known sequences, residues 592-632, contains 10 of the 33 conserved residues[52]. Several of the conserved residues are histidines involved in copper binding. Some conserved residues are also located at the active site. The consensus sequence Thr-X-X-Asn-Tyr-Asp/Glu (where X is any biological amino acid) has been demonstrated in several amine oxidases[53,54]. This tyrosine residue is the site of autogeneration of the redox cofactor[55].

The first crystal structure of any copper amine oxidase was recently reported by Knowles and coworkers[53]. The *E. coli* amine oxidase crystal structure was solved at 2 Å resolution. The enzyme is a mushroom-shaped homodimer consisting mainly of β sheets. The arrangement of secondary structure for this enzyme represents a new type of protein fold. Each monomer is 727 amino acids in size with a molecular weight of 81.24 kDa and a pI of 5.5. There is one active site per monomer, containing one mole of topaquinone (Figure 1.4), derived from Tyr466, and one mole of copper[56]. The active sites of the monomers are separated by 30 Å and are deeply shielded from solvent[53].

There is a prominent intersubunit interaction in which two β hairpins extend from each monomer into the other[53]. One of these hairpins from each monomer links the active sites and contains the conserved His440 residue. The conserved Asp467 and Thr462 residues in one subunit hydrogen bond with the His440 residue from the other subunit. This suggests the possibility that the two active sites in a functional homodimer "communicate" with one another[53]. The catalytic base is suggested to be Asp383 and is conserved in all reported CuAO amino acid sequences[57].

1.2.3 Determination of Topaquinone as the Redox Cofactor

Highly purified CuAOs are a peach-pink colour due to an absorbance at 470 nm that has been attributed to the essential organic cofactor, topaquinone (TPQ)[49,58]. The TPQ cofactor (Figure 1.4) is generated from a conserved tyrosine at the active site[55].

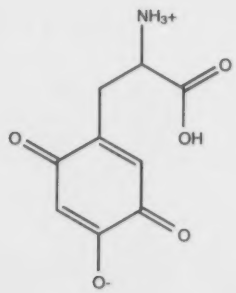

Figure 1.4 Molecular structure of topaquinone, the redox active cofactor of the copper amine oxidases, is the *p*-quinone anion of 2,4,5-trihydroxyphenylalanine.

Bovine serum amine oxidase (BSAO) was the first CuAO in which TPQ was unambiguously demonstrated to be the cofactor[49]. This was achieved by covalent derivatization of the BSAO redox cofactor with radioactive phenylhydrazine (Table 1.1). Phenylhydrazine is an irreversible inhibitor of CuAOs[59]. Proteolysis with thermolysin released peptides that contained the derivatized cofactor. Reverse-phase HPLC purification of the radioactive peptides provided a pentapeptide that had a molecular weight of 805. The amino acid sequence was determined as Leu-Asn-blank-Asp-Tyr. All the radioactivity was associated with the blank cycle from the amino acid sequencer. This established the unknown amino acid as the site of phenylhydrazine and, thus, cofactor attachment. The visible absorbance spectrum

of this pentapeptide was very similar to the spectrum of the derivatized BSAO before proteolysis.

Extensive characterization by mass spectrometry confirmed the sequencing results. Subtraction of the masses for the known amino acids from the pentapeptide mass yielded a molecular weight of 283 for the unknown (blank). A computer analysis provided seven empirical formulae fitting this mass. However, only one formula was consistent with the mass spectral fragmentation data[60]. The structure derived from the cofactor-phenylhydrazone adduct was thus tentatively proposed to be TPQ[49].

To confirm that TPQ was the authentic cofactor, a model compound was synthesized. Replacement of the amine and carboxylic acid moieties with a hydantoin, and derivatization with phenylhydrazine, provided a model TPQ compound (Figure 1.5)[49].

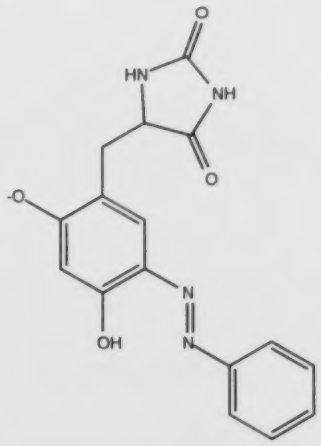

Figure 1.5 Topaquinone hydantoin phenylhydrazone (azo tautomer).

Comparison of the resonance Raman, NMR and visible spectra of the TPQ-hydantoin phenylhydrazone with the spectra obtained from 50 nanomoles of the pentapeptide validated the assignment of TPQ as the redox cofactor in BSAO[49].

A recent modification of this procedure employs pronase, a non-specific protease preparation, instead of trypsin or thermolysin, for the proteolysis of *p*-nitrophenylhydrazine (Table 1.1) adducts of pig kidney diamine oxidase and *E. coli* amine oxidase[61]. The released peptides were purified by reverse phase HPLC. Visible absorbance, NMR and mass spectral characterization of the major derivatized peptide (31 nanomoles, 47% yield) revealed the *p*-nitrophenylhydrazone adduct of a topaquinone-aspartate dipeptide (Figure 1.6).

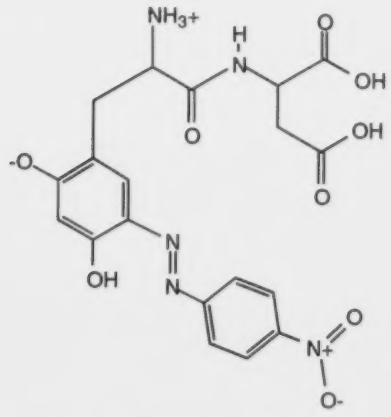

Figure 1.6 Topaquinone *p*-nitrophenylhydrazone C-terminal aspartate dipeptide.

This procedure provides a greater yield of TPQ-peptides (hydrazone) for some CuAOs compared with tryptic or thermolytic digests. This is advantageous as tryptic peptides may be produced in less than 0.1% yield[61,62]. The meager yield of tryptic peptides in certain cases has been attributed to the formation of N-terminally blocked cyclic peptides[60]. Amine oxidases from pea seedling, pig kidney, *E. coli.*, pig plasma, sheep plasma and chick pea have been determined as TPQ enzymes using these extensive physical-chemical characterization protocols[54,60,61].

However, a complete physical-chemical characterization of TPQ requires hundreds of nanomoles of high purity enzyme. This requirement precludes routine

characterization of TPQ in many amine oxidases. Therefore, an abbreviated procedure employing intact protein is now deemed sufficient[60]. TPQ is conveniently demonstrated by derivatization of the amine oxidase with *p*-nitrophenylhydrazine and measurement of the visible absorbance and resonance Raman spectra[63,64]. At neutral pH the *p*-nitrophenylhydrazine-treated enzyme displays a broad, intense absorbance at 460 nm that shifts to 580 nm at pH 14. This 120 nm pH-dependent shift is diagnostic for TPQ (Figure 1.7).

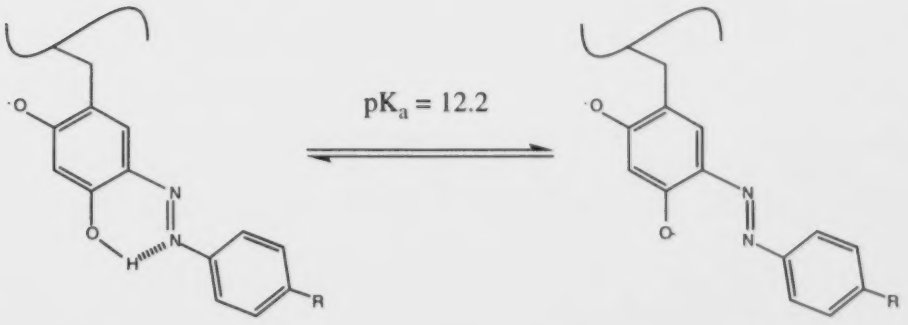

Figure 1.7 Topaquinone-hydrazine adducts display pH-dependent optical properties.

Phenylhydrazine is also a carbonyl reactive reagent and is used for derivatization of amine oxidases[63]. An absorbance at 440 nm is observed at neutral pH but only shifts 50 nm, to 490 nm, at higher pH. Also, significant absorbance at 440 nm is still observed for intact proteins. Therefore, *p*-nitrophenylhydrazine is preferred to phenylhydrazine as a derivatization reagent for characterization of TPQ in intact enzymes. However, if peptide characterization by MS is desired, then

phenylhydrazine is preferred because TPQ-phenylhydrazine adducts display superior ionization in the MS instrument[60].

Besides the visible spectral properties of derivatized amine oxidases, resonance Raman spectroscopy can be used to determine the presence of TPQ in intact proteins[64]. The enzyme is derivatized with phenylhydrazine or *p*-nitrophenylhydrazine and concentrated to an optical density of 2-10 absorbance units (1 cm path length). A 100-400 microlitre volume in a 5 mm tube cooled by nitrogen gas is irradiated with an Argon laser operating at 457.9 nm. Typically a photon flux of 20-50 milliwatts is sufficient[64].

The physical basis of the resonance Raman effect is that some of the 457.9 nm photons selectively excite vibronic transitions of the TPQ-hydrazine adduct. Energy has been removed from the incident photons and they shift to a longer wavelength (lower frequency). A detector at right angles to the incident beam records the resulting spectrum[65]. The resonance Raman spectrum displays vibrational modes of the TPQ-*p*-nitrophenylhydrazine adduct. This is to some extent similar to an infra-red spectrum[66]. The spectrum can be considered a "fingerprint" of the TPQ-hydrazine adduct. A comparison of this spectrum with standard spectra provides a very reliable indication of TPQ in an enzyme[64].

It should be noted that bovine and porcine aorta SSAOs have somewhat peculiar resonance Raman and visible absorbance spectra (see chapter 4). Thus, a more complete physical-chemical characterization is required to establish the nature of their redox cofactor (see chapter 4).

1.2.4 Enzymatic Reaction Mechanism

The proposed enzymatic reaction mechanism is an aminotransferase ping-pong type. An anaerobic half-reaction (Equation 1.2 A) is followed by

an aerobic half-reaction (Equation 1.2 B)[67].

$$E{=}O + R\text{-}CH_2\text{-}NH_2 + H_2O \rightarrow E\text{-}NH_2 + R\text{-}CHO \qquad (1.2\ A)$$

$$E\text{-}NH_2 + O_2 \rightarrow E{=}O + NH_3 + H_2O_2 \qquad (1.2\ B)$$

Topaquinone (TPQ) initially forms a Schiff's base with substrate amine (Figure 1.8 A)[67]. An active site base, recently proposed to be an aspartate residue, abstracts a proton from the alpha carbon (Figure 1.8 B)[54,67]. Thus, a resonance-stabilized carbanion is formed by electron delocalization into the π-orbital system of the TPQ-amine adduct, to yield TPQ-imine[68]. The TPQ-imine adduct is reprotonated at the C4 oxyanion and then undergoes nucleophilic attack by a water molecule to yield aminoquinone (aminoresorcinol) and free aldehyde (Figure 1.8 C)[68,69]. In the aerobic half-reaction the aminoquinone is oxidized by molecular oxygen, mediated by copper, to release hydrogen peroxide and ammonia (Figure 1.8 D). Electron paramagnetic resonance spectroscopy has demonstrated a Cu(I)-semiquinone generated from Cu(II) in the native holoenzyme under anaerobic conditions[1,70]. Autogeneration of the redox cofactor, which is essential for catalytic function, also requires copper and oxygen[71,72].

1.2.5 Enzyme Stereochemistry

Another aspect of CuAO enzymology that is investigated at the molecular level is enzyme stereochemistry. In general, enzymes in the same class have uniform stereochemistry since natural selection and the stereoelectronic constraints of the chemical reaction preserve the orientation of catalytic residues relative to bound substrate[73]. However, the CuAOs exhibit stereochemical heterogeneity in

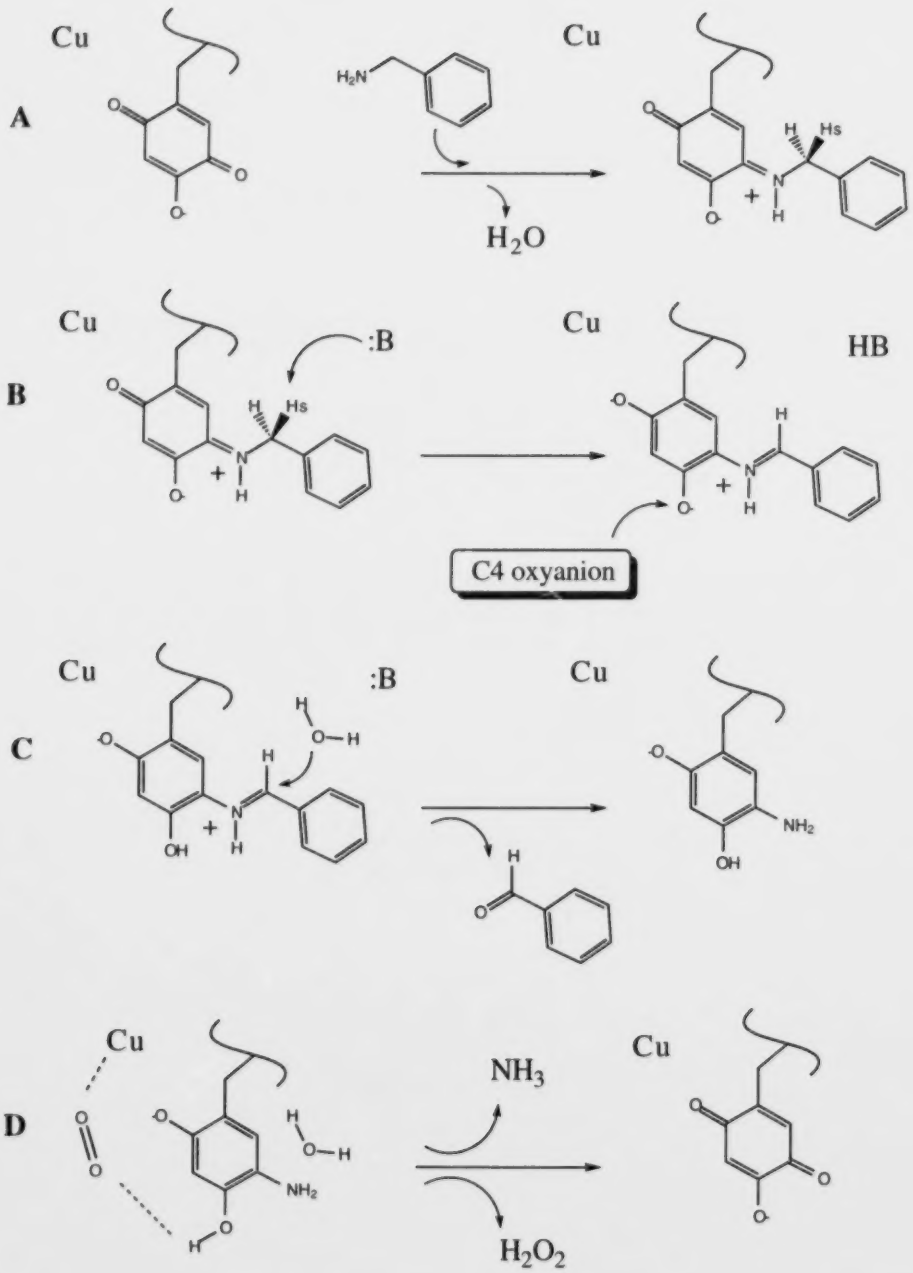

Figure 1.8 Mechanism of the copper amine oxidases. Schiff's base formation between TPQ and benzylamine (A), abstraction of the *pro*-S hydrogen (B), hydrolysis of product imine and release of benzaldehyde (C), copper mediated oxidation of TPQ and release of ammonia and hydrogen peroxide (D).

their reaction specificities. Source-dependent stereochemistry has been observed for tyramine, dopamine and phenethylamine oxidation (Figure 1.9)[74-79].

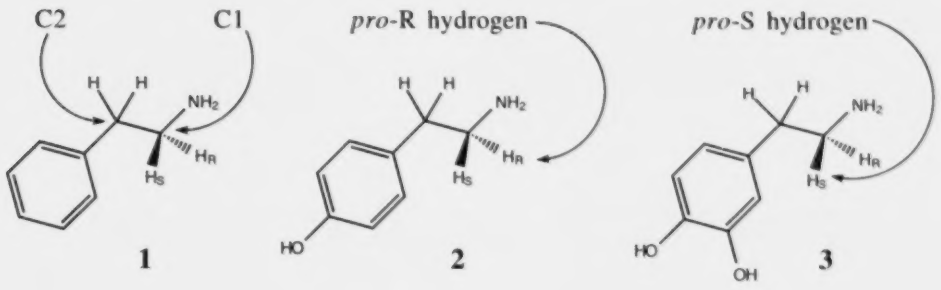

Figure 1.9 Stereochemical and configurational assignment of phenethylamine (1), tyramine (2) and dopamine (3). These amines are shown with the *pro*-S and *pro*-R hydrogens. This stereochemical classification is taken from the Cahn-Ingold-Prelog system that ranks the four groups of an asymmetric carbon (*Angew. Chem.*, **78**, 413-447, 1964). The alkyl carbons are labelled, starting from the nitrogen, as C1 and C2.

The porcine and horse CuAOs remove the *pro*-R hydrogen from C1 of tyramine or dopamine whereas pea seedling and porcine kidney CuAOs remove the *pro*-S hydrogen. In contrast, the enzymes from bovine, rabbit and sheep plasma display net nonstereospecific proton removal[80]. It should be noted that the nonstereospecificity of the bovine, rabbit and sheep enzymes is due to a mirror-image binding mode where substrate is bound in either of two absolute orientations. Thus, either the *pro*-S hydrogen or the *pro*-R hydrogen is abstracted from C1 of tyramine[78].

This unique alkylamine C1 stereochemistry of the CuAOs is correlated with solvent hydrogen exchange reactions at C2 of substrate amine[75]. It has been shown that the soluble enzymes that are *pro*-S specific at C1 of tyramine do not catalyze hydrogen exchange at C2, whereas the *pro*-R and nonstereospecific enzymes do catalyze exchange at C2 (Table 1.2)[7].

Table 1.2 Summary of the stereochemistry of proton abstraction and solvent exchange with tyramine, dopamine or phenethylamine substrates by amine oxidases[7].

Enzyme Source	C1 Proton Abstraction	C2 Solvent Exchange
Copper Amine Oxidases (EC 1.4.3.6)		
Porcine Plasma	*pro*-R	Yes
Horse Plasma	*pro*-R	Yes
Beef Plasma	nonstereospecific	Yes
Sheep Plasma	nonstereospecific	Yes
Rabbit Plasma	nonstereospecific	Yes
Pea Seedling	*pro*-S	No
Soybean Seedling	*pro*-S	No
Chick Pea Seedling	*pro*-S	No
Pig Kidney	*pro*-S	No
Semicarbazide-Sensitive Amine Oxidases		
Porcine Aorta	*pro*-S	Yes
Bovine Aorta	*pro*-S	Yes
Rat Aorta	*pro*-S	not determined
Lysyl Oxidase (EC 1.4.3.13)		
Beef Aorta	*pro*-S	Yes

Tissue-bound SSAO enzymes from porcine and bovine aorta are *pro*-S specific at C1 and catalyze C2 solvent exchange. They are therefore stereochemically distinct from the other CuAOs. The SSAO enzymes and lysyl oxidase have similar stereochemistry[76]. Solvent exchange at C2 of substrate amine was first demonstrated with the bovine plasma amine oxidase. It was observed that tritium was released from C2 of dopamine into bulk solvent[79]. This has been attributed to a reversible imine-enamine tautomerization side reaction that is unrelated to the main catalytic pathway[81]. All CuAO enzymes must hydrolyze imine, but those which do so more slowly (relative to tautomerization) would be expected to display this solvent exchange process (Figure 1.10). That is, if the rate of imine hydrolysis is fast relative to tautomerization, then no solvent exchange should be observed. An alternative explanation that has been suggested for the lack of solvent exchange in some enzymes is th.. tautomerization does occur but the abstracted proton is shielded from bulk solvent[75]. The loss of hydrogen from C2 has been termed "wash-out" and the reprotonation reaction has been termed "wash-in"[75]. Bovine plasma amine oxidase displays random wash-out of hydrogen from C2 of dopamine, neither *pro*-S nor *pro*-R loss is preferred[79]. However, reprotonation (wash-in) only occurs to the *pro*-R side[78]. This finding is very surprising since this appears to violate the principle of microscopic reversibility. This principle states that the forward and reverse directions of a reaction should be equivalent (i.e., have the same transition state)[82]. Since no enzyme nor chemical process has been shown to violate this principle and the bovine and porcine aorta SSAOs display stereospecific *pro*-R wash-in and wash-out at C2 it is probable that more than one process occurs in the bovine plasma enzyme. Stated another way, enamine reprotonation is not the microscopic reverse of imine exchange[78].

In contrast to the variable stereochemistry for tyramine and dopamine oxidation, benzylamine reacts exclusively with loss of the *pro*-S hydrogen for all

enzymes studied[80,83-85]. This is the expected result for enzymes with the same cofactor catalyzing the same chemical reaction. Enzymes that are *pro*-S specific for all substrates include bacterial (see chapter 3) and plant CuAOs as well as bovine and porcine aorta SSAOs (Table 1.2)[7].

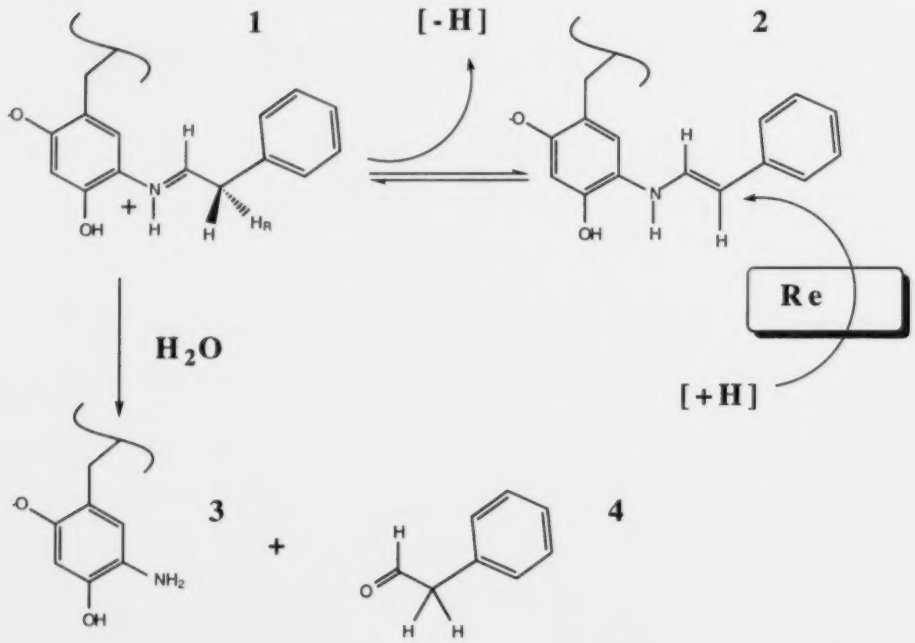

Figure 1.10 Reversible tautomerization of the phenethylamine-TPQ pre-hydrolysis complex. Loss of either C2 hydrogen from imine (**1**) yields the enamine (**2**). Reprotonation of enamine (**2**) occurs at the *pro*-R (Re face) position of C2. Hydrolysis of the phenethylamine-TPQ imine (**1**) yields aminoquinone (**3**) and phenylacetaldehyde (**4**).

BSAO is *pro*-S specific for benzylamine, *p*-hydroxybenzylamine and 3-methylbutylamine (Table 1.1) but catalyzes net nonstereospecific hydrogen abstraction from C1 of tyramine or dopamine[83,86,87]. However, it has been shown that *pro*-S abstraction is favoured by the BSAO enzyme[78]. Also, the CuAOs from

bovine, rabbit and sheep plasma exhibit smaller kinetic isotope effects for 1R-[^{2}H]tyramine than for 1S-[^{2}H]tyramine[75]. This was attributed to a partially rate limiting step other than C-H (or C-^{2}H) bond cleavage that is probably a conformational reorganization for a *pro*-R mode catalytic intermediate[75].

These observations suggest that *pro*-S stereospecificity is preferred for most CuAOs. Only the porcine and horse plasma enzymes display absolute *pro*-R specificity for hydrogen abstraction from C1 of tyramine. Thus, they must have an active site that prevents the formation of catalytically relevant intermediates from *pro*-S mode oriented substrate[80]. A crystal structure with resolution approaching 1.5 Å would provide the level of detail required to clarify active site geometric constraints in the CuAOs.

CuAO stereochemical analysis requires observation of the loss or retention of isotopic label subsequent to the enzymic oxidation of amine substrates[74,79-80,85]. Use of chiral deuterium labelling of the substrate amine is common. The advantage of deuterium, compared with tritium, is that it is not radioactive and it completely replaces hydrogen at a given position. This is not true of tritium, since only a small fraction (≤ 1PPB) of the molecules have tritium substituted for hydrogen at a given position. Thus tritium-labelled compounds require an analysis of the specific activity of both product and substrate.

Since enzymes are chiral catalysts, introduction of deuterium into amine substrate with high chiral selectivity is readily accomplished by enzyme-mediated transformation[83]. It is prudent to determine subsequently the chiral purity of the synthesized amine in order to draw correct conclusions regarding enzyme stereochemistry[80].

The retention or loss of deuterium from deuterium-labelled benzylamine or tyramine, subsequent to coupled enzymatic oxidation, is conveniently accomplished with ^{1}H NMR spectroscopy of the isolated product alcohols. In ^{1}H NMR the

deuterium nuclei are not directly observable. Thus, a substitution of 1 mole of deuterium for 1 mole of hydrogen results in a ^{1}H NMR peak integration (proton inventory) that is "missing" 1 proton. Indirect detection of deuterons is possible through observation of spin-spin (scalar) coupling. Typically, chemical shift information, integration of proton resonances and detection of deuterium-proton scalar coupling provide sufficient information to follow the deuterium content of labelled amines during the enzymatic reaction[80].

Experiments designed to determine the stereochemical course for the oxidative deamination of chirally deuterated tyramine and benzylamine are described in this thesis. Chapter 2 details the stereochemistry of benzylamine oxidation by six CuAOs. These enzymes represent the three different classes of stereochemistry for hydrogen removal from C1 of tyramine exhibited by CuAOs. Chapter 3 presents the stereochemistry of benzylamine and tyramine oxidation for four bacterial CuAO enzymes. This chapter also includes an evaluation of hydrogen exchange reactions at C2 of tyramine. In Chapter 4, the precise nature of the redox cofactor, proposed to be a TPQ-like molecule, was investigated in the SSAOs isolated from bovine and porcine aorta.

References

1. Mondovi, B. (1985) *Structure and Functions of Amine Oxidases*, CRC Press, Boca Raton, FL.

2. Blaschko, H. (1974) *Rev. Physiol. Biochem. Pharmacol.*, **70**, 84-148.

3. Hare, M.L.C. (1928) *Biochem J.*, **22,** 968-979.

4. Schnaitman, C., Erwin,V.G. and Greenawalt, J.W. (1967) *J. Cell. Biol.*, **32**, 719-735.

5. Tipton, K.F. (1968) *Biochim. Biophys. Acta*, **159**, 451-459.

6. Blaschko, H. (1952) *Pharmacol. Rev.*, **4**, 415-458.

7. Palcic, M.M., Scaman, C.H. and Alton, G. (1995) *Progress in Brain Research*, **106**, in press.

8. Sharman, D.F. (1973) *Br. Med. Bull.*, **29**, 110-115.

9. Loomer, H.P., Saunders, J.C. and Kline, N.S. (1957) *Psychiat. Res. Rep. Amer. Psychiat. Assoc.*, **8**, 129-141.

10. Riederer, P., and Youdim, M.B.H. (1986) J. *Neurochem.*, **46**, 1349-1356.

11. Kagan, H.M. (1986) In: Mecham, R.P. (ed.) *Regulation of matrix accumulation.* Academic Press, New York, pp. 322-398.

12. Pinnell, S.R. and Martin, G.R. (1968) *Proc. Natl. Acad. Sci. (USA)*, **61**, 708-716.

13. Robins, S.P. (1982) In: Weiss, J.B. & Jayson, M.I.Y. (eds.) *Collagen in health and disease.* Churchill Livingstone, Edinburgh, pp. 160-178.

14. Bailey, A.J., Robins, S.P. and Balian, G. (1974) *Nature*, **251**, 105-109.

15. Buffoni, F. (1985) in *Structure and Functions of Amine Oxidases*, Mondovi, B. (Ed) pp. 77-84 CRC Press, Boca Raton, Fl.

16. Krebs, C.J. and Krawetz, S.A. (1993) *Biochim. Biophys. Acta*, **1202**, 7-12.

17. Cronshaw, A.D., Fothergill-Gillmore, L.A. and Hulmes, D.J.S. (1995) *Biochem. J.*, **306**, 279-284.

18. Levene, C.I., O'Shea, M.P. and Carrington, M.J. (1988) *Int. J. Biochem.*, **20**, 1451-1456.

19. Lyles, G.A. and Singh, I. (1985) *J. Pharm. Pharmacol.* **37**, 637-643.

20. Williamson, P.R., Moog, R.S., Dooley, D.M. and Kagan, H.M. (1986) *J. Biol. Chem.*, **261**, 16302-16305.

21. Mu, D., Medzihradszky, K.F., Adams, G.W., Mayer, P., Hines, W.M., Burlingame, A.L., Smith, A.J., Cai, D. and Klinman, J.P. (1994) *J. Biol. Chem.*, **269**, 9926-9932.

22. Cai, D. and Klinman, J. P. (1994) *Biochemistry*, **33**, 7647-7653.

23. McIntire, W.S. and Hartmann, C. (1993) in *Principles and Applications of Quinoproteins,* Davidson, V.L. (Ed) pp. 97-109 Macel Dekker, Inc., New York, NY.

24. Maslinski C., Bieganski T., Fogel W.A., and Kitler M.E. (1985) in *Structure and Functions of Amine Oxidases*, Mondovi, B. (Ed) pp. 153-166 CRC Press, Boca Raton, Fl.

25. Callingham, B.A., Crosbie, A.E. and Rous, B.A. (1995) *Progress in Brain Research*, **106**, 305-321.

26. Blaschko, H. (1974) *Rev. Physiol. Biochem. Pharmacol.*, **20**, 83-148.

27. Callingham, B.A. and Barrand, M.A. (1987) *J. Neural Transm. [Suppl.]*, **23**, 37-45.

28. Tabor, H. (1985) in *Structure and Functions of Amine Oxidases*, Mondovi, B. (Ed) pp. 1-3 CRC Press, Boca Raton, Fl.

29. Kumagai, H. and Yamada, H. (1985) in *Structure and Functions of Amine Oxidases*, Mondovi, B. (Ed) pp. 37-43 CRC Press, Boca Raton, Fl.

30. Alton, G. and Palcic, M.M. (1995) Unpublished results.

31. Rinaldi, A., Floris, G. and Giartosio, A. (1985) in *Structure and Functions of Amine Oxidases,* pp. 51-62 CRC Press, Boca Raton, Fl.

32. Bolwell, G.P., Robbins, M.P. and Dixon, R.A. (1985) *Biochem. J.*, **229**, 693-699.

33. De Carolis, E., Chan, F., Balsevich, J. and De Luca, V. (1990)*Plant Physiol.*, **94**, 1323-1329.

34. Hashimoto, T., Mitani, A. and Yamada, Y. (1990) *Plant Physiol.*, **93**, 216-221.

35. Bardsley, E.G., Crabbe, M.J.C. and Scott, I.V. (1974) *Biochem. J.*, **139**, 169-181.

36. Conforti, L., Raimondi, L. and Lyles, G.A. (1993) *Biochem. Pharmacol.*, **46**, 603-607.

37. Yu, P.H. and Zuo, D-M. (1993) *Diabetes*, **42**, 594-603.

38. Yu, P.H. (1990) *J. Pharm. Pharmacol.*, **42**, 882-884.

39. Schayer, L., Smiley, L.R. and Kaplan, H.E. (1952) *J. Biol. Chem.*, **198**, 545-552.

40. Lyles, G.A., Holt, A. and Marshall, C.M.S. (1990) *J. Pharm. Pharmacol.*, **42**, 332-338.

41. Precious, E., Gunn, C.E. and Lyles, G.A. (1988) *Biochem. Pharmacol.*, **37**, 707-713.

42. Gibson, J.E. (1983) *Formaldehyde Toxicity*, Hemisphere Publishers, Washington, DC.

43. Hirsch, J.G. (1953) *J. Exp. Med.*, **97**, 345-355.

44. Morgan, D.M.L. (1990) *Biochem. Soc. Trans.*, **18**, 1080-1084.

45. Baylin, S.B. and Luk, G.D. (1985) in *Structure and Functions of Amine Oxidases*, Mondovi, B. (Ed) pp. 187-194 CRC Press, Boca Raton, Fl.

46. Petterson, G. (1985) in *Structure and Functions of Amine Oxidases*, Mondovi, B. (Ed) pp. 105-120 CRC Press, Boca Raton, Fl.

47. Holt, A. and Callingham, B.A. (1994) *J. Neural. Transm. [suppl.]*, **41,** 433-437.

48. Hysmith, R.M. and Boor, P.J. (1988) *Toxicology*, **51**, 133-145.

49. Janes, S.M., Mu, D., Wemmer, D., Smith, A.J., Kaur, S., Maltby, D., Burlingame, A.L. and Klinman, J.P. (1990) *Science*, **248**, 981-987.

50. Zhang, X., Fuller, J.H. and McIntire, W.S. (1993) J. Bacteriol., 175, 5617-5627.

51. Choi, Y-H., Matsuzaki, R., Fukui, T., Shimizu, E., Yorifuji, T., Sato. H., Ozaki, Y. and Tanizawa, K. (1995) *J. Biol. Chem.*, in press.

52. Tipping, A.J. and McPherson, M.J. (1995) *J. Biol. Chem.*, **270**, 16939-16946.

53. Parsons M.R., Convery M.A., Wilmot C.M., Yadav K.D.S., Blakely V., Corner A.S., Phillips S.E.V., McPherson, M.J. and Knowles P.F. (1995) *Structure*, **3**, 1171-1184.

54. Janes, S.M., Palcic, M.M., Scaman, C.H., Smith, A.J., Brown, D.E., Dooley, D.M., Mure, M. and Klinman, J.P. (1992) *Biochemistry*, **31**, 12147-12154.

55. Matsuzaki, R., Fukui, T., Sato, H., Ozaki, Y. and Tanizawa, K. (1994) *FEBS Lett.*, **351**, 360-364.

56. Yasunobu, K.T., Ishizaki, H. and Minamiura, N.(1976) *Mol. Cell. Biochem.*,**13**, 3-29.

57. Knowles, P.F. (1996) Personal communication.

58. Finazzi-Agro A. (1985) in *Structure and Functions of Amine Oxidases*, Mondovi, B. (Ed) pp. 121-125 CRC Press, Boca Raton, Fl.

59. Bardsley, W.G.(1985) in *Structure and Functions of Amine Oxidases*, Mondovi, B. (Ed) pp. 135-152 CRC Press, Boca Raton, Fl.

60. Janes, S.M. and Klinman, J.P. (1995) in *Methods in Enzymology vol. 258*, Klinman, J.P. (Ed.) pp. 20-34 Academic Press, New York, NY.

61. Steinebach, V., Groen, B.W., Wijmenga, S.S., Niessen, Wilfried M.A., Jongejan, J.A. and Duine, J.A. (1995) *Anal. Biochem.*, **230**, 159-168.

62. Klinman, J.P. and Mu, D. (1994) *Annu. Rev. Biochem.*, **63**, 299-344.

63. Palcic, M.M. and Janes, S.M. (1995) in *Methods in Enzymology vol. 258*, Klinman, J.P. (Ed.) pp. 34-38 Academic Press, New York, NY.

64. Dooley, D.M. and Brown, D.E. (1995) in *Methods in Enzymology vol. 258*, Klinman, J.P. (Ed.) pp. 132-140 Academic Press, New York, NY.

65. Laidler, K.J. and Mesier, J.H (1982) *Physical Chemistry*, pp. 607-611 Benjamin/Cummings Publishing Co., Menlo Park, CA.

66. Dooley, D.M. and Brown, D.E. (1993) in *Principles and Applications of Quinoproteins,* Davidson, V.L. (Ed) p. 275 Marcel Dekker, Inc., New York, NY.

67. Janes, S.M. and Klinman, J.P. (1991) *Biochemistry*, **30**, 4599-4605.

68. Hartmann, C. and Klinman, J. P. (1991) *Biochemistry*, **30**, 4605-4611.

69. Mure, M and Klinman, J.P. (1995) *J. Am. Chem. Soc.*, **117**, 8707-8718.

70. Dooley, D.M., McGuirl, M.A., Brown, D.E., Turowski, P.N., McIntire, W.S. and Knowles, P.F. (1991) *Nature (London),* **349**, 262-264.

71. Matsuzaki, R., Suzuki, S., Yamaguchi, K., Fukui, T. and Tanizawa, K. (1995) *Biochemistry*, **34**, 4524-4530.

72. Cai, D. and Klinman, J.P. (1994) *J. Biol. Chem.*, **269**, 32039-32042.

73. Hanson, K.R. and Rose, I.A. (1975) *Acc. Chem. Res.*, **8**, 1-10.

74. Scaman, C.H. and Palcic, M.M. (1992) *Biochemistry*, **31**, 6829-6841.

75. Coleman, A.A., Scaman, C.H., Kang, Y.J. and Palcic, M.M. (1991) *J. Biol. Chem.*,**266**, 6795-6800.

76. Shah, M.A., Scaman, C.H., Palcic, M.M. and Kagan, H.M. (1993) *J. Biol. Chem.*, **268**, 11573-11579.

77. Farnum, M., Palcic, M.M. and Klinman, J.P. (1986) *Biochemistry*, **25**, 1898-1904.

78. Farnum, M.F. and Klinman, J.P. (1986) *Biochemistry*, **25**, 6028-6036.

79. Summers, M.C., Markovic, R. and Klinman, J.P. (1979) *Biochemistry*, **18**, 1969-1979.

80. Alton, G., Taher, T.H., Beever, R.J. and Palcic, M.M. (1995) *Arch. Biochem. Biophys.*, **316**, 353-361.

81. Lovenberg, W. and Beaven, M.A. (1971) *Biochim. Biophys. Acta*, **251**, 452-455.

82. Jencks, W.P. (1969) *Catalysis in Chemistry and Enzymology*, p. 208, Dover Publications, Inc., New York, NY.

83. Battersby, A.R., Staunton, J., Klinman, J. and Summers, M.C. (1979) *FEBS. Lett.*, **99**, 297-298.

84. Battersby, A.R., Staunton, J. and Summers, M.C. (1976) *J. Chem. Soc. Perkin*, **1**, 1052-1056.

85. Yu, P.H. and Davis, B.A. (1988) *Int. J. Biochem.*, **20**, 1197-1201.

86. Suva, R.H. and Abeles, R.H. (1978) *Biochemistry*, **17**, 3538-3545.

87. Shibuya, M., Chou, H.M., Fountoulakis, N., Hassam, S., Kim, S.U., Kobayashi, K., Otsuka, H., Rogalska, E., Cassady, J.M. and Floss, H.G. (1990) *J. Am. Chem. Soc.*, **112**, 297-304.

Chapter Two

Stereochemistry of Benzylamine Oxidation by Copper Amine Oxidases[I]

2.1 Introduction

The copper-containing amine oxidases (EC 1.4.3.6) oxidatively deaminate a variety of primary amines yielding ammonia, hydrogen peroxide, and an aldehyde (Equation 1)[1].

$$RCH_2NH_2 + H_2O + O_2 \longrightarrow RCHO + NH_3 + H_2O_2 \qquad (1)$$

Highly purified amine oxidase preparations display a characteristic pink-peach color due to a broad absorbance at 470 nm[1], attributed to an essential organic cofactor. The cofactor has been identified as topaquinone in the amine oxidases isolated from bovine and sheep plasma, pea seedlings, and porcine kidney and plasma[2,3]. Recognition of the nature of the organic cofactor has facilitated the elucidation of mechanistic features of the copper amine oxidase reactions[4]. Topaquinone is reduced by substrate, concomitant with substrate oxidation in an anaerobic half-reaction, and is then reoxidized by molecular oxygen in a second aerobic reaction to complete the catalytic cycle[5]. However, little is known about the active site of these enzymes due to a lack of crystallographic structural information.

Previous studies on pea seedling and bovine plasma amine oxidases have shown that the oxidative deamination of benzylamine occurs with stereospecific

---

[I] A version of this chapter has been published in the Archives of Biochemistry and Biophysics, vol. 316 (1), 353-361 (1995). Authors: Gordon Alton, Taha H. Taher, Richard J. Beever and Monica M. Palcic.

removal of the *pro*-S hydrogen from the methylene carbon[6,7]. In contrast to benzylamine, the stereochemical course of tyramine oxidation is source dependent. The enzymes from pea seedling, soybean seedling, chick pea seedling, and porcine kidney also react with abstraction of the *pro*-S hydrogen from C-1 of tyramine whereas the enzymes from horse and porcine plasma remove the *pro*-R hydrogen[8-10]. The amine oxidases isolated from bovine, sheep, and rabbit plasma display rare mirror-image binding and catalysis with net nonstereospecific proton abstraction at C-1 of tyramine[8-12].

In the present study we have used ^{1}H NMR spectroscopy to determine the stereochemical course for the oxidative deamination of benzylamine by six copper amine oxidases. All six of the enzymes studied are stereospecific with the reaction occurring with removal of the *pro*-S hydrogen, irrespective of the stereochemical course for tyramine oxidation.

2.2 Experimental Procedures

Materials-The chemicals used were ACS reagent grade and used without further purification. Organic reactions were performed under a flowing dry argon stream in glassware that was oven dried at 150° C. Solvents were distilled and dried prior to use. Distilled water was further purified with a Milli-Q system. Column chromatography was carried out on silica gel 60 (EM Science) or C18 silica gel (Waters). C18 Sep-Pak cartridges were from Waters, DE-52 cellulose was from Whatman, alpha-deuterobenzaldehyde was from Merck, Sharp, and Dohme and deuterated NMR solvents were from Cambridge Isotope Laboratories. Hydrazine hydrate (99%) was from BDH, benzaldehyde was from Fisher Scientific and $^{2}H_{6}$-deuteroethanol was from Aldrich. *p*-Nitrophenylhydrazine hydrochloride and phthalimide-DBU were from Fluka. NADH, NAD, aminohexyl agarose (CNBr

activated), and [1S]-3-oxo-4,7,7-trimethyl-2 oxabicyclo [2.2.1] heptone-1-carbonyl chloride (camphanic acid chloride) were from Sigma. SDS-PAGE was done with pre-cast 4-20% acrylamide gels from Bio-Rad.

Enzymes-Horse liver alcohol dehydrogenase (ADH), bovine liver catalase, and bovine plasma amine oxidase were obtained from Sigma. Sheep and porcine plasma enzymes were isolated from fresh citrated blood obtained from local slaughterhouses; rabbit and horse amine oxidases were isolated from frozen serum (Pel-Freez Biologicals). Enzyme activity was measured at 25° C using 3.33 mM benzylamine as a substrate in 50 mM sodium phosphate buffer, pH 7.2 by monitoring the increase in absorbance at 250 nm[13]. One unit is defined as the quantity of enzyme which catalyzes the production of 1.0 µmol/min of benzaldehyde based on an extinction coefficient of 12.0 mM^{-1} cm^{-1}. Protein concentration was estimated by the Bradford method using a Bio-Rad kit with bovine serum albumin as a standard[14]. All centrifugations and precipitations were carried out at 17,000 x g at 4° C for 20 min. Concentration of enzymes was by ultrafiltration under 40 psi nitrogen gas pressure using PM-30 membranes (Amicon) in the ultrafiltration cells. Dialysis was done with 12,000 molecular weight cutoff membranes (Spectra/Por) for equilibration times of 4 h or overnight. Pea seedling amine oxidase with specific activity of 2 units/mg was available from previous work[8].

Plasma amine oxidases were isolated by a common methodology using slight modifications of published procedures[9,15]. When frozen serum samples were used as an enzyme source, 3 L of serum were centrifuged at 17,000 x g for 20 min to remove plasma lipoproteins. For fresh citrated blood samples, 10 L were centrifuged to remove red and white blood cells. The supernatants were fractionated by the addition of solid ammonium sulfate to 30% saturation and slowly stirring for 2 h. The solution was centrifuged and the supernatant solution brought to 60%

saturation with solid ammonium sulfate. The protein pellet precipitating at 30-60% ammonium sulfate saturation was dissolved in 10 mM sodium phosphate buffer, pH 7.0 (buffer A) and dialyzed extensively against this buffer. After dialysis the enzyme solution was applied to a 5 X 25 cm DE-52 anion exchange column equilibrated with buffer A. Protein was monitored in the column eluent by measuring the solution absorbance at 280 nm, and the column was washed with buffer A until the absorbance returned to baseline levels. Amine oxidase was then eluted with a 1.0 L linear gradient starting with buffer A (500 mL) up to 500 mL of 200 mM sodium phosphate, pH 7.0 (buffer B). The fractions containing enzyme were pooled, dialyzed against buffer A, and then concentrated by ultrafiltration to approximately 200 mL. The concentrated enzyme sample was applied to a 2.5 X 15 cm aminohexyl agarose column and the column was washed with buffer A until protein was no longer detected in the eluent. Then amine oxidase was eluted with a 500 mL linear gradient starting with 250 mL of buffer A up to 250 mL of buffer B. Following the linear gradient, higher purity amine oxidase could also be eluted from the affinity column with 20 mL buffer B containing 1.0 M NaCl. The partially purified amine oxidase was dialyzed against 50 mM sodium phosphate buffer, pH 7.2, and stored at 4^{o} C with no loss of activity for at least 4 weeks. For rabbit plasma enzyme isolations, potassium phosphate buffers and potassium chloride solutions were employed rather than sodium phosphate buffers and sodium chloride. Ion-exchange chromatography was carried out at pH 7.0, however, pH 8.0 was used for the aminohexyl affinity chromatography column step. The final specific activities of the oxidases were: bovine and horse 0.1 U/mL, rabbit 0.02 U/mL, sheep 0.2 U/mL, porcine, 0.01 U/mL, and pea seedling 2 U/mL.

p-Nitrophenylhydrazine Derivatization and Spectroscopy-Absorbance spectra were recorded with a Hewlett Packard 8451A diode array spectrophotometer using quartz cuvettes. An aqueous solution of *p*-

nitrophenylhydrazine hydrochloride (1.0 mM) was used for derivatizing the enzymes. Aliquots of 5 µL were added to a cuvette containing 1 mg of enzyme in 1.0 mL of 50 mM sodium phosphate buffer, pH 7.2 (buffer C). The length of time between aliquot additions was determined by monitoring the increase in absorbance at 464 nm until no further absorbance change was detected. The titration was continued until a slight excess of *p*-nitrophenylhydrazine was added. When the derivatization was complete the reaction mixture was applied to a Bio-Rad 10DG desalting column equilibrated in 50 mM NH_4HCO_3 to remove the excess *p*-nitrophenylhydrazine. Absorbance spectra from 350 nm to 700 nm were recorded for 0.2 mg/mL of enzyme in buffer C or 2.8 M KOH.

Benzylamine Oxidation by Amine Oxidases-Incubations were conducted in a coupled system containing 3.5 µmol of R- or S-[*methylene*-^{2}H]benzylamine hydrochloride, 13.1 µmol NADH, 1.3 units ADH, 7000 units catalase, and 0.4 mL of 50 mM sodium phosphate buffer, pH 7.2[6,9]. Amine oxidase (1.0 mL) was added to each incubation tube to initiate the reaction. After an 18 h incubation at 25° C the reactions were diluted to 10 mL with saturated NaCl and loaded onto reverse-phase C18 Sep-Pak cartridges. Each cartridge was rinsed with 5 mL saturated NaCl, followed by 5 mL ^2H_2O, and then the benzyl alcohol product was eluted directly into 5 mm NMR tubes with 0.7 mL C^2HCl_3.

R-[methylene-^{2}H]benzylamine hydrochloride-A modification of Battersby's procedure was used for the synthesis of this amine[7,16]. Briefly, [*formyl*-^{2}H]benzaldehyde was reduced to S-[*methylene*-^{2}H]benzyl alcohol with 79 units ADH and 31 mg NAD in 450 mL of 10% (v/v) ethanol and 20 mM sodium phosphate buffer, pH 7.2, incubated at 37° C for 16 h. After chromatography on silica gel, the S-[*methylene*-^{2}H]benzyl alcohol was converted to S-[*methylene*-^{2}H]benzyl *p*-toluenesulfonate. N-(R-[*methylene*-^{2}H]benzyl) phthalimide was prepared through inversion of configuration of the S-tosylate by a S_N2

displacement reaction (1.5 h, 25° C) with phthalimide-DBU. Heating the N-(R-[*methylene*-^{2}H]benzyl) phthalimide with hydrazine hydrate in 95% ethyl alcohol at 70° C overnight provided R-[*methylene*-^{2}H]benzylamine. After acidic workup from ethyl ether, 29 mg of R-[*methylene*-^{2}H]benzylamine hydrochloride were obtained in a final overall yield of 2%.

S-[methylene-^{2}H]benzylamine hydrochloride-To 1.4 L of 20 mM sodium phosphate buffer, pH 8.0, was added with rapid stirring 1.0 mL of benzaldehyde followed by 5 g $C^2H_3C^2H_2O^2H$ (deuteroethanol). The stirring rate was reduced and 195 mg NAD and 171 units ADH were added and the solution incubated at 37° C for 16 h. All other synthetic steps were similar to the synthesis of the R-deuterated enantiomer using proportionally adjusted quantities of reagents. The final overall yield was 3% representing 52 mg of S-[*methylene*^{2}H]benzylamine hydrochloride.

Chiral derivatization of benzylamine with camphanic acid-The R- and S-[*methylene*-^{2}H]benzylamines and diprotonated benzylamine were reacted with the chiral derivatization agent, camphanic acid chloride[17]. In 1.5 mL pyridine, 9 mmol of benzylamine and 51 mmol of camphanic acid chloride were stirred at 22° C. After 20 h, 3 mL of water were added to the reaction mixture and the solution was stirred vigorously for 1 h. The N-benzyl camphanamide was extracted into 5 mL CH_2Cl_2 and washed successively with 10 mL each 1 M HCl, twice with saturated $NaHCO_3$, and twice with water. After drying the solution over anhydrous Na_2SO_4, filtration, and evaporation the NMR spectrum was obtained with the sample dissolved in $C_6{}^2H_6$.

^{1}H and ^{2}H NMR spectroscopy-^{1}H NMR spectra were recorded at 500 MHz on a Varian Unity 500 instrument at 30° C, except for camphanamides (27° C). All compounds were dissolved in 0.7 mL of C^2HCl_3, except for amines (^2H_2O) and camphanamides ($C_6{}^2H_6$). NMR solvents were 99.9% deuterated or better. A T1

analysis indicated that a 3 s acquisition time followed by a 2 s relaxation delay was appropriate for compounds in C^2HCl_3 using a 60° (5 μs) pulse width. Chemical shifts are referenced to internal TMS, or residual ^2HOH (4.81 ppm) for amines, or residual $C_6{}^2H_5H$ (7.15 ppm) for camphanamides and are precise to 0.001 ppm. Spin-spin coupling constants are reported as first-order and are precise to 0.2 Hz. Digital resolution was 0.17 Hz/point. Resolution enhancement of spectra for benzyl alcohols used a line broadening factor of -1.8 and a Gaussian factor of 0.7. The ^2H-decoupled ^1H NMR was recorded at 400 MHz and the ^1H-decoupled ^2H NMR was recorded at 61.4 MHz on a Bruker AM-400 instrument operated by the Department of Chemistry NMR Service Laboratory, University of Alberta.

2.3 Results and Discussion

The purification of the copper amine oxidases followed well-established procedures with minor modifications[9,15]. Isolation steps included ammonium sulfate fractionation, anion exchange chromatography, and aminohexyl agarose affinity chromatography. Each enzyme was partially purified (60-300 fold) in one or two weeks with overall yields ranging from 12 to 21%. SDS-PAGE indicated that the enzymes all had similar levels of purity with a major band for the expected molecular weight of 91 ± 6 kDa.

Prior to the investigation of the stereochemical course of benzylamine oxidation, topaquinone was confirmed to be the cofactor in the horse plasma and rabbit plasma amine oxidases using visible absorbance spectroscopy. This was important for comparison of stereochemical results to ensure that all enzymes studied contained the same cofactor.

The visible absorbance spectra of *p*-nitrophenylhydrazine derivatized horse plasma amine oxidase are shown in Figure 2.1.

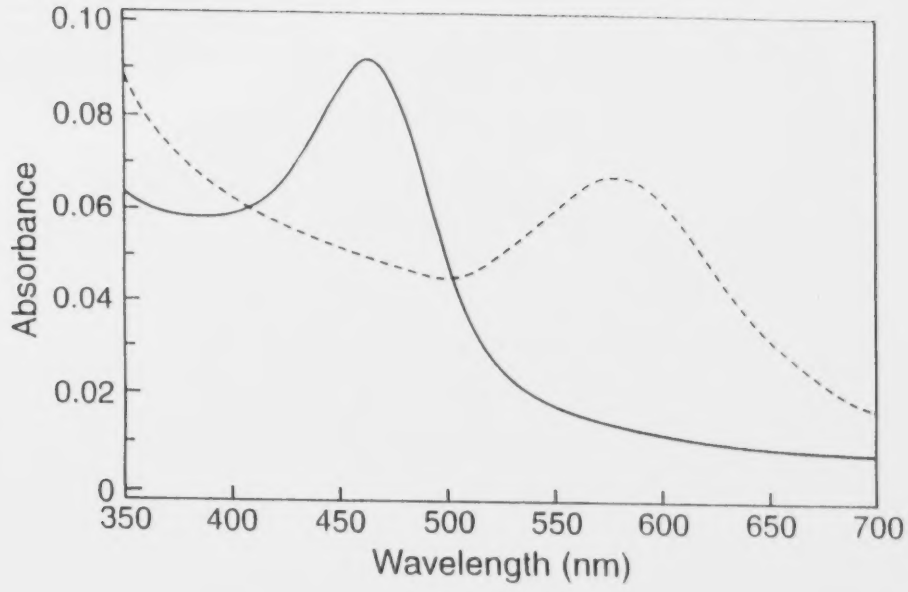

Figure 2.1 Absorbance spectra of the *p*-nitrophenylhydrazine derivatized horse plasma amine oxidase. Spectra were obtained with 0.2 mg of enzyme in 1 mL of 50 mM sodium phosphate buffer, pH 7.2 (—) or in 2.8 M KOH (---).

The derivatized enzyme exhibits a peak at 464 nm in neutral solution (pH 7.2), which undergoes a 116 nm redshift to 580 nm in basic solution. The derivatized rabbit plasma enzyme also has a λ_{max} of 462 nm at pH 7.2 which redshifts to 584 nm in basic solution (Appendix I). These results closely parallel the unique spectral properties reported for other topaquinone containing amine oxidases and topaquinone model compounds suggesting that the horse and rabbit plasma enzymes also contain this cofactor[3].

Horse liver alcohol dehydrogenase was used to synthesize stereospecifically deuterated benzyl alcohols which were then converted to amines *via* chemical procedures. The reduction of benzaldehyde catalyzed by alcohol dehydrogenase has been studied in detail[7,16]. NAD^{2}H is produced *in situ* by transfer of deuterium from $^2H_6$-deuteroethanol to NAD. R-[*methylene*-^{2}H]benzyl alcohol is generated by the stereospecific transfer of the deuteron from NAD^{2}H to the *Re* face of benzaldehyde[18]. The opposite process, proton transfer to deuterobenzaldehyde from NADH, yields S-[*methylene*-^{2}H]benzyl alcohol. The hydroxyl group is converted to a leaving group by transformation to a *p*-toluenesulfonate. Inversion of configuration is achieved by displacement of the toluenesulfonate with a phthalimide. Deprotection of the phthalimide affords stereospecifically alpha-deuterated benzylamine. The synthesis of S-[*methylene*-^{2}H]benzylamine is outlined in Scheme 2.1.

The ^{1}H NMR spectrum (Figure 2.2 a) of R-[*methylene*-^{2}H]benzylamine shows a resonance at 4.175 ppm. Integration of this benzylic proton resonance *vs.* the aromatic signals of the spectrum indicates 105% deuterium incorporation. A small signal (1.5%) for the benzylic protons of the diprotonated amine was observed at 4.189 ppm. The ^{1}H NMR spectrum (Figure 2.2 b) of S-[*methylene*-^{2}H]benzylamine was similar to the R-labelled benzylamine but only 92% deuterium

was incorporated at the benzylic position. A signal for the diprotonated benzylamine (8%) was observed at 4.190 ppm.

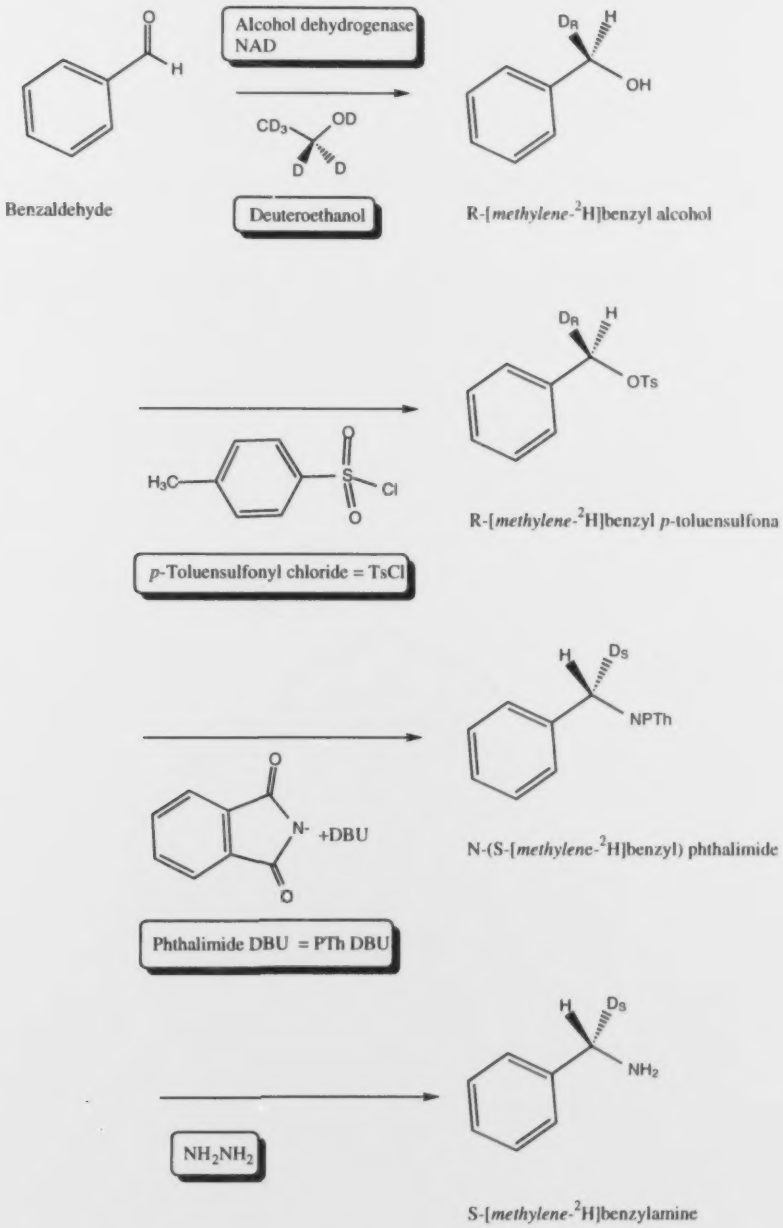

Scheme 2.1 Synthesis of S-[*methylene*-^{2}H]benzylamine.

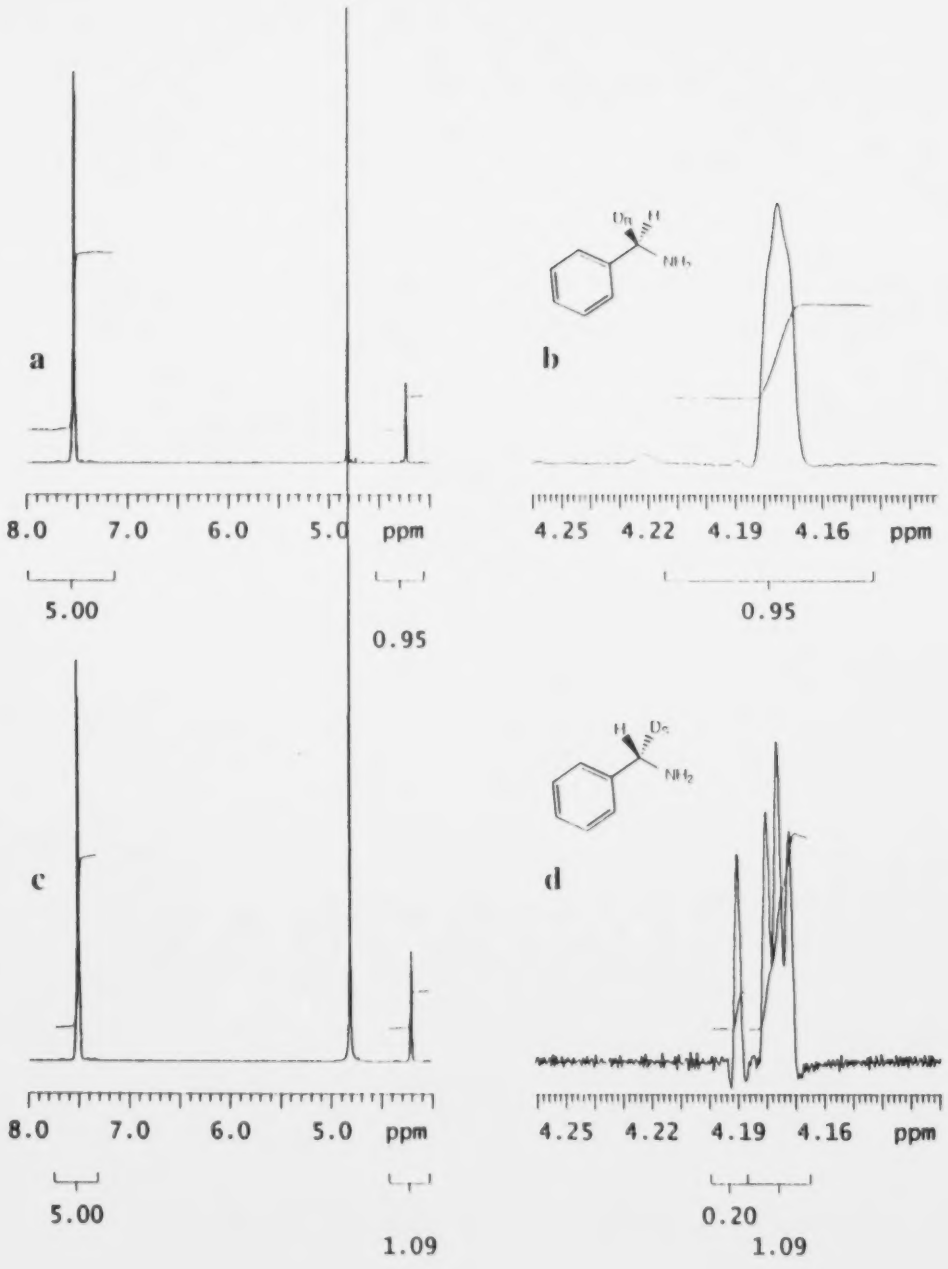

Figure 2.2 Partial 500 MHz ^{1}H NMR spectra of R-[*methylene*-^{2}H]benzylamine, (a) and (b). The spectra for S-[*methylene*-^{2}H]benzylamine is shown in (c) and (d). Panels (a) and (c) show the integration of aromatic protons *vs* benzylic protons. The large resonance at 4.81 ppm is residual HO^{2}H. Panels (b) and (d) are expansions of the spectra around the benzylic proton region.

Resolution enhancement shows a 1:1:1 triplet with a geminal deuterium-proton coupling constant of 2.02 Hz. It is possible that the lower deuterium incorporation for the S-enantiomer was due to a chemical exchange process prior to the ADH-mediated reduction, as has been suggested by others[12]. The lower incorporation of deuterium did not interfere with the subsequent stereochemical analysis. The enantiomeric purity of the R- and S-deuterated amines can be evaluated by use of chiral derivatization agents. Examples of such reagents are acetylmandelic acid[19], Mosher's reagent[20], and camphanic acid chloride[17,21,22]. By chiral derivatization enantiotopic protons can be made magnetically nonequivalent by transformation to the corresponding diastereotopomers. Direct integration of the diasterotopic resonances provides a precise estimate of the relative amounts of each isomer and hence of the original enantiomers. Camphanic acid chloride is a facile derivatization agent for primary amines and provides significant chemical shift nonequivalence to the diastereotopic protons of N-benzyl camphanamide.

Figure 2.3 A shows the partial ^{1}H NMR spectra of camphanic acid chloride derivatized benzylamine. The *pro*-S hydrogen of N-benzyl camphanamide resonates to a higher frequency (4.250 ppm) as compared to the *pro*-R hydrogen which is observed at 4.125 ppm[21,22]. Figure 2.3 B shows the partial spectrum for the R-labelled compound. A 0.05 ppm upfield shift (to lower frequency) is observed due to the *geminal* deuterium isotope effect. No S-deuterated material was observed. The spectrum of derivatized S-[*methylene*-^{2}H]-benzylamine is displayed in Figure 2.3 C and indicates 90% S-labelled, approximately 10% diprotonated, and no R-labelled material. The diprotonated material does not affect subsequent stereochemical analysis. The *geminal* deuterium isotope effect for this diastereomer provides an approximate 0.03 ppm upfield shift. Based on ^{1}H NMR spectroscopy the stereospecifically deuterated enantiomers of benzylamine possess a high degree of chiral purity.

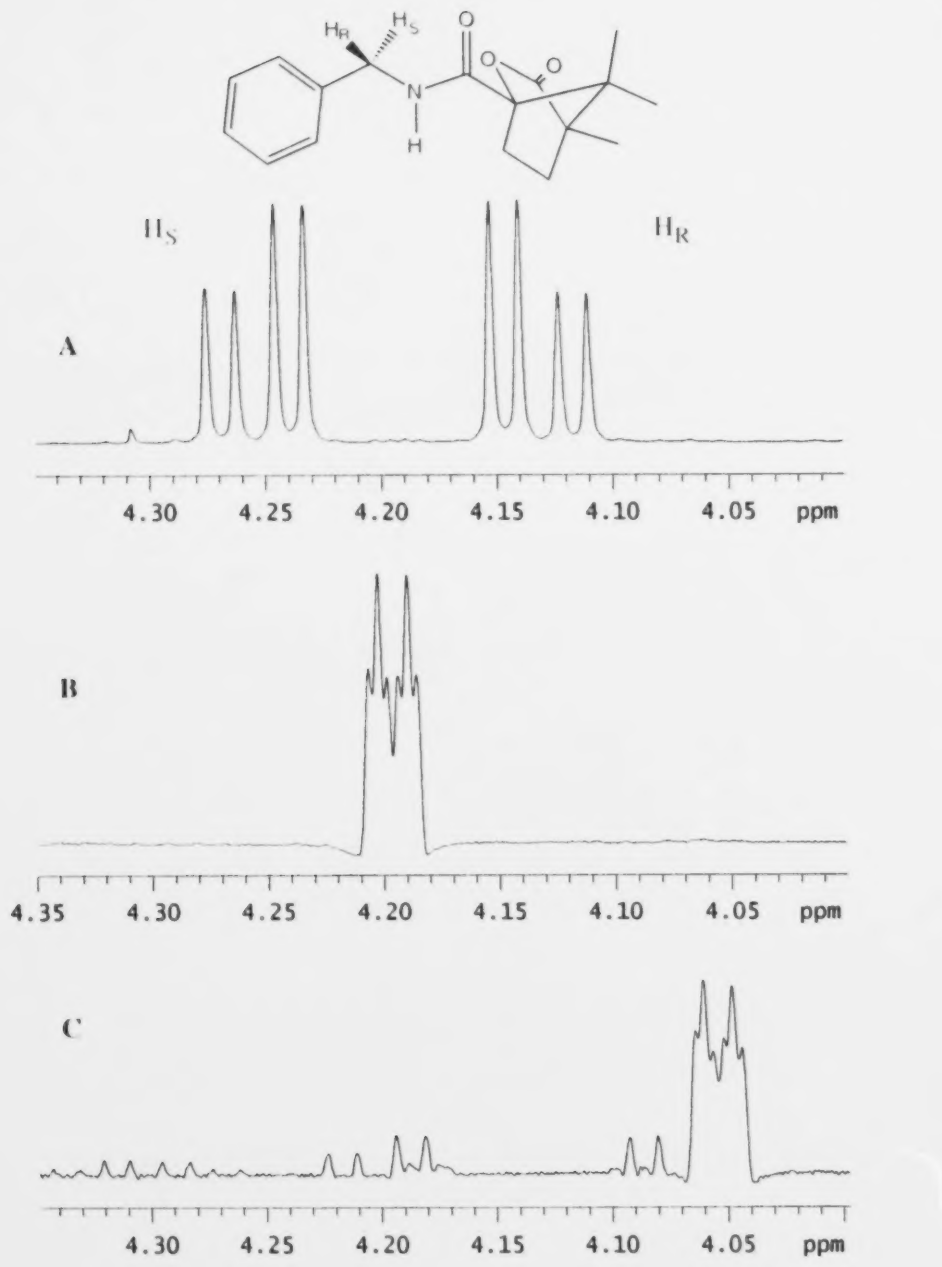

Figure 2.3 Partial 500 MHz ^{1}H NMR spectra of products from the camphanic acid chloride derivatization of benzylamine (A), R-[methylene-^{2}H]benzylamine (B), and S-[methylene-^{2}H]benzylamine (C). The deuterium-labelled benzylamines show a geminal deuterium isotope effect on the chemical shift of the methylene proton.

The stereochemical outcome for the enzymic oxidation of the chiral deuterium-labelled benzylamines can be determined by NMR spectroscopy to establish if label has been retained or lost in the product benzyl alcohols. Proton resonances as small as 1% (relative to the major compound observed) are easily detected. Thus, we conservatively estimate the quantitative error as ± 2%, and can observe greater than 98% loss or retention of deuterium in the product benzyl alcohols. Figure 2.4 A shows the ^{1}H NMR of the benzyl alcohols isolated from the ADH-coupled incubation of S-[*methylene*-^{2}H]benzylamine with the pea seedling amine oxidase. The left panel displays the aromatic region which is identical to a commercial sample of benzyl alcohol (spectra not shown). The large singlet resonance at 7.192 ppm is residual $CHCl_3$ from the NMR solvent. The centre panel depicts a broad resonance at 4.628 ppm which integrates to 2.12 protons *vs.* the aromatic region and is thus attributed to two benzylic protons. A small resonance (≤ 0.01 protons) at approximately 4.61 ppm is observed, but detailed expansions indicate that it is probably not deuterated material.

The right panel of Figure 2.4 A presents the resolution enhanced signal for the benzylic protons. The spin-spin coupling constant of 0.9 Hz results from *vicinal* deuterium coupling through the alcohol oxygen atom. The alcohol oxygen has a deuteron attached to it due to the work-up conditions for the benzyl alcohol which include $^{2}H_2O$ as a wash solvent for the C18 Sep-Paks. The pea seedling amine oxidase coupled incubation produced diprotonated benzyl alcohol and therefore demonstrates ≥ 98% loss of deuterium during the enzymic oxidation of S-[*methylene*-^{2}H]benzylamine. The small amount of diprotonated benzylamine in the original S-labelled material becomes diprotonated benzyl alcohol and, as such, does not affect the conclusions regarding enzyme stereochemistry.

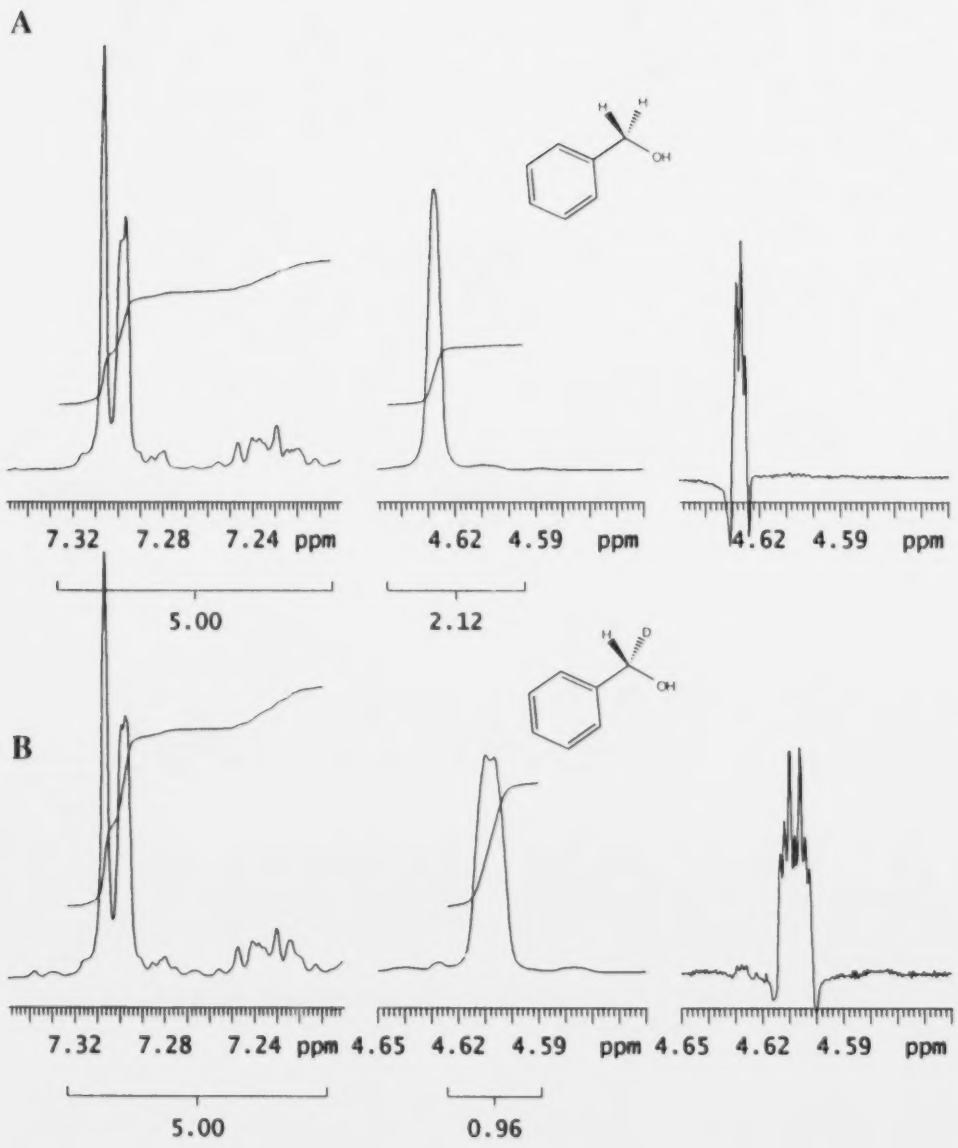

Figure 2.4 Partial 500 MHz ^{1}H NMR spectra of benzyl alcohols derived from coupled incubations of pea seedling amine oxidase with S-[*methylene*-^{2}H]benzylamine (A), and R-[*methylene*-^{2}H]benzylamine (B).

Similarly, the isolated benzyl alcohols from coupled incubations of S-[*methylene*-^{2}H]benzylamine with the other amine oxidases yield ^{1}H NMR spectra similar to the pea seedling incubation product NMR spectrum (Appendix II). Therefore, it can be concluded that all six amine oxidases studied completely (≥ 98%) remove deuterium from S-deuterated benzylamine consistent with stereospecific *pro*-S proton abstraction. The overall reaction stereochemistry for the oxidative deamination of S-[*methylene*-^{2}H]benzylamine is depicted in Figure 2.5 A. Figure 2.4 B shows the ^{1}H NMR of the product isolated from the incubation of R-[*methylene*-^{2}H]benzylamine with the pea seedling amine oxidase. The centre panel depicts a broad resonance at 4.608 ppm which integrates to 0.96 protons *vs.* the aromatics and is thus attributed to a single benzylic proton. A small resonance is observed at 4.628 ppm which represents approximately 1.5% diprotonated benzyl alcohol. This is derived from the diprotonated benzylamine impurity in the original R-labelled material. The right panel of Figure 2.4 B shows the resolution enhanced signal for the benzylic proton. The spin-spin coupling pattern results from *geminal* and *vicinal* deuterium-proton coupling with coupling constants of 1.8 Hz and 0.9 Hz respectively.

Broadband ^{2}H-decoupling results in the collapse of this heptaplet to a singlet (data not shown). The broadband ^{1}H-decoupled ^{2}H NMR spectrum shows a 1:1:1 triplet (data not shown) attributed to *vicinal* deuterium-deuterium coupling. Based on the NMR analysis it is clear that the pea seedling amine oxidase coupled incubation produced monodeuterated benzyl alcohol and therefore demonstrates complete (≥ 98%) retention of deuterium during the enzymic oxidation of R-[*methylene*-^{2}H]benzylamine.

Isolated benzyl alcohols from coupled incubations of R-[*methylene*-^{2}H]benzylamine with the other amine oxidases yielded ^{1}H NMR spectra similar to the pea seedling incubation product NMR (Appendix II). Therefore, it can be

concluded that all six amine oxidases studied do not remove deuterium from the R-deuterated amine consistent with the overall reaction stereochemistry as depicted in Figure 2.5 B. This is the expected result for enzymes which remove only the *pro*-S hydrogen.

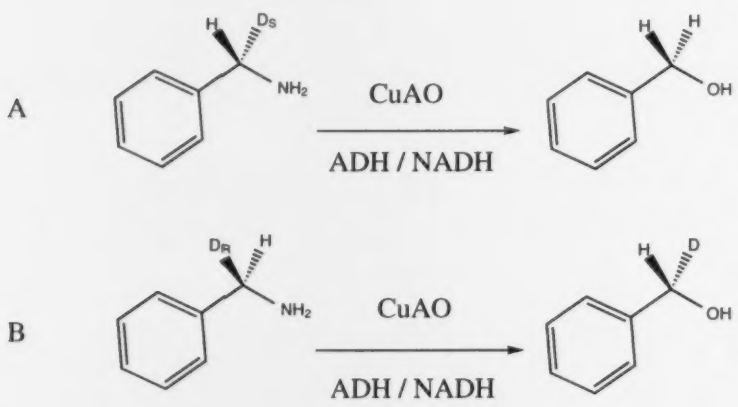

Figure 2.5 Overall reaction for S-[*methylene*-^{2}H]benzylamine producing diprotonated benzyl alcohol (A), and R-[*methylene*-^{2}H]benzylamine producing monodeuterated benzyl alcohol (B). Monodeuterated S-[*methylene*-^{2}H]benzyl alcohol is formed in (B) due to the stereospecific transfer of hydrogen to the Re face of [*formyl*-^{2}H]benzaldehyde by alcohol dehydrogenase.

For all six of the amine oxidases studied the *pro*-S hydrogen of benzylamine is stereospecifically removed during the enzymic oxidation. With the exception of the pea seedling enzyme, which exhibits *pro*-S stereospecificity for C-1 hydrogen removal for all substrates studied, the specificity for benzylamine oxidation contrasts with the stereochemical course of oxidation of tyramine and dopamine[9]. For example, the bovine, sheep, and rabbit enzymes catalyze net nonstereospecific removal of hydrogen from C-1 of either dopamine or tyramine[9]. The porcine[8] and horse[10] plasma amine oxidases abstract the *pro*-R hydrogen from C-1 of tyramine

and the porcine enzyme exhibits the same specificity for dopamine oxidation as well.

Previous stereochemical studies on bovine plasma amine oxidase have suggested that *pro*-S hydrogen abstraction from C-1 of substrates is favored. Dopamine oxidation catalyzed by the bovine enzyme is nonstereospecific due to the existence of alternate binding modes for this substrate[11]. However, a larger steady state kinetic isotope effect on k_{cat}/K_m for 1S-^{2}H-dopamine suggests that dopamine bound in the *pro*-S abstraction mode is preferentially positioned for subsequent hydrolysis[12]. Further support that the *pro*-S mode of proton abstraction is favored for the bovine enzyme comes from the studies on *p*-hydroxybenzylamine and 3-methylbutylamine for which substrate oxidation proceeds with *pro*-S hydrogen abstraction[24, 25]. Our results for the six amine oxidases studied, which demonstrate *pro*-S proton abstraction from benzylamine, further extend the idea that *pro*-S specificity for proton abstraction is favored for the topaquinone amine oxidases.

Model building exercises portraying substrate-cofactor bound in a catalytically competent manner might provide further insight concerning the geometric constraints of the active site of copper amine oxidases. Figures 2.6-2.8 were generated with the commercial software package Chem3D Plus (Cambridge Scientific Computing). The topaquinone adducts displayed in Figures 2.6-2.8 are shown as a neutral species only for clarity of presentation. The most probable structure from a mechanistic viewpoint is the zwitterionic species with the C4 oxyanion and the C5 iminium cation[4]. In Figures 2.7 and 2.8 the adducts are shown without the tyramine phenolic OH group for clarity.

Figure 2.6 A is a top view of a partial structure for the benzylamine-topaquinone adduct displayed in a planar conformation. Figure 2.6 B shows a side view and clearly demonstrates that the *pro*-S hydrogen is below the plane of the adduct whereas the *pro*-R hydrogen is situated above the molecule. The C1-H

sigma bond of the *pro*-S hydrogen is presumed to be labilized when it becomes perpendicular to the π electron system of the topaquinone ring. Therefore, if a single active site base is responsible for *pro*-S hydrogen abstraction then, according to the structure as depicted, it must be located below the plane of the molecule in order to allow for correct orbital overlap to occur. There is both stereochemical evidence and kinetic data which suggest a single catalytically important base for amine oxidation[11, 26].

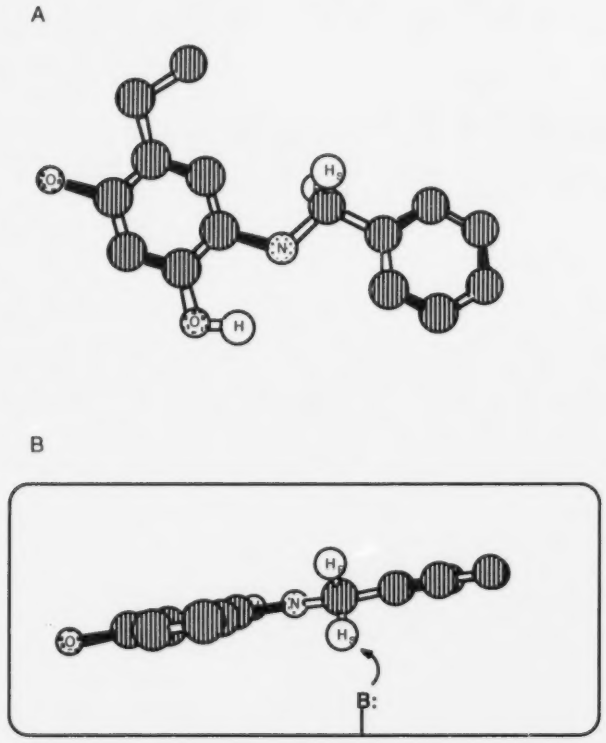

Figure 2.6. Side view (A) and a top view (B) of the partial structure of a topaquinone-benzylamine adduct. The relative orientation between views is 105 degrees. A potential active site base is depicted with a bold type **B:**. The *pro*-S hydrogen of benzylamine is positioned for abstraction by the active site base.

Figure 2.7 A and 2.7 B show the top and side view, respectively, of the tyramine-topaquinone adduct with the C1 *pro*-S hydrogen positioned below the plane of the molecule. This structure is very similar to that of benzylamine and provides a potential picture of the active site alignment of tyramine in the amine oxidases which are C1 *pro*-S specific.

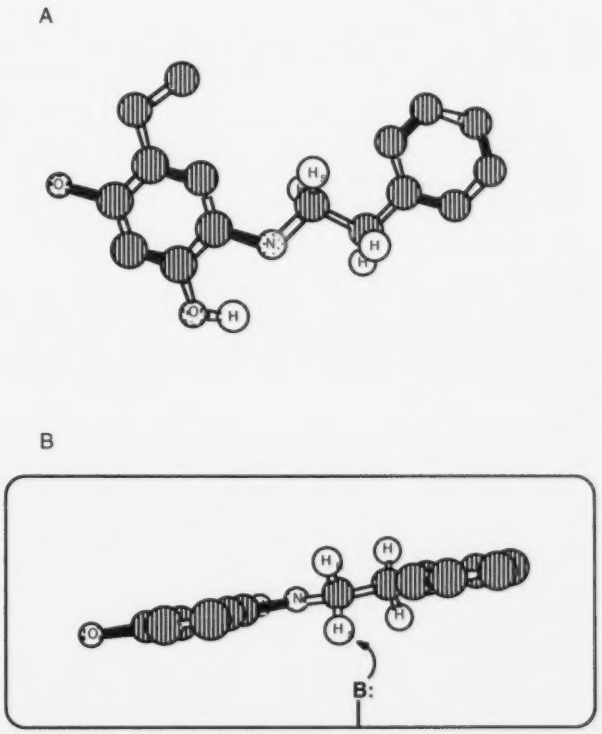

Figure 2.7. Side view (A) and a top view (B) of the partial structure of a topaquinone-tyramine adduct. The relative orientation between views is 105 degrees. The *pro*-S hydrogen of tyramine is positioned for abstraction by the active site base. The phenolic OH moiety of tyramine has been omitted for clarity.

One consequence of the alignment of tyramine and benzylamine as shown in Figures 2.6 B and 2.7 B is that a hydrophobic cavity must exist that is co-planar to the aromatic ring of tyramine and benzylamine. A detailed series of structure-function studies by Hartmann *et al* indicated that a hydrophobic pocket is present at

the active site of the bovine amine oxidase[4]. This allows for docking of benzylamine or tyramine at the active site with correct positioning of the *pro*-S hydrogen for abstraction. If the relative orientation of the topaquinone ring system and the active site base are preserved in enzymes which are C1 *pro*-R stereospecific for tyramine, then a molecular reorganization of tyramine must occur to reposition the *pro*-R hydrogen. Figure 2.7 B again shows the fully planar conformation of tyramine bound at the active site, a 120^{o} single bond rotation around the C1 carbon-nitrogen sigma bond while holding the topaquinone ring system fixed in space results in the tyramine conformer shown in Figure 2.8 A. The C1 *pro*-R hydrogen is now correctly positioned relative to the active site base for hydrogen abstraction. However, the aromatic ring of tyramine is now in an orientation very different than the one depicted in Figure 2.7 B. Since the enzymes which are *pro*-R stereospecific for C1 hydrogen abstraction from tyramine are still *pro*-S specific for benzylamine, it is reasonable to assume a similar hydrophobic docking site for the aromatic rings of these substrates. Therefore a 90^{o} single bond rotation around the C2 carbon-aryl carbon bond results in a conformer that does have the required co-planarity as shown in Figure 2.8 B. Figures 2.6-2.8 provide a potential model to account for both *pro*-R and *pro*-S hydrogen abstraction *via* a single active site base mechanism. Enzymes exhibiting net nonstereospecific hydrogen abstraction might have active sites that allow sufficient reorganization of substrate such that both modes are expressed. Thus a single active site base can account for all observed modes of hydrogen abstraction.

If two bases are located at the active site, one above and one below the plane of the substrate-cofactor adduct then this might explain the results for the enzymes which exhibit net nonstereospecificity for C1 hydrogen abstraction from tyramine. However, the absolute *pro*-S stereospecificity for benzylamine cannot be reconciled with a two base mechanism. Although a single active site base would seem more

probable, crystallographic analyses are required to answer definitively questions about the active site geometry of this class of enzymes.

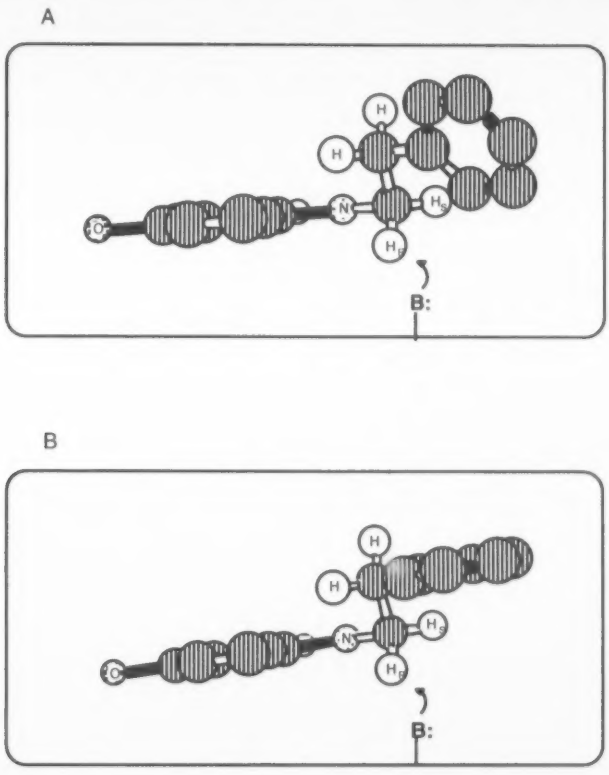

Figure 2.8. Top view of the partial structure of a topaquinone-tyramine adduct drawn in a conformation that presents the *pro*-R hydrogen for abstraction (A). Top view with the anticipated reorientation of the tyramine aromatic ring to accommodate interaction with the putative active site hydrophobic pocket (B). The phenolic OH moiety of tyramine has been omitted for clarity.

The EC 1.4.3.6 enzyme class of copper amine oxidases displays a uniquely variable stereochemistry for tyramine and dopamine oxidation yet is uniform with regard to benzylamine oxidation. Configurational characterization of products derived from chiral substrate incubations has furnished information which allows hypotheses to be formulated concerning the active site geometry of the copper

amine oxidases. Further delineation of stereochemical preferences *via* kinetic evaluation of isotope-labelled substrate oxidations can provide a yet more detailed representation of the active site.

References

1. Mondovi, B. (1985) *Structure and Function of Amine Oxidases*, CRC Press, Boca Raton, FL.

2. Janes, S.M., Mu, D., Wemmer, D., Smith, A.J., Kaur, S., Maltby, D., Burlingame, A.L. and Klinman, J.P. (1990) *Science*, **248**, 981-987.

3. Janes, S.M., Palcic, M.M., Scaman, C.H., Smith, A.J., Brown, D.E., Dooley, D.M., Mure, M. and Klinman, J P. (1992) *Biochemistry*, **31,** 12147-12154.

4. Hartmann, C. and Klinman, J.P. (1991) *Biochemistry*, **30,** 4605-4611.

5. Turowski, P.N., McGuirl, M.A. and Dooley, D.M. (1993) *J. Biol. Chem.*, **268,** 17680-17682.

6. Battersby, A.R., Staunton, J., Klinman, J. and Summers, M.C. (1979) *FEBS Lett.*, **99,** 297-298.

7. Battersby, A.R., Staunton, J. and Summers, M.C. (1976) *J. Chem. Soc. Perkin,* **1,** 1052-1056.

8. Coleman, A.A., Hindsgaul, O. and Palcic, M.M. (1989) *J. Biol. Chem.*, **264,** 19500-19505.

9. Coleman, A.A., Scaman, C.H., Kang, Y.J. and Palcic, M.M. (1991) *J. Biol. Chem.*, **266,** 6795-6800.

10. Palcic, M.M., Scaman, C.H. and Alton, G. (1995) *Progress in Brain Research*, **106**, in press.

11. Summers, M.C., Markovic, R. and Klinman, J. P. (1979) *Biochemistry*, **18,** 1969-1979.

12. Farnum, M. F., and Klinman, J. P. (1986) *Biochemistry*, **25,** 6028-6036.

13. Tabor, C.W., Tabor, H. and Rosenthal, S.M. (1954) *J. Biol. Chem.*, **208,** 645-661.

14. Bradford, M.M. (1976) *Anal. Biochem.*, **72,** 248-254.

15 Schallinger, L.E. (1980) *Diss. Abstr. Int. B*, **41,** 176-177.

16. Battersby, A.R., Staunton, J. and Wiltshire, H.R. (1975) *J. Chem. Soc. Perkin*, **1,** 1156-1161.

17. No, Z., Sanders, C.R., Dowhan, W. and Tsai, M.-D. (1988) *Biorg. Chem.*, **16,** 184-188.

18. Walsh, C. (1979) *Enzymatic Reaction Mechanisms*, W. H. Freeman and Company, San Francisco.

19. Whitesell, J.K. and Reynolds, D. (1983) *J. Org. Chem.*, **48,** 3548-3551.

20. Dale, J.A., Dull, D.L. and Mosher, J.S. (1969) *J. Org. Chem.*, **34,** 2543-2549.

21. Gerlach, H. and Zagalak, B. (1973) *J. Chem. Soc., Chem. Commun.*, 274-275.

22. Parker, D. (1983) *J. Chem. Soc. Perkin Trans. II*, 83-88.

23. Gani, D., Wallis, O.C. and Young D.W. (1983) *Eur. J. Biochem.*, **136,** 303-311.

24. Suva, R. H. and Abeles, R. H. (1978) *Biochemistry*, **17,** 3538-3545.

25. Shibuya, M., Chou, H.-M., Fountoulakis, M., Hassam, S., Kim, S.-U., Kobayashi, K., Otsuka, H., Rogalska, E., Cassady, J.M. and Floss, H.G. (1990) *J. Am. Chem. Soc.*, **112,** 297-304.

26. Farnum, M., Palcic, M. and Klinman, J.P. (1986) *Biochemistry*, **25**, 1898-1904.

Chapter Three

Stereochemistry of Bacterial Copper Amine Oxidase Reactions[I,II]

3.1 Introduction

Enzymes are stereospecific and a knowledge of enzyme stereochemistry can provide insight concerning reaction mechanisms[1]. The copper amine oxidases [EC 1.4.3.6] oxidatively deaminate primary amines with atypical stereochemistry[2,3]. Contrary to virtually all other classes of enzymes, there is little stereochemical uniformity amongst the copper amine oxidases (CuAO)[4]. CuAO enzymes display substrate- and source-dependent stereochemistry[3].

The soluble CuAO enzymes isolated from pea seedling, soybean seedling, chick pea seedling, and pig kidney have been shown to be *pro*-S specific for C1 hydrogen abstraction from tyramine[4,5]. Tissue-bound semicarbazide-sensitive amine oxidases (SSAO) from rat, pig and bovine aorta are also *pro*-S specific for C1 hydrogen abstraction from tyramine[6,7]. The CuAO enzymes from porcine and horse plasma are *pro*-R specific for C1 of tyramine or dopamine[4,8]. Amine oxidase enzymes that catalyze net nonstereospecific C1 hydrogen abstraction have been characterized from the plasma of bovine, sheep, and rabbit[4,9].

In contrast to tyramine C1 stereochemistry (Figure 3.1), the oxidative deamination of benzylamine (Figure 3.2 A) occurs with stereospecific removal of the *pro*-S hydrogen for all enzymes studied[3,8,10,11]. Also, the bovine enzyme has

---

I A version of this chapter is to be submitted to Archives of Biochemistry and Biophysics. Authors: Gordon Alton, Ayse Hacisalihoglu, Johannis A. Duine, K. Tanizawa and Monica M. Palcic.

II Additionally, the *E. coli* stereochemical results will be included in a crystal structure publication with Knowles and coworkers (Leeds, U.K.), concerning the position of the active site base relative to a covalently-bound inhibitor.

been shown to be *pro*-S specific for *p*-hydroxybenzylamine and 3-methylbutylamine[12,13].

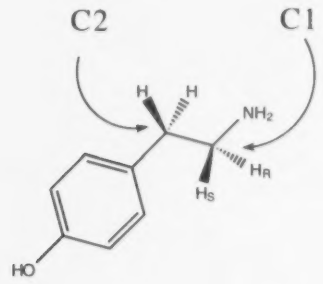

Figure 3.1 Stereochemical and configurational nomenclature for tyramine. The *pro*-R hydrogen of is behind the plane of the molecule (aromatic ring is coplanar with the paper) and the *pro*-S hydrogen is in front. The carbon covalently bonded to the amine is labelled C1 and the carbon one bond further away is labelled C2.

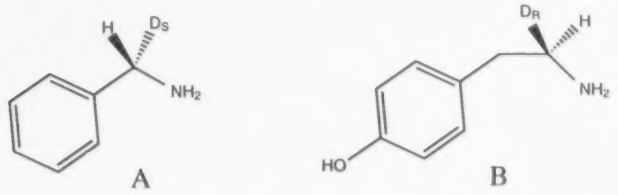

Figure 3.2 Molecular structure of S-[*methylene*-^{2}H]benzylamine (A) and [1(R)-^{2}H]tyramine (B).

A reversible imine-enamine tautomerization preceding imine hydrolysis has been demonstrated in many amine oxidases which allows exchange of C2 hydrogens from tyramine or dopamine into bulk solvent (Scheme 3.1)[14]. Furthermore, the stereochemistry of C1 hydrogen abstraction from tyramine (Figure 3.2 B) or dopamine is correlated with the hydrogen exchange reactions at C2 of these substrates[8,9]. The soluble CuAO enzymes that are *pro*-S specific do not catalyze hydrogen exchange at C2, whereas *pro*-R and net nonstereospecific

CuAOs do catalyze C2 exchange[4,14]. The tissue-bound SSAO enzymes, which are *pro*-S specific for all substrates, also catalyze hydrogen exchange at C2[7]. In this regard, the SSAO enzymes are similar to lysyl oxidase [EC 1.4.3.13][15].

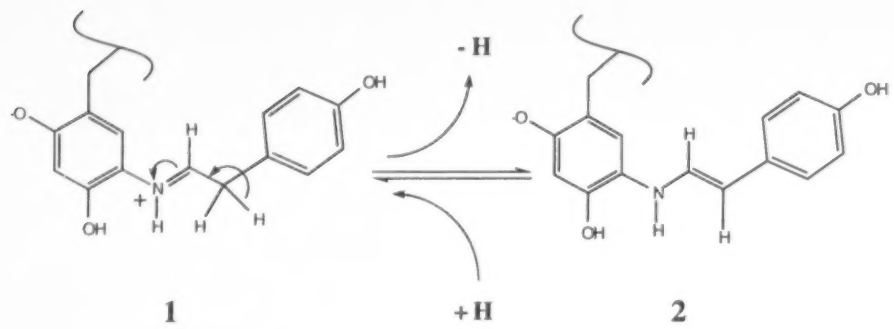

Scheme 3.1 Reversible tautomerization of the tyramine-TPQ pre-hydrolysis complex. Loss of hydrogen from imine (1) yields the enamine (2). Reprotonation of enamine can occur from bulk solvent.

We have used ^{1}H NMR spectroscopy to determine the stereochemical course for the oxidative deamination of benzylamine and tyramine by four bacterial topaquinone-containing CuAOs. Two enzymes were obtained from the gram negative bacteria, *Escherichia coli* and *Klebsiella oxytoca*, and two enzymes were from the Coryneform gram positive bacterium, *Arthrobacter globiformis*.

All four enzymes studied are stereospecific with the reaction occurring with removal of the *pro*-S hydrogen from all substrates. In addition, no tyramine C2 hydrogen exchange was observed for any of these enzymes.

3.2 Experimental Procedures

Materials-Chemicals were of ACS reagent grade and were used without further purification. Distilled water was further purified with a Milli-Q system. C18

Sep-Pak cartridges were from Waters. Deuterated NMR solvents were from Cambridge Isotope Laboratories and 2-(4-hydroxyphenyl)ethyl-2,2-d_2-amine (C2 dideuterated tyramine) hydrochloride was from MSD Isotopes. NADH and 4-hydroxyphenethylamine were from Sigma.

Enzymes-Horse liver alcohol dehydrogenase (ADH) and catalase were obtained from Sigma. *E. coli* (ATCC 25256) amine oxidase was obtained from Professor P. Knowles (Leeds, U.K.)[16]. *K. oxytoca* (ATCC 43863) amine oxidase was a kind gift from A. Hacisalihoglu and Professor J.A. Duine (T.U. Delft, the Netherlands). *A. globiformis* (ATCC 8010) histamine oxidase and phenethylamine oxidase were from Professor K. Tanizawa (Osaka, Japan)[17]. Enzyme activity was measured at 25° C with 2 mM semicarbazide and 1 mM phenethylamine as a substrate in 100 mM sodium phosphate buffer, pH 6.8 by monitoring the production of phenylacetaldehyde semicarbazone at 230 nm[18]. One unit is defined as the quantity of enzyme that catalyzes the production of 1.0 µmol/min of phenylacetaldehyde semicarbazone based on an extinction coefficient of 16.0 mM^{-1} cm^{-1}. The relative rate of benzylamine oxidation was approximately 1% of the rate of phenethylamine oxidation, whereas tyramine and phenethylamine are oxidized at similar rates[19]. Protein concentrations were estimated by the Bradford method using a Bio-Rad kit with bovine serum albumin as a standard[20].

The enzymatic activity of the oxidases were: *E. coli*, 48 U/mL; *K. oxytoca*, 5U/mL; *A. globiformis* histamine oxidase, 150 U/mL; *A. globiformis* phenethylamine oxidase, 1000 U/mL.

R- and S-[methylene-^{2}H]benzylamine hydrochloride and [1(R)- and [1(S)-^{2}H]tyramine hydrochloride-These amines were available from previous work[3,7].

Benzylamine Oxidation by Amine Oxidases-Incubations were conducted in a coupled system containing 10.0 µmol of R- or S-[*methylene*-^{2}H]benzylamine hydrochloride, 13.1 µmol NADH, 1.3 U ADH, 37,000 U catalase in a total volume

of 1 mL with 100 mM sodium phosphate buffer, pH 6.8. Amine oxidase (5 U) was added to each incubation tube to initiate the reaction[3]. After a 48 h incubation at 25° C the reaction mixtures were diluted to 10 mL with saturated NaCl and loaded onto reverse-phase C18 Sep-Pak cartridges. Each cartridge was rinsed with 5 mL saturated NaCl, followed by 5 mL ^2H_2O, and then the benzyl alcohol product was eluted directly into 5 mm NMR tubes with 0.7 mL C^2HCl_3.

Tyramine Oxidation by Amine Oxidases-For analysis of C1 stereochemistry incubations were conducted in a coupled system containing 10.5 µmol of [1(R)- or [1(S)-^{2}H]tyramine hydrochloride, 13.1 µmol NADH, 4.0 U ADH, and 37,000 U catalase in a total volume of 1 mL with 100 mM sodium phosphate buffer, pH 6.8[4,10]. Amine oxidase (0.2 U) was added to each incubation tube to initiate the reaction. After a 48 h incubation at 25° C the reaction mixtures were diluted to 10 mL with saturated NaCl and the *p*-hydroxyphenethyl alcohols extracted into 10 mL ethyl acetate. The organic layer was taken to dryness and the resulting material was dissolved in 0.7 mL 4:1 $(^2H_3C)_2CO$:^2H_2O prior to ^{1}H NMR spectroscopy.

For C2 stereochemical analysis, incubations were conducted in a coupled system containing 0.5 U amine oxidase, 24.5 µmol of C2 dideuterated tyramine hydrochloride (or tyramine hydrochloride), 50.4 µmol NADH, 8.0 U ADH, and 28,000 U catalase in a total volume of 2 mL with 100 mM sodium phosphate buffer, pH 6.8 (or deuterated sodium phosphate buffer for the incubation containing tyramine hydrochloride). The *p*-hydroxyphenethyl alcohol extraction conditions were as described for the C1 stereochemical analysis above.

^{1}H NMR spectroscopy-^{1}H NMR spectra were recorded at 500 MHz on a Varian Unity 500 instrument at 30° C (benzyl alcohols) or 22° C (*p*-hydroxyphenethyl alcohols). Benzyl alcohols were dissolved in 0.7 mL of C^2HCl_3 and *p*-hydroxyphenethyl alcohols were dissolved in 0.7 mL of 4:1 $(^2H_3C)_2CO$:^2H_2O. NMR solvents were at least 99.9% deuterated. A T1 analysis

indicated that a 3 s acquisition time followed by a 2 s relaxation delay was appropriate for benzyl alcohols in C^2HCl_3 using a 60^o (5 μs) pulse width, whereas a 10 s relaxation delay for *p*-hydroxyphenethyl alcohols in 4:1 $(^2H_3C)_2CO$:^2H_2O was required. Chemical shifts for benzyl alcohols were referenced to internal TMS (0.000 ppm) and for *p*-hydroxyphenethyl alcohols, to residual acetone (2.190 ppm), and are precise to 0.001 ppm. Spin-spin coupling constants are reported as first-order and are precise to 0.2 Hz. Digital resolution was 0.17 Hz/point. Resolution enhancement of spectra for benzyl alcohols used a line broadening factor of -1.8 and a Gaussian factor of 0.7. The spectra of *p*-hydroxyphenethyl alcohols normally had a Gaussian factor of 0.5 and a squared Gaussian factor of 0.4 applied prior to Fourier transformation of the free induction decay.

3.3 Results and Discussion

The R-[*methylene*-^{2}H]benzylamine was shown previously to be enantiomerically pure and to contain 1.5% diprotonated benzylamine[3]. The S-[*methylene*-^{2}H]benzylamine was also enantiomerically pure but contained 8% diprotonated benzylamine[3]. The lower incorporation of deuterium does not interfere with the subsequent stereochemical analysis. Similarly, [1(R)- and [1(S)-^{2}H]tyramine were greater than 98% enantiomerically pure and contained less than 2% C1 diprotonated tyramine[7]. The C2 dideuterated tyramine was greater than 98% deuterated at C2.

The amine oxidases produce aldehydes from the amine substrates (Equation 1)[2].

$$RCH_2NH_2 + H_2O + O_2 \rightarrow RCHO + NH_3 + H_2O_2 \qquad (1)$$

Since undesirable Schiff's base formation might occur between the product aldehydes and the amines, the stereochemical studies were conducted in a coupled enzymatic fashion. The aldehydes were converted to alcohols by ADH in the presence of NADH (Scheme 3.2). The alcohols are inert and unreactive towards any of the components of the coupled incubations and are easily extracted from the solution. The use of ADH does not perturb the deuterium content of the aldehyde intermediate.

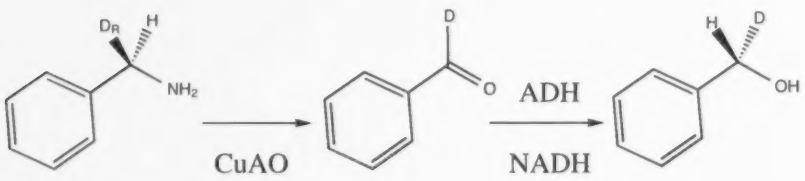

Scheme 3.2 *Pro*-S specific oxidative deamination of R-[*methylene*-^{2}H]benzylamine coupled to alcohol dehydrogenase (ADH).

The retention or loss of deuterium from deuterium-labelled benzylamine or tyramine during the coupled enzymatic oxidation is conveniently followed by ^{1}H NMR spectroscopy of the isolated alcohol products. In ^{1}H NMR, deuterium nuclei are not directly observable. Thus, a substitution of 1 mole of deuterium for 1 mole of hydrogen results in an NMR peak integration (proton inventory) that is "missing" 1 proton. A conservative estimate for the quantitative precision of integration is 0.05 protons for the reported spectra.

The magnitude of deuteron-proton coupling indicates whether the nuclei are *geminal* or *vicinal* to one another. *Geminal* spin-spin (scalar) coupling between protons and deuterons is readily observable, with a typical value of 2 Hz[3]. Additionally, when a carbon atom with two or more bound hydrogens has one of these substituted by a deuterium then an upfield shift is observed for the remaining

proton resonance(s). The deuterium isotope effect on proton chemical shifts is approximately 0.02 ppm[3]. Thus, chemical shift information, integration of proton resonances and detection of deuterium-proton scalar coupling provide sufficient information to follow the deuterium content of labelled amines during the course of the reaction.

Figure 3.3 A shows the ^{1}H NMR of the product isolated from the incubation of R-[*methylene*-^{2}H]benzylamine with the *A. globiformis* phenethylamine oxidase. The left panel displays the aromatic region that is identical to a commercial sample of benzyl alcohol dissolved in $C^{2}HCl_3$. Neither the resonance of the aromatic hydrogen, that is *para* relative to the benzylic carbon, nor its integration, are included in this figure. A resonance at 4.608 ppm that integrates to 1.05 protons *vs.* the aromatics is shown in the centre panel and is attributed to a single benzylic proton. A small resonance is observed at 4.628 ppm that represents approximately 1.5% diprotonated benzyl alcohol. This is derived from the diprotonated benzylamine impurity in the original R-labelled material. The right panel of Figure 3.3 A shows the resolution enhanced signal for the benzylic proton. The spin-spin coupling pattern results from *geminal* and *vicinal* deuterium-proton coupling with coupling constants of 1.8 Hz and 0.9 Hz, respectively.

The *A. globiformis* phenethylamine oxidase coupled incubation with R-[*methylene*-^{2}H]benzylamine produced monodeuterated benzyl alcohol. Isolated benzyl alcohols from coupled incubations of R-[*methylene*-^{2}H]benzylamine with the other bacterial amine oxidases yielded ^{1}H NMR spectra similar to the *A. globiformis* phenethylamine incubation product NMR (Appendix III). Therefore, it can be concluded that all bacterial amine oxidases studied do not remove deuterium from the R-deuterated amine since complete ($\geq$ 98%) retention is observed. This is consistent with the overall reaction stereochemistry as depicted in Figure 3.4 A and is the expected result for *pro*-S enzymes.

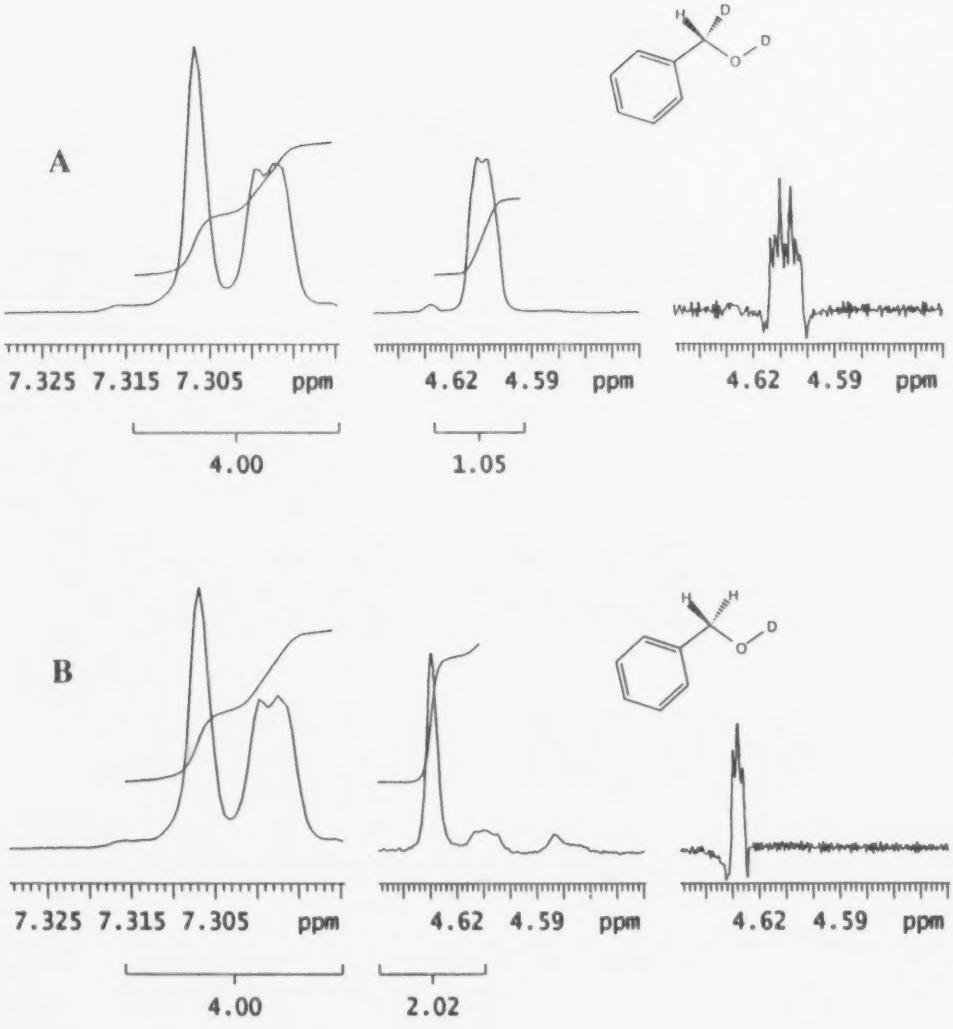

Figure 3.3 Partial 500 MHz ^{1}H NMR spectra of benzyl alcohols derived from coupled incubations of *A. globiformis* phenethylamine oxidase with R-[*methylene*-^{2}H]benzylamine (A) and S-[*methylene*-^{2}H]benzylamine (B).

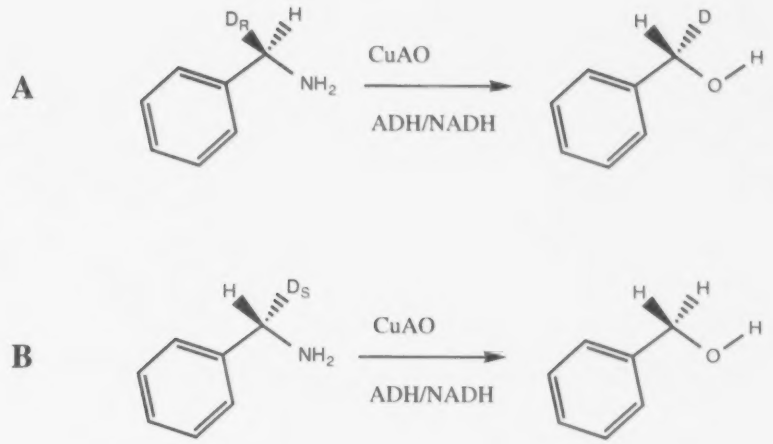

Figure 3.4 Overall reaction for R-[*methylene*-^{2}H]benzylamine producing monodeuterated benzyl alcohol (A), and S-[*methylene*-^{2}H]benzylamine producing diprotonated benzyl alcohol (B). Monodeuterated S-[*methylene*-^{2}H]benzyl alcohol is formed in (A) due to the stereospecific transfer of hydrogen to the *Re* face of [*formyl*-^{2}H]benzaldehyde by alcohol dehydrogenase.

Figure 3.3 B shows the ^{1}H NMR of the benzyl alcohols isolated from the ADH-coupled incubation of S-[*methylene*-^{2}H]benzylamine with the *A. globiformis* phenethylamine oxidase. The left panel displays the aromatic region that is identical to a commercial sample of benzyl alcohol dissolved in C^2HCl_3. Neither the resonance of the aromatic hydrogen, that is *para* relative to the benzylic carbon, is included in this figure, nor its integration. The centre panel depicts a resonance at 4.628 ppm that integrates to 2.02 protons *vs.* the aromatic region and is thus attributed to two benzylic protons. The right panel of Figure 3.3 B presents the resolution enhanced signal for the benzylic protons. The spin-spin coupling constant of 0.9 Hz results from *vicinal* deuterium coupling through the alcohol oxygen atom. The alcohol oxygen has a deuteron attached to it due to the extraction conditions for the benzyl alcohol that include ^2H_2O as a wash solvent for the C18 Sep-Paks. The *A. globiformis* phenethylamine oxidase coupled incubation

produced diprotonated benzyl alcohol and therefore demonstrates ≥ 98% loss of deuterium during the enzymic oxidation of S-[*methylene*-^{2}H]benzylamine.

Similarly, the isolated benzyl alcohols from coupled incubations of S-[*methylene*-^{2}H]benzylamine with the other three bacterial amine oxidases yield ^{1}H NMR spectra identical to the *A. globiformis* phenethylamine oxidase incubation product NMR spectrum (Appendix IV). Therefore, it can be concluded that all bacterial amine oxidases studied completely (≥ 98%) remove deuterium from S-deuterated benzylamine, consistent with stereospecific *pro*-S proton abstraction. The overall reaction stereochemistry for the oxidative deamination of S-[*methylene*-^{2}H]benzylamine is depicted in Figure 3.4 B. For all four bacterial amine oxidases studied the *pro*-S hydrogen of benzylamine is stereospecifically removed during the enzymic oxidation (Appendix III).

In contrast to the uniform stereochemistry of benzylamine oxidation the CuAOs display heterogeneity for C1 hydrogen abstraction from tyramine or dopamine[2,3]. Figure 3.5 A displays the partial 500 MHz ^{1}H NMR spectrum for [1(R)-^{2}H]tyramine. The C1 methylene region shows a triplet integrating to 1.01 protons at 3.27 ppm with a deuterium-proton scalar coupling of 1.65 Hz. Figure 3.5 C displays the corresponding spectrum of [1(S)-^{2}H]tyramine showing a triplet that integrates as 1.09 protons *vs.* the C2 protons. These spectra indicate that the deuterated tyramines are monodeuterated at the C1 methylene carbon.

Figure 3.5 B displays a spectrum of the *p*-hydroxyphenethyl alcohol isolated from the coupled incubation of *A. globiformis* phenethylamine oxidase with [1(R)-^{2}H]tyramine. The C2 protons of the product alcohol are observed as a doublet at 2.78 ppm. The C1 proton(s) are observed as a triplet at 3.72 ppm that integrates as 0.91 protons. A deuterium-proton *geminal* coupling constant of 1.38 Hz can be discerned in resolution enhanced spectra. Within experimental error these results show no loss of deuterium from [1(R)-^{2}H]tyramine during the reaction.

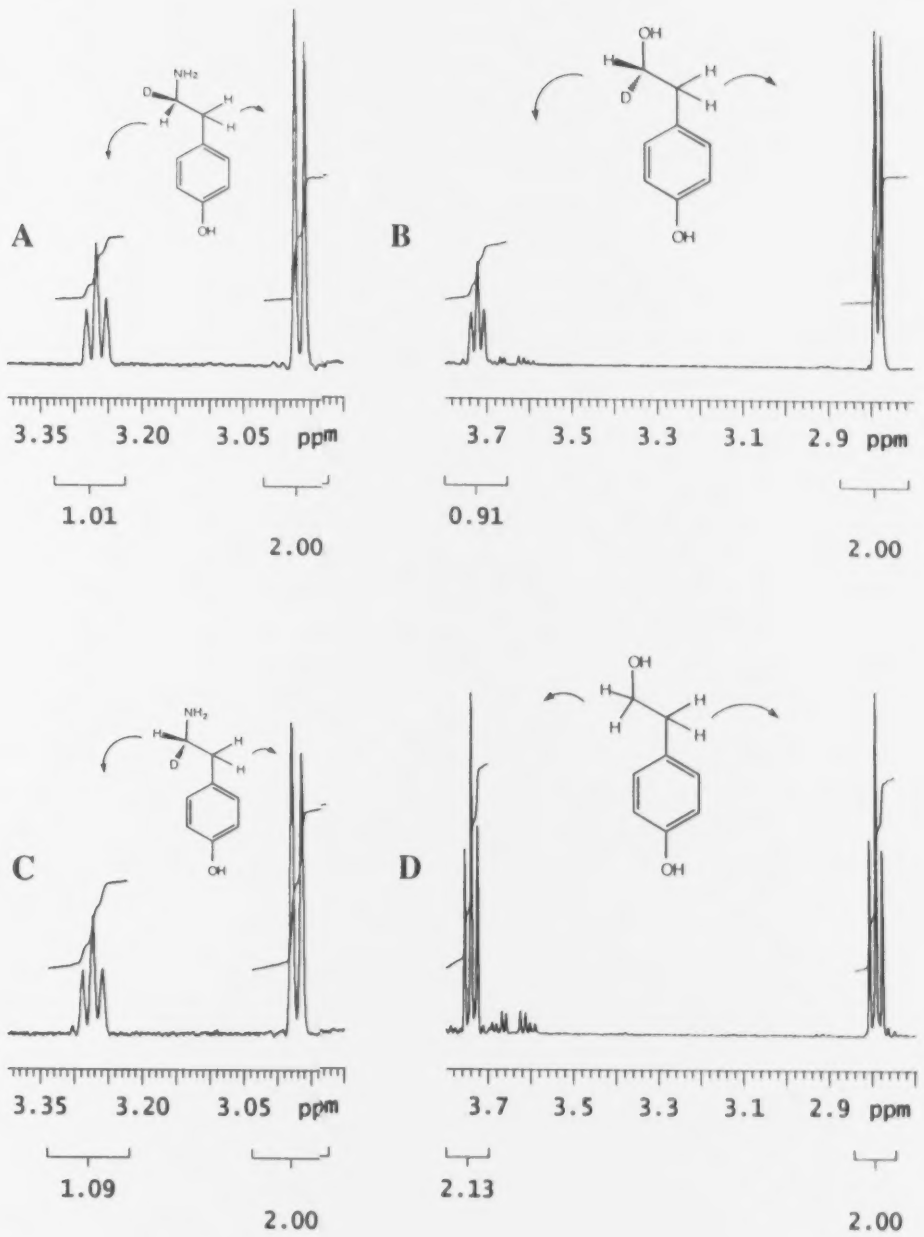

Figure 3.5 Partial 500 MHz ^{1}H NMR spectra of [1(R)-^{2}H]tyramine (A) and [1(S)-^{2}H]tyramine (C). Spectra of the *p*-hydroxyphenethyl alcohols derived from coupled incubations of the deuterated amines with *A. globiformis* phenethylamine oxidase, (B) and (D).

Figure 3.5 D displays the spectrum of the *p*-hydroxyphenethyl alcohol isolated from the coupled incubation of *A. globiformis* phenethylamine oxidase with [1(S)-^{2}H]tyramine. In this instance, triplets are observed for both the C1 and C2 protons. Integration of the C1 triplet at 3.74 ppm indicates 2.13 protons. Both the integration and the scalar coupling pattern indicate that the isolated *p*-hydroxyphenethyl alcohol is fully protonated. Thus, during the enzymic reaction of [1(S)-^{2}H]tyramine the deuterium was fully removed. These results, taken together, indicate that the *A. globiformis* phenethylamine oxidase displayed only *pro*-S stereochemistry during the oxidative deamination of tyramine. Appendix V shows the spectra for the *E. coli*, *A. globiformis* histamine oxidase and *K. oxytoca* enzymes. These spectra show that the bacterial enzymes are also *pro*-S specific for hydrogen abstraction from C1 of tyramine.

There is a correlation between C1 stereochemistry and C2 hydrogen exchange reactions[8,9]. Soluble CuAO enzymes that are *pro*-S specific for hydrogen abstraction at C1 do not catalyze hydrogen exchange at C2 of product. To investigate the loss or retention of hydrogen from C2, duplicate coupled incubations were set up. One incubation was performed in protiated buffer containing C2 dideuterated tyramine and the other in deuterated buffer with fully protonated tyramine. Figure 3.6 A shows the partial 500 MHz ^{1}H NMR spectrum for [2,2-^{2}H]tyramine and shows approximately 98% deuteration at C2. Figure 3.6 C shows the spectrum of tyramine. The ^{1}H NMR spectrum of the product *p*-hydroxyphenethyl alcohol derived from dideuterated tyramine and *A. globiformis* phenethylamine oxidase (in protiated buffer) is shown in Figure 3.6 B. A very small increase of 0.04 protons at C2 is observed. Since this is smaller than the estimated error for integration it can be concluded that there was no significant "wash-out" of deuterium during the course of the enzymic reaction. Similarly the other bacterial enzymes displayed no wash-out (Appendix VI).

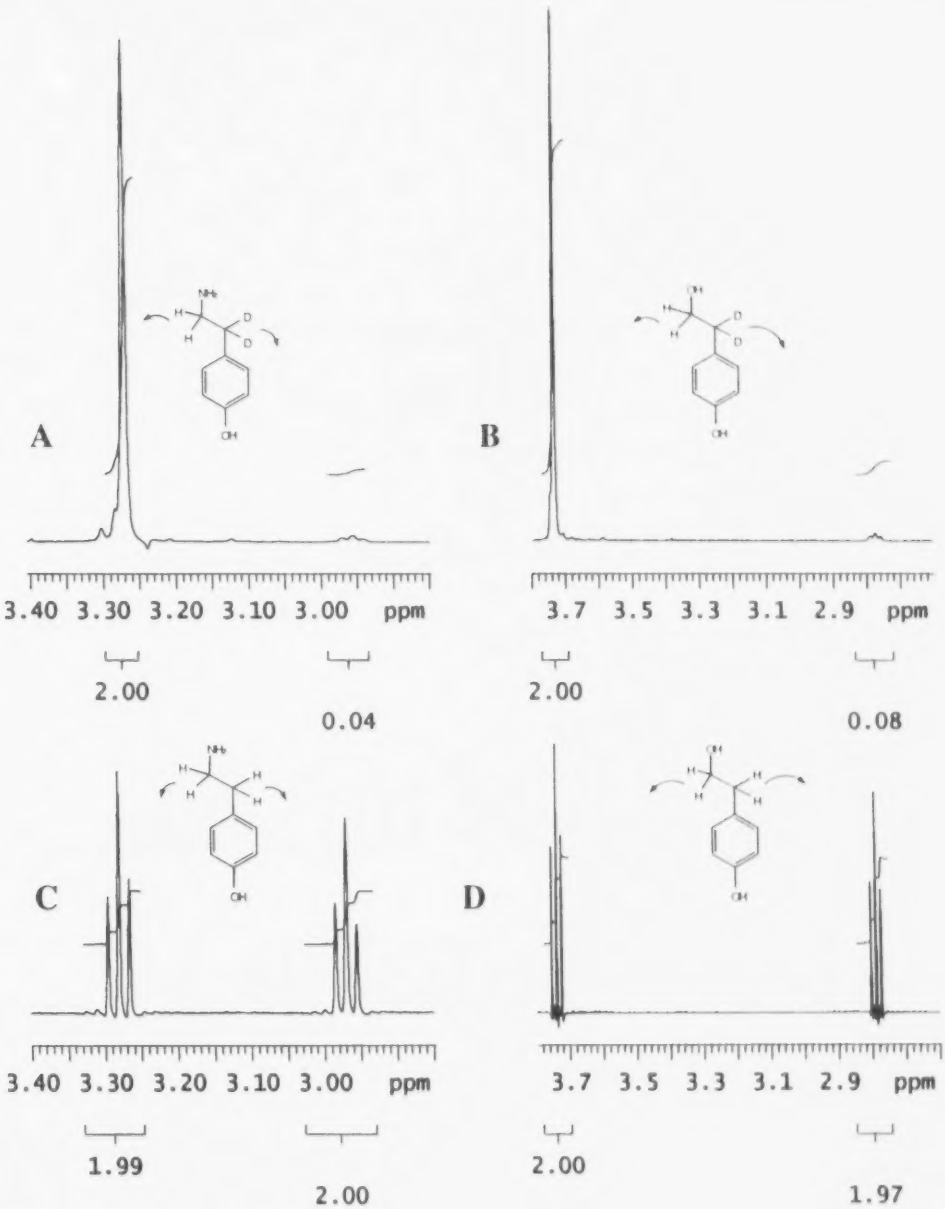

Figure 3.6 Partial 500 MHz ^{1}H NMR spectra of [2,2-^{2}H]tyramine (A) and tyramine (C). Spectra of the *p*-hydroxyphenethyl alcohols derived from coupled incubations of the amines with *A. globiformis* phenethylamine oxidase, (B) and (D).

Figure 3.6 D demonstrates that the oxidative deamination of tyramine in deuterated buffer by *A. globiformis* phenethylamine oxidase resulted in complete retention of hydrogen and no wash-in of deuterium from the deuterated buffer. Again, a small but insignificant decrease of 0.03 protons is observed at C2 of the product *p*-hydroxyphenethyl alcohol. The other bacterial enzymes studied also displayed similar spectra (Appendix VI) indicating no wash-in. Thus, all bacterial enzymes studied do not exchange C2 hydrogens with solvent. This conforms to the results for all other known soluble CuAO enzymes that are C1 *pro*-S specific.

Our results for the four bacterial amine oxidases studied demonstrate *pro*-S hydrogen abstraction from benzylamine and tyramine and no hydrogen exchange at C2 of tyramine. Thus, the bacterial enzymes join a growing list of *pro*-S specific soluble copper amine oxidases that includes pea, chick pea and soybean seedling amine oxidases and pig kidney diamine oxidase.

References

1. Fersht, A. (1985) *Enzyme Structure and Mechanism* p. 221, W.H. Freeman and Company, New York, NY.

2. Mondovi, B. (1985) *Structure and Functions of Amine Oxidases*, CRC Press, Boca Raton, FL.

3. Alton, G., Taher, T.H., Beever, R.J. and Palcic, M.M. (1995) *Arch. Biochem. Biophys.*, **316**, 353-361.

4. Coleman, A.A., Scaman, C.H., Kang, Y.J. and Palcic, M.M. (1991) *J. Biol. Chem.*, **266**, 6795-6800.

5. Coleman, A.A., Hindsgaul O. and Palcic, M.M. (1989) *J. Biol. Chem.*, **264**, 19500-19505.

6. Yu, P.H. (1988) *Biochem. Cell. Biol.*, **66**, 853-861.

7. Scaman, C.H. and Palcic, M.M. (1992) *Biochemistry*, **31**, 6829-6841.

8. Palcic, M.M., Scaman, C.H. and Alton, G. (1995) *Progress in Brain Research*, **106**, in press.

9. Farnum, M.F. and Klinman, J.P. (1986) *Biochemistry*, **25**, 6028-6036.

10. Battersby, A. R., Staunton, J., Klinman, J.P. and Summers, M. C. (1979) *FEBS Lett.*, **99,** 297-298.

11. Battersby, A. R., Staunton, J. and Summers, M. C. (1976) *J. Chem. Soc. Perkin,* **1,** 1052-1056.

12. Suva, R.H. and Abeles, R.H. (1978) *Biochemistry*, **17**, 3538-3545.

13. Shibuya, M., Chou, H.-M., Fountoulakis, N., Hassam, S., Kim, S.-U., Kobayashi, K., Otsuka, H., Rogalska, E., Cassady, J.M. and Floss, H.G. (1990) *J. Am. Chem. Soc.*, **112**, 297-304.

14. Lovenberg, W. and Beaven, M.A. (1971) *Biochim. Biophys. Acta*, **251**, 452-455.

15. Shah, M.A., Scaman, C.H., Palcic, M.M. and Kagan, H.M. (1993) *J. Biol. Chem.*, **268**, 11573-11579.

16. Parsons M.R., Convery M.A., Wilmot C.M., Yadav K.D.S., Blakely V., Corner A.S., Phillips S.E.V., McPherson M.J. and Knowles P.F. (1995) *Structure*, **3**, 1171-1184.

17. Tanizawa, K., Matsuzaki, R., Shimizu, E., Yorifuji, T. and Fukui, T. (1994) *Biochem. Biophys. Res. Comm.*, **199**, 1096-1102.

18. Parrott, S., Jones, S. and Cooper, R.A. (1987) *J. Gen. Microbiol.*, **133**, 347-351.

19. Alton, G. and Palcic, M.M. (1996) Unpublished results.

20. Bradford, M. M. (1976) *Anal. Biochem.*, **72,** 248-254.

Chapter Four

Identification of Topaquinone as the Redox Cofactor in Tissue-Bound Semicarbazide-Sensitive Amine Oxidases[I]

4.1 Introduction

Mammalian tissue-bound semicarbazide-sensitive amine oxidases (SSAO) have been characterized in many different tissues, including white and brown adipocytes, umbilical artery, aorta, vasculature, uterus, ureter, vas deferens, chondrocytes and odontoblasts[1-10]. Vascular SSAO enzymes are found in the smooth muscle cell layers (tunica media) of blood vessels[5,6,11]. Subcellular localization studies indicate that the aorta enzymes are cell-surface-associated and have an extracellular active site[12]. These membrane glycoproteins are considered to be homodimers with a subunit molecular weight of approximately 95 kDa[13].

The tissue-bound SSAO enzymes and the soluble copper amine oxidases (EC 1.4.3.6) oxidatively deaminate primary amines to produce ammonia, hydrogen peroxide and an aldehyde (Equation 4.1).

$$RCH_2NH_2 + H_2O + O_2 \rightarrow RCHO + NH_3 + H_2O_2 \qquad (4.1)$$

The membrane-bound enzymes have a greater affinity for benzylamine than do the soluble enzymes (Table 4.1). However, benzylamine has not been found endogenously in mammals. Methylamine and aminoacetone may be the physiologically relevant substrates[13,14]. The rate of inhibition of the tissue-bound enzymes by semicarbazide is less than the rate for most soluble enzymes (Table

---

[I] A version of this chapter is to be submitted to Biochemistry. Authors: Gordon Alton, Glen Loppnow, Andy Holt and Monica Palcic.

4.1). However, both are irreversibly and completely inhibited by 1 mM semicarbazide[13].

Table 4.1 Benzylamine affinity and semicarbazide sensitivity of the amine oxidases.

Enzyme source	K_m Benzylamine	Inactivation by Semicarbazide	Reference
Copper Amine Oxidases (EC 1.4.3.6)			
Bovine plasma	1.7 mM	90%, 2 hr @ 10 μM	15, 16
Porcine plasma	90 μM	no data	17
Human plasma	225 μM	35%, 20 min @ 10μM	8
Semicarbazide-Sensitive Amine Oxidases			
Bovine aorta	16 μM	27%, 2 hr @ 10 μM	16
Porcine aorta	8 μM	37%, 2 hr @ 10 μM	16
Rat aorta	7 μM	35%, 20 min @ 10 μM	5
Human umbilical artery	207 μM	35%, 20 min @ 10 μM	5

These enzymes are also inhibited by other carbonyl-reactive reagents, such as aromatic and alkyl hydrazines, but are insensitive to inhibition by the acetylenic aromatic amine inhibitors of MAO[13]. The inhibition of the soluble copper amine oxidases by carbonyl reagents has been attributed to irreversible covalent derivatization of the essential redox cofactor, topaquinone (Figure 4.1).

Topaquinone was first determined in bovine plasma amine oxidase by Janes and coworkers in 1990[18]. ^{14}C-Phenylhydrazine-derivatized enzyme was

proteolyzed with thermolysin in 2M urea and the resultant peptides purified by reverse-phase HPLC.

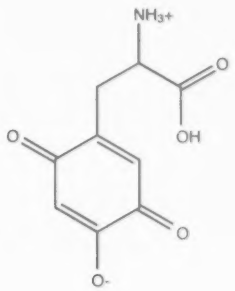

Figure 4.1 Topaquinone, the redox active cofactor of the copper amine oxidases. Shown as the *p*-quinone anion form of 2,4,5-trihydroxyphenylalanine.

A pentapeptide, shown to be L-N-X-D-Y, was recovered in 40% yield. The unknown residue at the third position (X) was determined by scintillation counting to be the site of ^{14}C-phenylhydrazine attachment. Structural characterization of this pentapeptide and of a topaquinone-hydantoin model compound, by high-resolution mass spectrometry, proton NMR and visible absorbance spectroscopy, confirmed that topaquinone is the redox cofactor in bovine plasma amine oxidase. Resonance Raman and visible absorbance spectroscopy of intact phenylhydrazine (PHZ) or *p*-nitrophenylhydrazine (pNPHZ)-derivatized enzyme is now deemed sufficient to establish topaquinone as the redox cofactor in putative copper amine oxidases[19]. Enzymes isolated from the plasma of cattle, sheep, rabbit, horse and pig, from gram positive and gram negative bacteria, from porcine kidney, from pea and chick pea seedling and from yeast are known to contain topaquinone[18,20-25].

Although the soluble copper amine oxidases and the tissue-bound SSAO enzymes have similar reaction mechanisms and carbonyl-reactive inhibitor sensitivity, no direct evidence has been reported supporting topaquinone as the redox cofactor in the tissue-bound enzymes[13,26]. Also, the copper requirement for

the tissue-bound enzymes has not been demonstrated conclusively[27,28]. This paucity of information may be due to difficulties that are typically encountered during the purification of membrane-bound proteins[29]. Bovine plasma amine oxidase can be purified to a specific activity of 0.44 U/mg protein, whereas a specific activity of 0.04 U/mg protein is the highest yet reported for bovine aorta SSAO[30,31].

In addition to subtle substrate and inhibitor differences, certain physical-chemical features of the tissue-bound enzymes distinguish them from the soluble copper amine oxidases. The pH-dependent visible absorbance spectra of PHZ derivatized bovine aorta SSAO were somewhat different from spectra reported for known copper amine oxidases[26]. Normally, the absorbance maximum undergoes a 50 nm red-shift as the pH is changed from neutral to approximately pH 14, but the bovine spectrum bleaches at high pH. Furthermore, soluble enzymes that display *pro*-S hydrogen abstraction at C1 of tyramine do not exchange hydrogens at C2 of product aldehyde, whereas the tissue-bound enzymes (*pro*-S at C1) do exchange hydrogens at C2[16]. It should be noted that lysyl oxidase is also *pro*-S specific and exchanges hydrogens at C2[32]. These stereochemical and visible absorbance results may suggest a different cofactor, or alternatively, a different active site configuration.

To clarify further the nature of the redox cofactor in the tissue-bound amine oxidases the pH-dependent visible absorbance spectra and resonance Raman spectra of pNPHZ-derivatized enzymes were investigated. Active site peptides were partially purified following proteolysis of derivatized enzymes with thermolysin or trypsin. Additionally, the derivatized enzymes were proteolyzed with pronase to liberate cofactor-containing peptides that were then characterized by mass spectrometry. Topaquinone is thus shown to be the redox cofactor in bovine and porcine aorta SSAO.

4.2 Experimental Procedures

Materials-All chemicals were ACS reagent grade. Acetonitrile, methyl alcohol and trifluoroacetic acid (TFA) were of HPLC grade and were obtained from Fisher. Triton X-100, urea, ammonium bicarbonate, Na_2HPO_4 and NaH_2PO_4 were also from Fisher. Pronase E was from Merck. Phenylhydrazine hydrochloride and *p*-nitrophenylhydrazine hydrochloride were from Fluka. All buffers were prepared with Milli-Q water. Nitro blue tetrazolium, glycine, octylglucoside, methyl-α-D-glucopyranoside, benzylamine hydrochloride and α-cyano-4-hydroxycinnamic acid were from Aldrich. Thermolysin (*Bacillus thermoproteolyticus rokko*) was from Boehringer-Mannheim. DEAE fast flow, lentil lectin, butyl, octyl, phenyl and alkylamino agaroses, 2-(N-Morpholino)ethanesulfonic acid (MES), TPCK-treated bovine pancreatic trypsin and Brilliant Blue G colloidal concentrate were from Sigma. The Bioscale Q2 column, 10DG desalting column, pre-cast 12% acrylamide gels, DC protein assay kit and the Biologic FPLC system were from BioRad. The Resource-S column, Hi-prep Sephacryl S100 (16/60) column and Superdex 200 (15/30) column were from Pharmacia. Whole aortas were obtained from a local slaughterhouse (Gainers) or Pel-Freez Biologicals. C18 Sep-Pak cartridges were from Millipore.

Enzymes-Pea seedling amine oxidase (PSAO) was available from previous work[25]. Porcine kidney diamine oxidase (PKDAO) was purified essentially as described by Steinbach and coworkers[33]. The purification of tissue-bound SSAO from bovine and porcine aorta followed previously reported procedures with only slight modification[16]. Briefly, 600 g of aorta were cleaned of adhering adventitia and ground with a 4 mm sieve meat grinder, washed with 4 L of 30 mM sodium phosphate pH 7.6 (buffer A), minced in a blender with 3 L of buffer A and centrifuged to pellet tissue-bound enzyme. The pellets were rehomogenized in 4 L

of buffer A and Triton X-100 was added to 1% (w/v) final concentration. After 4 hr of rapid stirring the thick slurry was centrifuged. The resultant 3 L of supernatant were filtered through Whatman number 2 filter paper and applied to a 5.0 X 50 cm DEAE fast flow anion exchange column. After washing unbound protein from the column with 4 L of 30 mM sodium phosphate pH 7.6 containing 1% Triton X-100 (buffer B) the enzyme was eluted with a NaCl gradient in buffer B at 2.5 mL/min. The active enzyme fractions eluted at approximately 0.5 M NaCl and were pooled and applied to a 2.5 X 20 cm lentil lectin column at 1 mL/min. After washing unbound protein from the column with 350 mL of buffer B the column was further washed with 350 mL of buffer A until the absorbance at 280 nm did not change so as to reduce the Triton X-100 concentration to a low level. The bovine or porcine aorta SSAO was eluted as a faint yellowish solution with 500 mL of 1 M α-methylglucoside at 0.2 mL/min. This yellowish solution was dialyzed against buffer A and concentrated to provide 0.04 U/mg of enzyme with a typical recovery of 2 units (10% yield) for the bovine enzyme and 0.5 units (7% yield) for the porcine enzyme. For some preparations of the aorta enzymes a protein with an absorbance at 410 nm was partially removed by use of a 2 mL Q2 quaternary anion exchange FPLC column using the Biologic FPLC system (BioRad). Enzyme was applied to the column, washed with buffer A and eluted at 0.6 mL/min with a 100 mL linear gradient of buffer A containing 1 M NaCl. This procedure did not increase the specific activity. Superdex 200 size-exclusion chromatography was performed in 50 mM sodium phosphate, pH 7.6 containing 0.5 M NaCl at a flow rate of 0.1 mL/min. Other protein chromatographic procedures described in "Results and Discussion" did not improve the specific activity or electrophoretic purity of the enzymes, and no experimental details are reported for these procedures. SDS-PAGE was performed on 12% pre-cast gels using the Laemmli procedure[34]. Protein bands were stained with colloidal Brilliant Blue G stain and

quinoproteins were detected with a nitroblue tetrazolium redox cycling assay as previously described[35]. Enzyme activity was measured at 37° C with 0.2 mM benzylamine hydrochloride as substrate in 50 mM sodium phosphate buffer, pH 7.6, by monitoring the increase in absorbance at 250 nm[36]. One unit is defined as the quantity of enzyme that catalyzes the production of 1.0 µmol/min of benzaldehyde, based on an extinction coefficient of 12.0 mM^{-1} cm^{-1}. Protein concentration was estimated by a detergent compatible method using a Bio-Rad DC protein assay kit (as directed by the supplier) with bovine serum albumin as a standard.

Phenylhydrazine and p-Nitrophenylhydrazine Derivatization and Spectroscopy-Absorbance spectra were recorded with a Hewlett Packard 8451A diode array spectrophotometer using quartz cuvettes. An aqueous solution of 0.2 mM *p*-nitrophenylhydrazine (or phenylhydrazine) hydrochloride was used for derivatizing the enzymes. Aliquots of 2 µl were added to a cuvette containing 0.1 U of enzyme in 1.0 mL of 50 mM sodium phosphate buffer, pH 7.6 (buffer C). The increase in absorbance at 464 nm was monitored until no further absorbance change was detected. The titration was continued until a slight excess of *p*-nitrophenylhydrazine (or phenylhydrazine) had been added. When the derivatization was complete, the reaction mixture was applied to a Bio-Rad 10DG column equilibrated in 50 mM NH_4HCO_3 to remove the excess hydrazine reagent. Absorbance spectra from 350 nm to 650 nm were recorded for 2.0 mg/mL of enzyme in buffer C, 2 M KOH, or 2.8 M KOH, as noted in the relevant figure legends.

Peptide spectra were recorded on fractions eluting from the HPLC column (see *Isolation of cofactor-p-nitrophenylhydrazine containing peptides*). Approximately 0.2 nanomoles of peptide, based on an extinction coefficient of 22 mM^{-1} cm^{-1} for the topaquinone-*p*-nitrophenylhydrazone adduct, were added to a

quartz cuvette in a final volume of 0.8 mL. The eluant from the first HPLC column, in 0.2 mM NH_4HCO_3, had a pH of 7.8. The high pH spectra were recorded after the addition of solid KOH to provide a KOH concentration of 2 M.

Resonance Raman Spectroscopy-Room-temperature resonance Raman spectra of the *p*-nitrophenylhydrazine derivatives of PSAO, and bovine and porcine SSAO were obtained with 150-300 µL sample solutions of absorbance 0.3 - 0.7 OD/cm at 468 nm (PSAO) or 456 nm (bovine or porcine SSAO). The extensive concentration of derivatized enzyme necessary to provide these required absorbance values resulted in solution turbidity that was removed by microfiltration with Millex-GV 0.22 µm filters (Millipore). Resonance Raman scattering was excited by spherically focusing the laser onto a spinning 5 mm i.d. NMR tube containing the sample solution in a 135° backscattering geometry. Laser excitation at 457.9 nm was obtained with an argon ion laser (Coherent, Santa Clara, CA). The laser power was typically 30 mW at the sample. Multi-channel detection of the resonance Raman scattering was obtained with a liquid nitrogen-cooled charged-coupled device (CCD) (Princeton Instruments, Trenton, NJ) connected to the first half of a double monochromator (Spex Industries, Metuchen, NJ). Spectral slit widths were 5-7 cm^{-1}. Frequency calibration was done by measuring the Raman scattering of solvents of known frequencies (benzene, chloroform and carbon tetrachloride). Reported frequencies are accurate to $\pm$ 2 cm^{-1}. The resonance Raman spectra were analyzed by using a 486DX2-66V computer (Gateway Computers, North Sioux City, SD). A 50 mM NH_4HCO_3 buffer solution background spectrum was subtracted from all spectra. In addition, fluorescence was removed by subtracting multiple joined line segments from the spectrum. Spectra were smoothed using a 5-point Savitsky-Golay function. It should be noted that exposure of the *p*-nitrophenylhydrazine-derivatized enzymes to the laser for times in excess of 30 min resulted in photochemical degradation of the chromophore. Thus, the data were

acquired over a shorter period of time to minimize this degradation, despite the reduction in the signal-to-noise of the acquired spectra.

Isolation of cofactor-p-nitrophenylhydrazine-containing peptides-A Waters HPLC system consisting of model 501 and 590 pumps, automated gradient controller and a 590E multiwavelength detector was used for all purifications. On-line column injections were performed with a model 7010 Rheodyne valve fitted with a 100 µL volume sample loop. Approximately 2 units of amine oxidase were derivatized with *p*-nitrophenylhydrazine as previously described and concentrated to a volume of 3 mL. Pronase E was added to provide a 1:1 (w/w) ratio of pronase to protein. After 24 hr (PKDAO or bovine SSAO) or 42 hr (porcine SSAO) at 37° C the solution was diluted to 10 mL with 0.1% trifluoroacetic acid (TFA) and applied to a C18 Sep-Pak cartridge. The cartridge was washed with 10 mL of 0.1% TFA and eluted with 5 mL of 90% CH_3CN in 0.1% TFA. The yellowish eluted material was freeze-dried and then dissolved in 0.2 mM NH_4HCO_3. This was injected onto a 0.39 X 15 cm C18 Deltapak HPLC column (Waters, 5 µm particle size) equilibrated in 0.2 mM NH_4HCO_3. Peptides were eluted with 0.2 mM NH_4HCO_3 containing 50% methyl alcohol at a flow rate of 0.8 mL/min with a 21 min linear gradient. The major peak at 450 nm was concentrated to approximately 50 µL and diluted to 1 mL with 0.2% TFA. This fraction was injected onto the Deltapak C18 column, pre-equilibrated in 0.2% TFA. Peptide elution was achieved with a linear gradient over 22 min with 0.2% TFA containing 55% CH_3CN at a flow rate of 1 mL/min. C4 and C8 columns provide lower purity peptides and thus were not used.

Alternatively, derivatized bovine SSAO was digested at 37° C with either thermolysin (11 mg), or trypsin (5 mg) in 2 M urea. The tryptic digestion mixture was diluted to 15 mL with 50 mM NH_4HCO_3 prior to placing the reaction tube into the 37° C incubator. The bovine thermolytic digestion (24 hr) or bovine tryptic digestion (48 hr) was adsorbed to and eluted from C18 cartridges as previously

described. The freeze dried eluants were applied to the C18 Deltapak HPLC column equilibrated in 0.1% TFA.

For the tryptic digestion, elution of peptides occurred with a linear gradient of 0.1% TFA containing 85% CH_3CN over 28 min at a flow rate of 1.1 mL/min. Various fractions absorbing at 400 nm were concentrated to a small volume. These fractions were applied to a 0.39 X 15 cm Novapak C8 HPLC column (Waters, 4 μm particle size) equilibrated in 0.1% TFA. Elution of peptides was achieved with a linear gradient of 0.1% TFA containing 55% CH_3CN over 18 min at a flow rate of 1.0 mL/min.

For the thermolytic digestion, elution of peptides occurred with a linear gradient of 0.1% TFA containing 27% CH_3CN over 20 min followed by a linear gradient from 27% CH_3CN to 45% CH_3CN over the next 30 min, at a flow rate of 1.1 mL/min. The major fraction with absorbance at 400 nm was freeze-dried and redissolved in 0.2 mM NH_4HCO_3. This fraction was applied to a 0.39 X 15 cm Novapak C8 HPLC column (Waters, 4 μm particle size) equilibrated in 0.2 mM NH_4HCO_3. Elution of peptides was achieved with a linear gradient of 0.2 mM NH_4HCO_3 containing 50% methyl alcohol over 50 min at a flow rate of 0.7 mL/min. All peptide retention times are precise to within 5%.

Mass spectrometry-Matrix-assisted laser desorption and ionization time-of-flight (MALDI-TOF) mass spectra were acquired on a Hewlett-Packard G2025A instrument. Peptides were dissolved in 50% CH_3CN to a concentration of 5 μM. One μL of 33 mM α-cyano-4-hydroxycinnamic acid (ACN) matrix in 50% acetonitrile was applied to each sample zone on the MALDI probe tip and allowed to evaporate. One μL of a 1:1 mixture of the peptide solution and the ACN matrix solution was applied to the dried matrix spots and allowed to evaporate. At least 100 separate laser shots, at 1 μJ laser power, were accumulated and averaged to provide the final MALDI-TOF mass spectra.

4.3 Results and Discussion

Enzyme purification-The partial purification of bovine and porcine SSAO followed previously established protocols that include DEAE and lentil lectin chromatography[16]. Analytical SDS-PAGE was used at all chromatographic steps to evaluate enzyme purity. Quinone-positive bands at approximately 97 kDA showed increased protein staining intensity as the specific activity of the enzyme increased throughout the chromatographic procedures. A typical gel profile and a quinone staining procedure have been reported previously[26,35]. The active enzyme fractions eluting from the lentil lectin column were yellowish in colour. This is correlated with a protein impurity, possibly a heme-containing protein, that absorbs at 410 nm. This impurity was found in variable amounts from one isolation to another but could be partially removed by use of a Bioscale Q2 (quaternary amine) anion exchange FPLC column by injecting small ($\leq$0.2 U) amounts of enzyme and eluting with a shallow salt gradient.

Many different purification procedures were evaluated to improve the specific activity of the enzymes after the lentil lectin column. Bovine SSAO eluted in the void volume of a Superdex 200 size-exclusion column. The SDS-PAGE profile of this fraction revealed the 97 kDA enzyme band and several smaller and larger molecular weight protein bands. No increase in specific activity or electrophoretic purity was obtained. Since the exclusion limit of this column is 600 kDa and the smaller molecular weight bands were observed, this implies that a multimolecular aggregate of an active enzyme and the other proteins is found under these chromatographic conditions. Size exclusion chromatography in sodium phosphate buffer, pH 7.6 with denaturants (either 1% Triton X-100, 1% octylglucoside, or 3 M urea) using a Sephacryl S-100 column, again resulted in elution of a multimolecular aggregate at the void volume (exclusion limit 150 kDa).

Alkylamino agarose columns, which have proved so successful for other copper amine oxidase purifications, failed to retain the tissue-bound SSAO. Butyl, phenyl and octyl agarose columns were unable to improve the electrophoretic purity and inactivated the enzymes. Cation exchange with a Resource-S column at pH 5.5 (0.1 M MES) resulted in no improvement of specific activity.

A non-chromatographic procedure using a Rotofor free-solution isoelectric focusing device (BioRad) resulted in the irreversible precipitation and loss of activity of the enzymes at approximately pH 4.5. None of these procedures increased the specific activity (0.04 U/mg) or enhanced the SDS-PAGE electrophoretic purity of the enzymes relative to that of the lentil lectin-eluted material. This is certainly due to the tendency of intrinsic membrane proteins to associate tightly with detergent micelles and to aggregate with other hydrophobic proteins, thus reducing the efficacy of the purification techniques[29]. Therefore, all subsequent procedures described in this paper used partially purified enzyme (0.04 U/mg) resulting from the lentil lectin eluate.

Visible absorbance spectroscopy-The identification of topaquinone as the redox cofactor in a copper amine oxidase enzyme is usually quite straightforward. The pH-dependent visible absorbance properties of phenylhydrazine or *p*-nitrophenylhydrazine-derivatized enzymes are recorded and compared to the spectra of known topaquinone-containing copper amine oxidases[37]. Phenylhydrazone derivatives of topaquinone show absorbance maxima near 445 nm at pH 7.0, with an incomplete red-shift of 50 nm in 1-2 M KOH solutions (Figure 4.2)[21]. The pNPHZ-derivatized topaquinone-containing enzymes display absorbance maxima near 462 nm at pH 7.0 with a characteristic 120 nm red-shift at high pH (Figure 4.2)[21]. Only topaquinone has been shown to have these pH-dependent spectral properties. Neither pyrroloquinoline quinone (PQQ) nor tryptophan

tryptophylquinone (TTQ), the redox cofactors in certain other quinoproteins, display similar spectra[38,39].

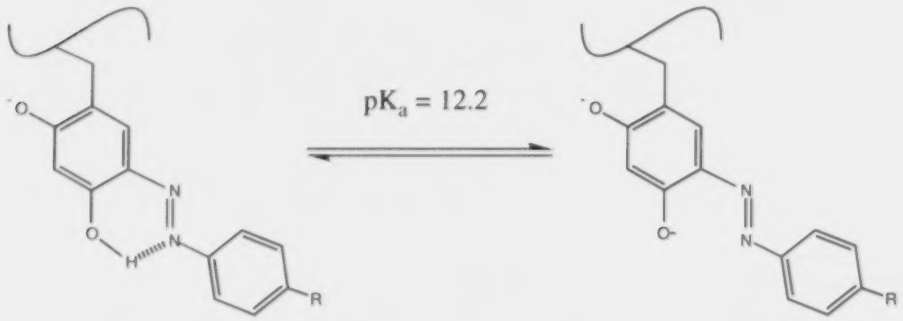

Figure 4.2 pH-Dependent spectral properties of topaquinone. Topaquinone-hydrazine adduct solutions are yellow at neutral pH. The *p*-nitrophenylhydrazine adduct is purple at high pH. This pH-induced shift in the absorbance maximum is attributed to the deprotonation of the azo form (pK$_a$ =12.2) of the topaquinone-hydrazone.

Figure 4.3 A shows the visible absorbance spectrum of phenylhydrazine-derivatized bovine aorta SSAO at pH 7.6 and in 2.0 M KOH. The maximum absorbance at neutral pH is at 428 nm. This wavelength is approximately 15 nm lower than previously reported spectra for derivatized copper amine oxidases that contain topaquinone[21]. Interestingly, the maxima for the intact bovine aorta enzyme at 428 nm is near the maxima (433-435 nm) reported for active site derived phenylhydrazone adduct peptides[21]. The high pH spectrum in Figure 4.3 A shows a complete bleaching of the 428 nm absorbance and no other absorbances are observed. This is very different from the high pH spectra of copper amine oxidases that show a maximum absorbance near 483 nm[21].

Figure 4.3 Absorbance spectra of the phenylhydrazine-derivatized bovine aorta SSAO (A). Absorbance spectra of the *p*-nitrophenylhydrazine-derivatized bovine aorta SSAO (B) and PSAO (C). Spectra were obtained with 0.2 mg of enzyme in 1 mL of 50 mM sodium phosphate buffer, pH 7.6 (—) or in 2.0 M KOH (---).

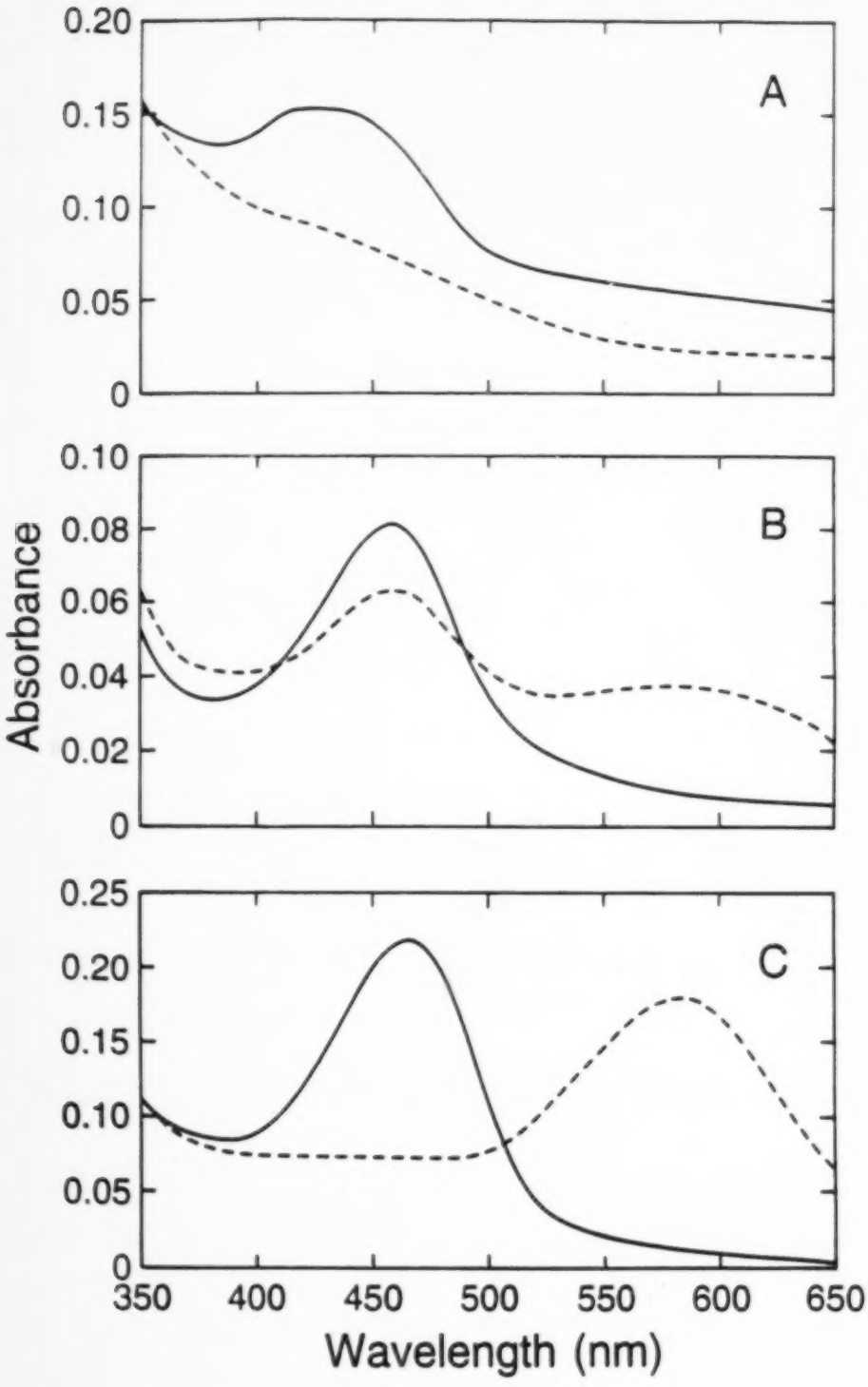
A
B
C
Absorbance
Wavelength (nm)
0.20
0.15
0.10
0.05
0
0.10
0.08
0.06
0.04
0.02
0
0.25
0.20
0.15
0.10
0.05
0
350
400
450
500
550
600
650

Figure 4.3 B shows the neutral and high pH spectra of bovine aorta SSAO that has been derivatized with pNPHZ and Figure 4.3 C shows the corresponding spectra for PSAO. The neutral pH spectra (Figures 4.3 B and C) show absorbance maxima at 456 nm (bovine SSAO) or 468 nm (PSAO). These spectra are similar to those derived from known topaquinone-containing copper amine oxidases. In 2 M KOH a complete spectral shift to higher wavelength (586 nm) is observed in Figure 4.3 C for the pea enzyme but an incomplete shift (580 nm) is seen in Figure 4.3 B for the bovine enzyme. Most topaquinone-containing copper amine oxidases display a complete spectral shift with no absorbance remaining at 460 nm in the high pH solution[21]. However, an incomplete shift has been reported for the derivatized *Hansenula polymorpha* enzyme and for a thermolytic peptide derived from PSAO[37,40]. A spectrum of the pNPHZ-derivatized bovine aorta enzyme in 2.8 M KOH shows a complete shift to 586 nm (data not shown). The significance of these incomplete shifts for the bovine pNPHZ-treated enzyme, and the bleaching of the PHZ-treated enzyme, at high pH, is not well understood but may reflect differences in the pK_a of the hydrazine adducts[37].

Figure 4.4 A shows the neutral and high pH spectra of pNPHZ-derivatized porcine aorta SSAO. Figure 4.4 B shows the spectra for a pronase-liberated peptide from the porcine SSAO enzyme (see page 101). At neutral pH (Figure 4.4 A) the absorbance maximum is at 466 nm and this shifts to 580 nm in 2 M KOH. This spectrum demonstrates a complete shift with no residual absorbance at 466 nm. The pH-dependent spectral properties of pNPHZ-derivatized porcine aorta SSAO are similar to known topaquinone-containing enzymes. Since the properties of the bovine enzyme were somewhat different, the pNPHZ-derivatized SSAO enzymes were further characterized by resonance Raman spectroscopy.

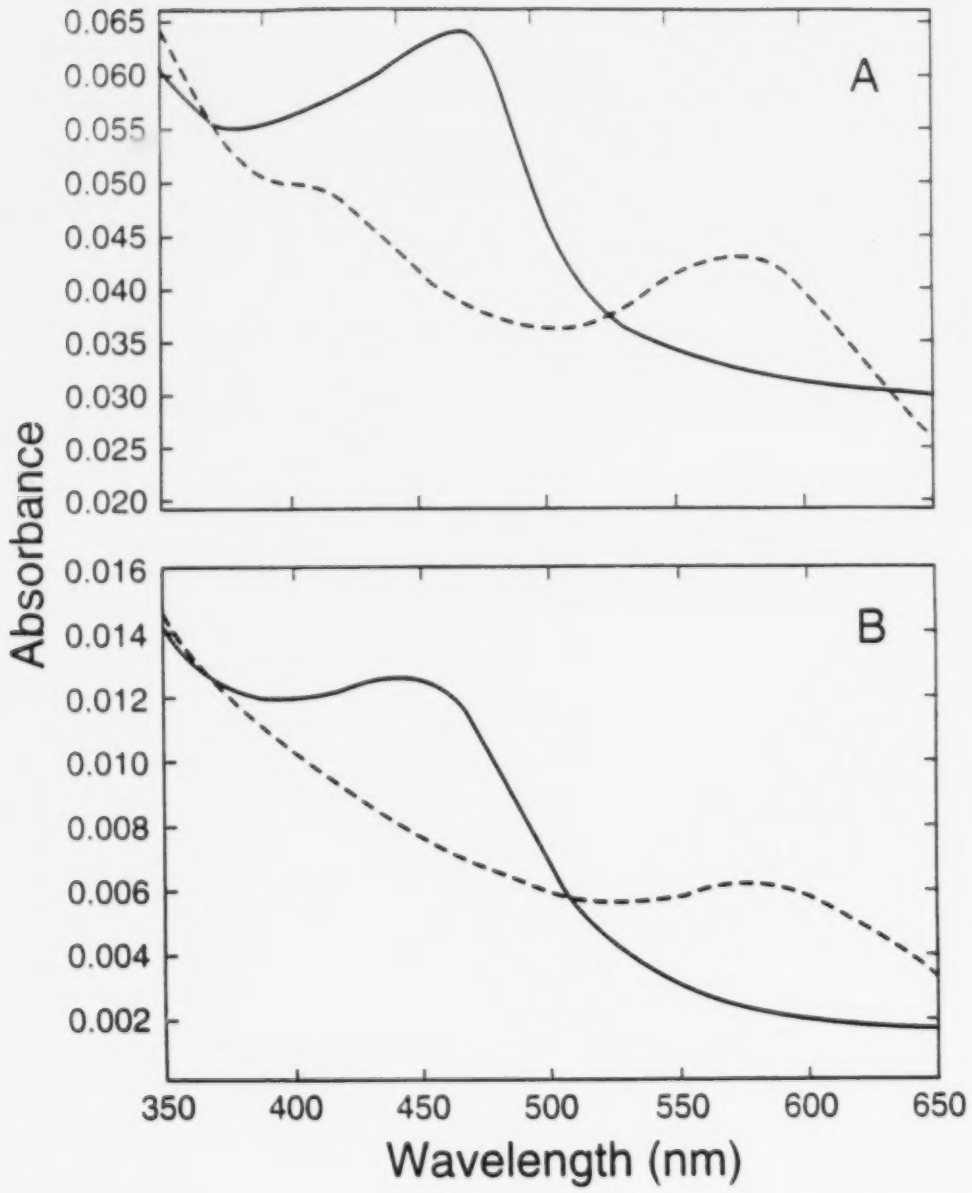

Figure 4.4 Absorbance spectra of the *p*-nitrophenylhydrazine-derivatized porcine SSAO (A). Absorbance spectra of the isolated peptide released from *p*-nitrophenylhydrazine-derivatized porcine SSAO with pronase (B). Spectra were obtained at pH 7.6-7.8 (—) or in 2.8 M KOH (---).

Resonance Raman spectroscopy[II]-The resonance Raman spectra of the *p*-nitrophenylhydrazine derivatives of the soluble PSAO, the tissue-bound bovine SSAO and porcine SSAO are shown in Figure 4.5. A number of spectral features require comment. The most striking observation is that the spectra of all three are essentially identical, with similar frequencies and relative intensities. This similarity indicates that the chromophore, and hence the cofactor, is identical in the three enzymes. In addition, the resonance Raman spectra of pNPHZ-derivatized PSAO, bovine SSAO and porcine SSAO are similar to the spectra of other pNPHZ-derivatized copper amine oxidases with known topaquinone cofactors[21,22,41]. Finally, the X-ray crystal structure of pea seedling amine oxidase clearly shows a topaquinone cofactor near, but not bound to, the copper active site[42]. Thus, *the resonance Raman spectra indicate that the cofactors in PSAO, bovine SSAO and porcine SSAO are identical topaquinones.*

Based on previous stereochemical data it has been suggested that the cofactor in the tissue-bound enzymes and lysyl oxidase are the same[26]. The cofactor in lysyl oxidase has been shown to be similar to, but distinct from, topaquinone[43]. However, the resonance Raman spectrum of derivatized lysyl oxidase does not resemble the spectra of the derivatized tissue-bound SSAO enzymes[44]. This information, in conjunction with our resonance Raman data, preclude the lysyl oxidase cofactor and confirm topaquinone as the redox cofactor in bovine and porcine SSAO.

A closer examination of the resonance Raman spectra reveal slight differences in intensities and frequencies. These differences may elucidate the molecular source of the different C2 hydrogen exchange characteristics that distinguish the soluble amine oxidases from the tissue-bound enzymes[26]. The most

---

II The resonance Raman spectra presented in this chapter were kindly provided by Dr. Glen Loppnow, Department of Chemistry, University of Alberta.

Figure 4.5 Resonance Raman spectra of the *p*-nitrophenylhydrazine derivatives of PSAO, bovine SSAO and porcine SSAO. Spectra were excited with 30 mW of laser light at 457.9 nm. Total accumulation time was 400-450 sec. Frequencies were calibrated using a mixture of carbon tetrachloride, chloroform and benzene, and are accurate to ± 2 cm^{-1}. Except for slight differences in relative intensities, the spectra of bovine and porcine SSAO are identical and very similar to the PSAO spectrum.

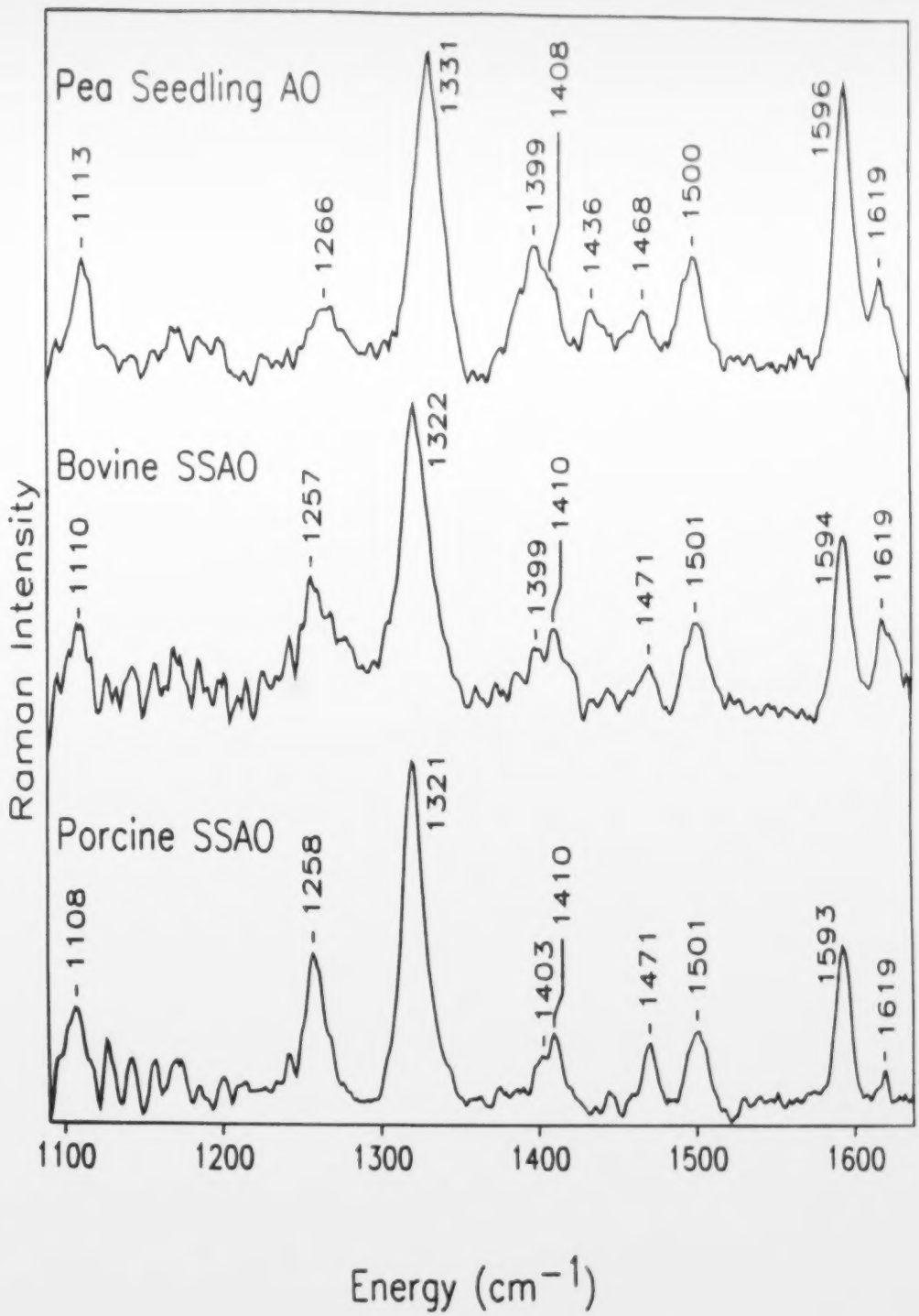
Pea Seedling AO
1113
1266
1331
1399
1408
1436
1468
1500
1596
1619
Bovine SSAO
1110
1257
1322
1399
1410
1471
1501
1594
1619
Porcine SSAO
1108
1258
1321
1403
1410
1471
1501
1593
1619
Raman Intensity
1100
1200
1300
1400
1500
1600
Energy (cm⁻¹)

significant difference among these three spectra is a downshift of the 1266 and 1331 cm^{-1} modes in PSAO to 1257 and 1321 cm^{-1}, respectively, in the bovine and porcine SSAOs. The resonance Raman spectra of the pNPHZ derivative of *A. globiformis* histamine oxidase also exhibits 10 cm^{-1} downshifts in these two modes compared to the spectrum for a topaquinone hydantoin model compound[45].

Resonance Raman spectroscopy of PHZ-derivatized topaquinone-containing amine oxidases has progressed little beyond the comparison of spectral frequencies and relative intensities[21,22,41,45,46]. Recently, isotopic derivatives of *E. coli* amine oxidase (ECAO) and a *tert*-butyltopaquinone anion model compound have been prepared. Their resonance Ramna spectra have been taken in an effort to assign the observed modes[47]. They assigned the 1200 to 1400 cm^{-1} region of the spectra to C-C strectching, C-O stretching or C-H bending modes. ECAO exhibits intense modes at 1269 cm^{-1} and 1334 cm^{-1}, that did not shift on isotopic substitution with ^{2}H or ^{18}O. In contrast, the 1354 cm^{-1} mode in the model compound shifted 10 cm^{-1} with ^{2}H substitution. The pNPHZ-derivatized PSAO exhibits a resonance Raman band at approximately 1330 cm^{-1} that is not seen in the PHZ derivative. Thus, we assign the observed mode at 1331 cm^{-1} in PSAO to the symmetric NO_2 stretch that is seen at 1347 cm^{-1} in pNPHZ. The mode at 1266 cm^{-1} is more difficult to assign. A mode at 1269 cm^{-1} is seen in the resonance Raman spectra of underivatized ECAO and is also seen at 1249 cm^{-1} in the *tert*-butyltopaquinone model compound. However, a mode at 1288 cm^{-1} is one of the strongest modes in the Raman spectrum of pNPHZ. No strong modes are observed in this region in *p*-benzoquinone[48]. Because the derivatized SSAO enzymes exhibit an absorption band at approximately 456 nm that is due primarily to the topaquinone moiety, we tentatively assign the mode at 1269 cm^{-1} to the C-O stretch of topaquinone in the pNPHZ-derivatized enzymes. The downshifts of both of these modes in comparing the PSAO and the SSAOs suggests specific perturbations from the enzyme near the

NO_2 group of the pNPHZ derivative and near C2 of topaquinone. Since C2 of topaquinone is near the proposed site of reaction, the different resonance Raman frequencies of this mode may directly reflect the differences in active site environment responsible for the different C2 hydrogen exchange characteristics for the two different types of enzymes[26].

Peptide purification and cofactor characterization[III]-The topaquinone-containing CuAO enzymes have an active site consensus sequence, (T-X-X-N-Y-D/E), where X is any amino acid, in which the tyrosine (Y) is the autocatalytic site of topaquinone generation[21,49]. The amino acid sequences derived from pNPHZ-derivatized active site peptides are very hydrophobic, as judged by reverse-phase HPLC chromatography. In order to resolve one hydrophobic peptide from another, two different solvent systems are typically used with the same HPLC column. Usually, a neutral pH solvent system is used first with an organic modifier (e.g., methyl alcohol) to achieve elution of peptides. Peptides collected from this step are reinjected onto the same reverse-phase column, but at a low pH and with elution by a second organic modifier (e.g., acetonitrile). The rationale behind this two-step procedure is that, since peptides have different pI values, peptides that co-elute at one pH may be separated at a different pH. The different organic modifiers may also affect some resolution of the peptides.

Thermolysin, trypsin and pronase have been used previously to release cofactor-containing peptides from the active site of PHZ-derivatized copper amine oxidases[18,21,33]. Trypsin generally provides peptides that are 10-20 amino acids in length whereas thermolysin provides shorter peptides of approximately 5 amino

---

III Pig kidney diamine oxidase (PKDAO) and the chromatographic data for the pronase digestion of pNPHZ-derivatized PKDAO and porcine SSAO were kindly provided by Dr. Andrew Holt, Department of Chemistry, University of Alberta.

acids in length[21]. Thermolysin, in contrast to trypsin, normally does not require denaturing agents such as urea to digest the protein effectively. Trypsin would normally be preferred as the longer peptide sequences generated would provide a superior starting point for the design of oligonucleotide probes. Pronase, a nonspecific protease, releases *p*-nitrophenylhydrazone-topaquinone aspartate dipeptide (Figure 4.6) from the topaquinone-containing pig kidney diamine oxidase (PKDAO) and *E. coli.* amine oxidase[33]. Although this short dipeptide does not provide extensive sequence information it does facilitate physical-chemical determination of the topaquinone adduct.

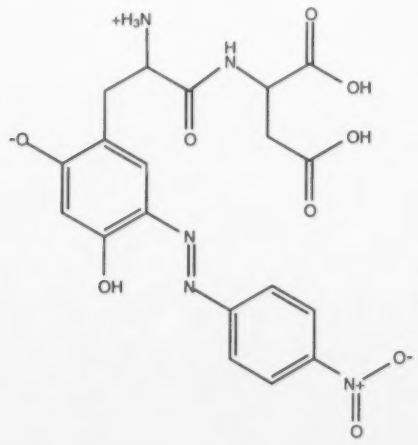

Figure 4.6 The azo tautomer of *p*-nitrophenylhydrazone-topaquinone aspartate.

Initial peptide isolation experiments focused on tryptic digestion of the *p*-nitrophenylhydrazine-derivatized bovine aorta SSAO enzyme in 2 M urea. This protocol has been shown previously to release cofactor-containing peptides from bovine serum amine oxidase (BSAO), porcine serum amine oxidase and PKDAO[18,21]. The tryptic digestion mixture was applied to a C18 reverse-phase cartridge and washed with water to remove buffer salts, hydrophilic peptides and glycopeptides. The hydrophobic pNPHZ-labelled cofactor-containing peptides were

eluted with acetonitrile and the solution concentrated to a small volume. This solution was diluted with the HPLC column equilibration mobile phase (0.1% TFA) and injected onto the column. Elution was achieved with increasing acetonitrile concentration. Figure 4.7 A displays the 400 nm absorbance chromatogram of the first HPLC column step (low pH) for the tryptic digestion of the bovine enzyme. Major peaks were observed at 7.850, 11.916, 15.800 and 19.333 min, each representing approximately 2% of the chromophore relative to the intact derivatized enzyme. The peak at 7.850 min was observed to have a slightly larger peak area at approximately 36 hours but the chromatogram was more reproducible with a 48 hour incubation. Each of these peaks were collected and reinjected onto the HPLC column with modified elution conditions (see Experimental Procedures). Figure 4.7 B displays the 400 nm absorbance chromatogram for the purification of the 7.850 min fraction from the first column with the new elution conditions. The major peaks at 1.400, 6.333, 7.133 and 10.950 min were collected and sent for amino acid sequencing. Only the peak at 6.333 min revealed any sequence and this was ambiguous. This ambiguity may be related to the small amount of peptide ($\leq$ 15 picomoles) such that each cycle of the amino acid sequencer provided only background signals. Alternatively the peak fraction may have been impure. The inability of the amino acid sequencer to obtain any sequence from the other peptides may be due to N-terminal blockage that has been observed by other researchers[50]. It has been determined that cyclic peptide formation by condensation of the N-terminus with topaquinone-phenylhydrazone was responsible for this blockage[50]. No other peaks isolated from the tryptic digest provided any sequence information. Figure 4.8 A displays the low pH chromatogram of the peptides released from the thermolytic digestion of pNPHZ-derivatized bovine aorta SSAO. The major peak with absorbance at 400 nm was

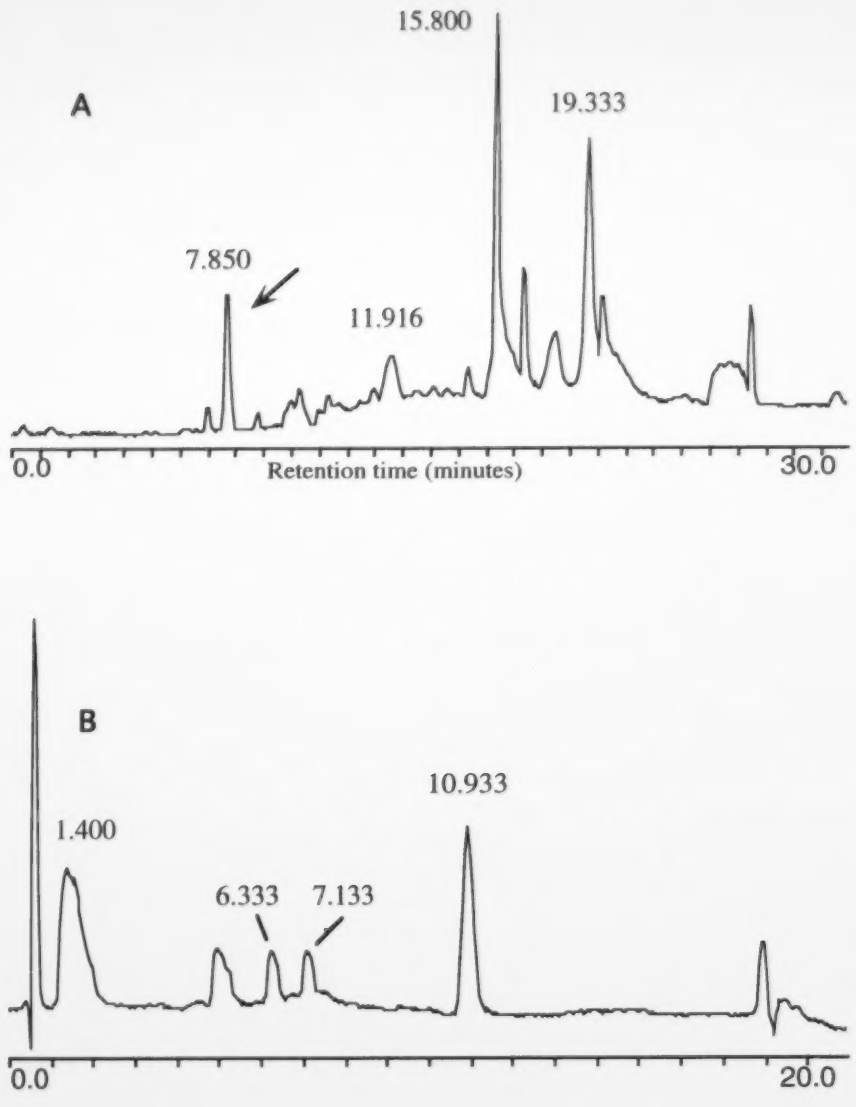

Figure 4.7 The HPLC chromatograms of the chromophoric peptides derived from the tryptic digestion of *p*-nitrophenylhydrazine-derivatized bovine SSAO. The peak at retention time 7.850 min (arrow) in chromatogram (A) was rechromatographed with different elution conditions as described in the text (B). Both traces show absorbance at 400 nm.

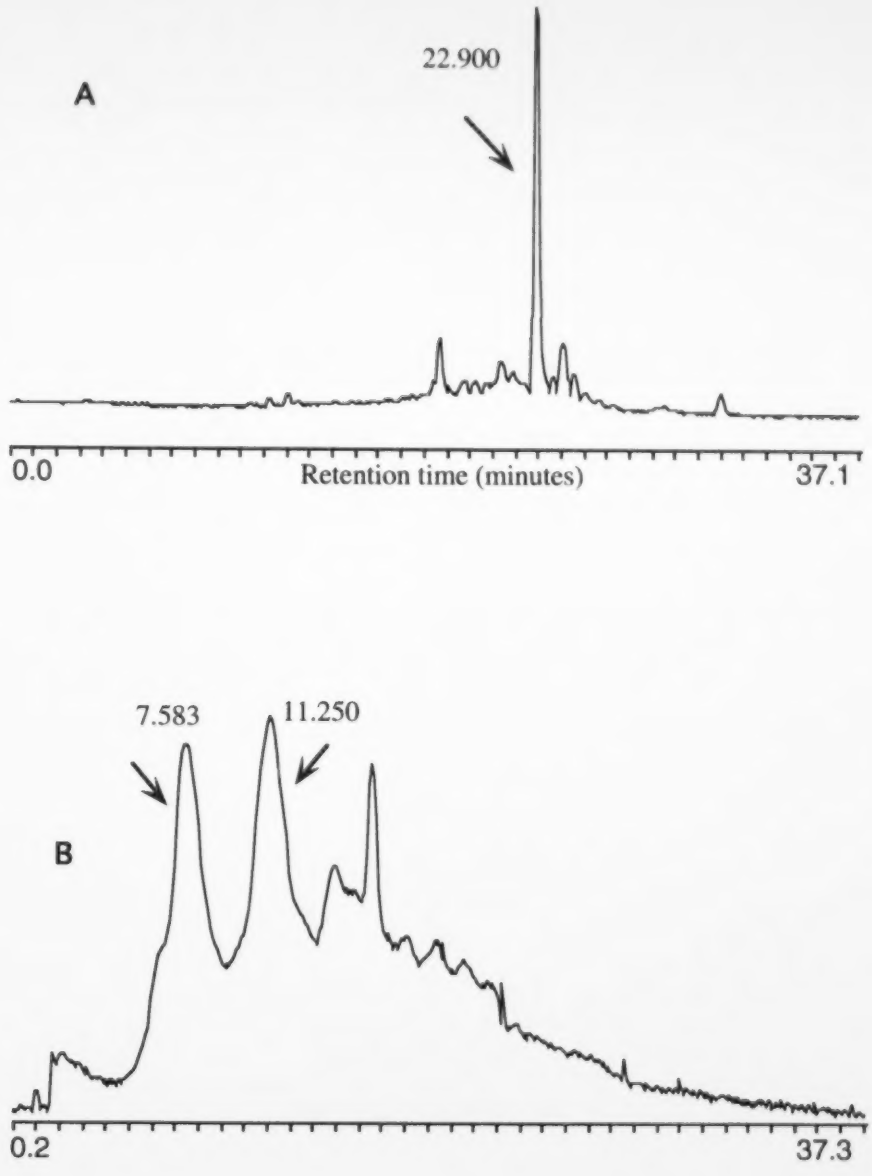

Figure 4.8 The HPLC chromatograms of the chromophoric peptides derived from the thermolytic digestion of *p*-nitrophenylhydrazine-derivatized bovine SSAO. The low pH (A_{400} nm) chromatogram is shown at top (A). The peak at retention time 22.900 min (arrow) in the upper trace was rechromatographed at neutral pH, as shown by the lower (A_{450} nm) chromatographic trace (B). The 7.583 min peak in B was sent for amino acid analysis.

observed at a retention time of 22.900 min and represents 750 picomoles of peptide, assuming topaquinone-*p*-nitrophenylhydrazone as the chromophore. This peak fraction, representing a 7% yield from the enzyme, was collected and injected onto a reverse-phase C8 column, as described in Experimental Procedures. Figure 4.8 B displays the absorbance at 450 nm for the peptide elution and shows a broad peak at a retention time of 7.583 min containing approximately 150 picomoles of chromophore. Preliminary amino acid sequence analysis of this fraction suggests that it is a pentapeptide. Another broad peak at a retention time of 11.250 min contains approximately 100 picomoles of chromophore. The two major peaks shown in Figure 4.8 B will be analyzed by high energy collision-induced-dissociation tandem mass spectrometry.

The low yields from tryptic and thermolytic proteolysis have been observed by other researchers and this has led to the development of higher yield procedures[38,50]. Duine and coworkers have recently published such a protocol using pronase digestion of either PHZ or pNPHZ-derivatized copper amine oxidases[33]. Total proteolysis of pNPHZ-derivatized bovine and porcine SSAO and PKDAO was achieved with pronase. The reverse-phase HPLC purification of the released cofactor-containing peptides followed Duine's reported procedure quite closely.

Figures 4.9 A-C show the neutral pH HPLC purification step chromatograms (450 nm absorbance) for bovine SSAO, porcine SSAO and PKDAO, respectively. This chromatographic step was performed with an NH_4HCO_3 solvent system and elution achieved by increasing methyl alcohol concentration. The major peak at 17.600 min was collected and rechromatographed at low pH, as described in Experimental Procedures. Figures 4.9 D-F display the chromatograms for the second HPLC purification step for bovine SSAO, porcine SSAO and PKDAO, respectively. Clearly, all three enzymes release chromophoric

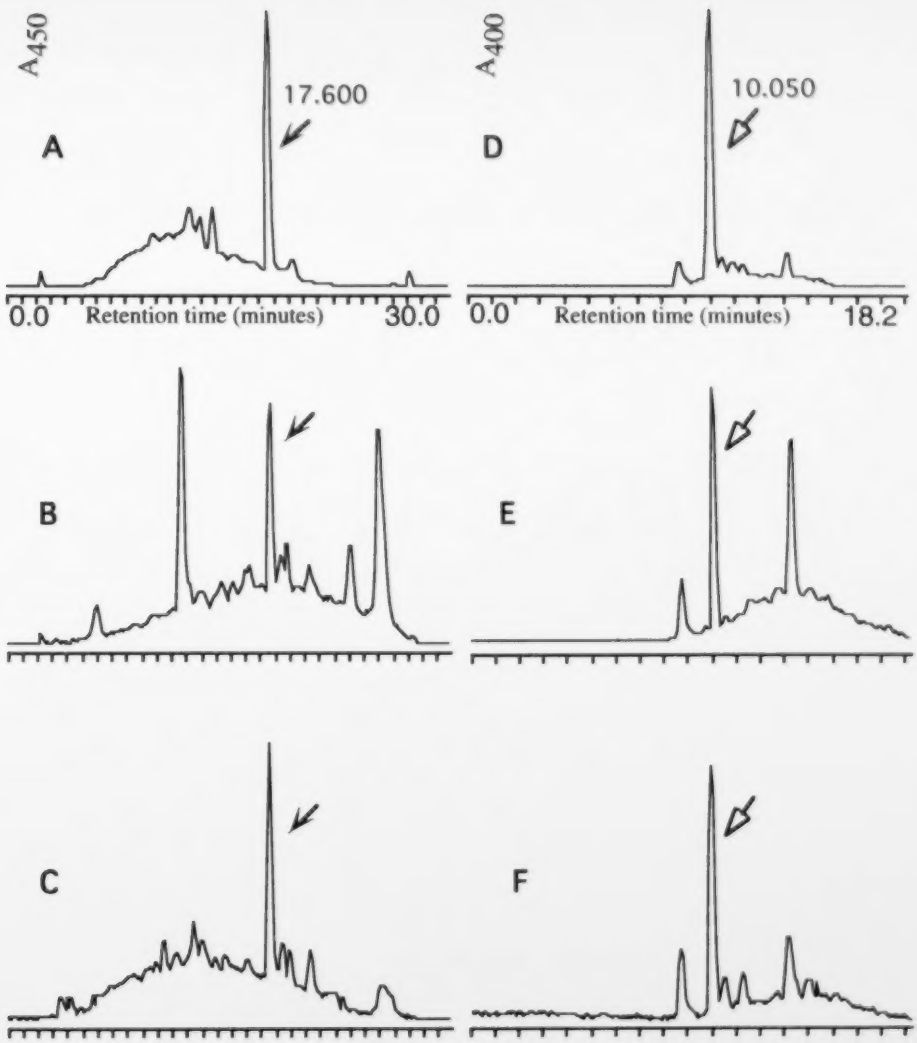

Figure 4.9 HPLC purification of cofactor-containing peptides released by pronase from pNPHZ-derivatized enzymes. The left-hand panels show the 450 nm absorbance chromatograms (neutral pH) for bovine SSAO (A), porcine SSAO (B) and PKDAO (C). The right-hand panels show the 400 nm absorbance chromatograms (low pH) for the bovine (D), porcine (E) and PKDAO (F) enzymes.

peptides that display very similar chromatographic properties. The peptides observed at 17.600 min from the first HPLC step (Figure 4.9 A-C) elute at approximately 41% methyl alcohol concentration. Duine and coworkers reported a peak eluting at a methyl alcohol concentration of 38% for a pNPHZ-derivatized PKDAO pronase digest, representing a 41% recovery of chromophore (150 nanomoles)[33].

The bovine SSAO pronase digestion provided a 17.600 min peak with 2.0 nanomoles (9% yield) of cofactor, assuming topaquinone-pNPHZ as the chromophore. The porcine SSAO peak at 17.600 min provided 1.2 nanomoles (7% yield) of cofactor-pNPHZ and the PKDAO peak provided 0.6 nanomoles (10% yield) of cofactor-pNPHZ. These yields are smaller than the yield reported by Duine and coworkers and may be due to the lower purity of the enzymes, although it is possible that certain components of the HPLC system may be catalyzing hydrolysis of the pNPHZ-cofactor. Figure 4.4 B shows the pH-dependent visible absorbance spectra of the 17.600 min fraction from the porcine SSAO digestion (Figure 4.9 B). This peptide fraction had an absorbance maximum, at neutral pH, of 450 nm that shifts to 580 nm at high pH. This was very similar to the shifts (457-584 nm) reported for topaquinone-pNPHZ peptides isolated from other copper amine oxidases[21]. The 17.600 min fraction for the bovine enzyme (Figure 4.9 A) had similar pH-dependent visible absorbance spectra.

Duine and coworkers showed a maximum absorbance at 450 nm for their peak fraction from the first column, but failed to report if a high pH shift occurred. They also indicated that the low pH of the second HPLC chromatography step shifts the absorbance maximum to 418 nm and reduces the molar absorbance of the pNPHZ-cofactor, but they did not provide a quantitative estimate. Experiments in our laboratory suggest that, in 0.1% TFA, the molar absorbance was 40% of the value observed at neutral pH and that the maximum absorbance shifts to

approximately 420 nm. The 10.050 min peak observed in Figure 4.9 D (bovine) thus represents 1.1 nanomoles of cofactor-pNPHZ. This provides an overall recovery of 5% for the pNPHZ-cofactor.

The peptide fraction eluting at 10.050 min for the bovine enzyme digestion (Figure 4.9 D) was characterized by matrix-assisted laser desorption and ionization time-of-flight (MALDI-TOF) mass spectrometry. Figure 4.10 A shows the positive ion MALDI-TOF mass spectrum for this peptide obtained with α-cyano-4-hydroxycinnamic acid (ACN) matrix. Figure 4.10 B shows the MALDI-TOF mass spectrum of the ACN matrix alone. Despite the large matrix-associated peaks, a molecular ion mass of 462.3 Da is observed for the 10.050 min peptide fraction. The theoretical average mass for protonated topaquinone-pNPHZ aspartate dipeptide is 462.4 Da. Duine and coworkers unequivocally determined the structure of a topaquinone-pNPHZ aspartate dipeptide by nuclear magnetic resonance spectroscopy and electrospray mass spectrometric fragmentation, providing a molecular ion of 462 Da. The mass peak at 447 Da may be a fragment ion of TPQ.

The similarity of our HPLC chromatographic data and mass spectra, as compared to Duine's findings, confirm the resonance Raman result that the cofactor of bovine and porcine SSAO is topaquinone. Additionally, the dipeptide released by the pronase treatment shows that the bovine and porcine SSAO enzymes contain aspartate, which is part of the consensus sequence in other topaquinone-containing copper amine oxidases. The bleaching of the bovine SSAO phenylhydrazine-derivatized spectrum and the incomplete shift of the absorbance maximum for the *p*-nitrophenylhydrazine-derivatized spectrum at high pH may simply reflect different active site configurations for the membrane-bound SSAO enzymes. This correlates with the spectral shifts observed in the Raman modes and may provide insight concerning the different C2 hydrogen exchange characteristics of the tissue-bound enzymes compared to the soluble amine oxidases.

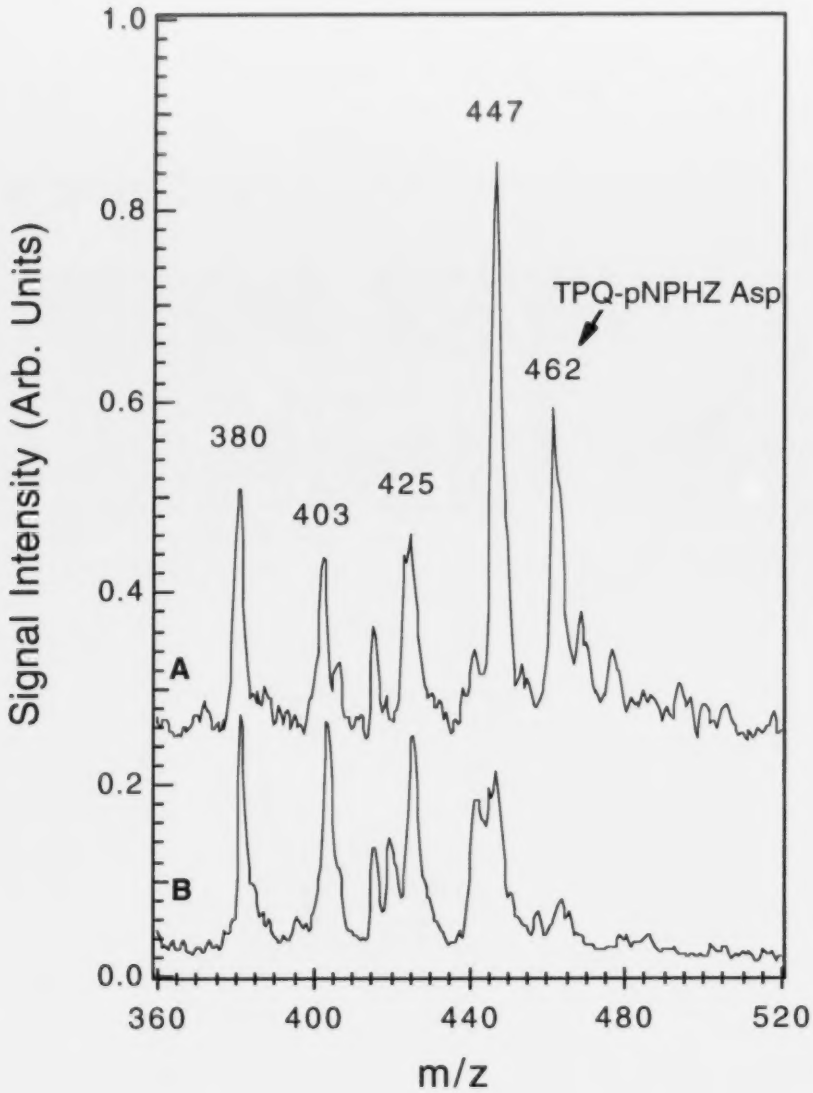

Figure 4.10 The MALDI-TOF mass spectrum of the major pNPHZ-derivatized peptide isolated from pronase digestion of bovine SSAO (A). A mass spectrum of ACN matrix is shown below (B). The ratio of the 380 (m/z) signal intensities was set to one in order to normalize peak heights.

References

1. Rucker, R.B. and O'Dell, B.L. (1971) *Biochim. Biophys. Acta.*, **235**, 32-43.

2. Lewinsohn, R. (1981) *J. Pharm. Pharmacol.*, **33**, 569-575.

3. Lyles, G.A. and Bertie, K.H. (1987) *Pharmacol. Toxicol.*, **60 (Suppl. 1)**, 33.

4. Norqvist, A., Fowler, C.J. and Oreland, L. (1981) *Biochem. Pharmacol.*, **30**, 403-409.

5. Precious, E., Gunn, C.E. and Lyles, G.A. (1988) *Biochem. Pharmacol.*, **37**, 707-713.

6. Lyles, G.A. and Singh, I. (1985) *J. Pharm. Pharmacol.* **37**, 637-643.

7. Precious, E. and Lyles, G.A. (1988) *J. Pharm. Pharmacol.* **40**, 627-633.

8. Lyles, G.A., Holt, A. and Marshall, C.M.S. (1990) *J. Pharm. Pharmacol.* **42**, 332-338.

9. Yu, P.H. (1990) *J. Pharm. Pharmacol.* **42**, 882-884.

10. Conforti, L., Raimondi, L. and Lyles, G.A. (1993) *Biochem. Pharmacol.*, **46**, 603-607.

11. Lewinsohn, R. (1984) *Braz. J. Med. Biol. Res.*, **17**, 223-256.

12. Holt, A. and Callingham, B.A. (1993c) *Br. J. Pharmacol.*, **108**, 158P.

13. Lyles, G.A. (1995) *Int. J. Biochem. Cell Biol.*, in press.

14. Callingham, B.A., Crosbie, A.E. and Rous, B.A. (1995) *Progress in Brain Research*, **106,** 305-321.

15. Palcic, M.M. and Klinman, J.P. (1983) *Biochemistry*, **22**, 5957-5966.

16. Scaman, C.H. and Palcic, M.M. (1992) *Biochemistry*, **31**, 6829-6841.

17. Gorkin, V.Z. (1983) *Amine Oxidases in Clinical Research*, Pergamon Press, Toronto.

18. Janes, S.M., Mu, D., Wemmer, D., Smith, A.J., Kaur, S., Maltby, D., Burlingame, A.L. and Klinman, J.P. (1990) *Science*, **248**, 981-987.

19. Dooley, D.M. and Brown, D.E. (1995) in *Methods in Enzymology 258*, Klinman, J.P. (Ed.) pp. 132-140 Academic Press, New York, NY.

20. Mu, D., Janes, S.M., Smith, A.J., Brown, D.E., Dooley, D.M. and Klinman, J.P. (1992) J. *Biol. Chem.*, **267**, 7979-7982.

21. Janes, S.M., Palcic, M.M., Scaman, C.H., Smith, A.J., Brown, D.E., Dooley, D.M., Mure, M. and Klinman, J.P. (1992) *Biochemistry*, **31**, 12147-12154.

22. Dooley, D.M., McIntire, W.S., McGuirl, M.A., Cote, C.E. and Bates, J.L. (1990) *J. Am. Chem. Soc.*, **112**, 2782-2789.

23 Cooper, R.A., Knowles, P.F., Brown, D.E., McGuirl, M.A. and Dooley, D.M. (1992) *Biochem. J.*, **288**, 337-340.

24. Matsuzaki, R., Fukui, T., Sato, H., Ozaki, Y. and Tanizawa, K. (1994) *FEBS Lett.*, **351**, 360-364.

25. Alton, G., Taher, T.H., Beever, R.J. and Palcic, M.M. (1995) *Arch. Biochem. Biophys.*, **316**, 353-361.

26. Palcic, M.M., Scaman, C.H. and Alton, G. (1995) *Progress in Brain Research*, **106**, in press.

27. Lyles, G.A., Garcia-Rodriguez, J. and Callingham, B.A. (1983) *Biochem. Pharmacol.*, **32**, 2515-2521.

28. Barrand, M.A. and Callingham, B.A. (1984) *Biochem. J.*, **222**, 467-475.

29. Jagow, G.V., Link, T.A. and Schagger, H. (1994) *A Practical Guide to Membrane Protein Purification*, Jagow, G.V. and Schagger, H. (Eds.) pp. 3-21 Academic Press, New York, NY.

30. Janes, S.M. and Klinman, J.P. (1991) *Biochemistry*, **30**, 4599-4605.

31. Barrand, M.A. and Callingham, B.A. (1982) *Biochem. Pharmacol.*, **31**, 2177-2184.

32. Shah, M.A., Scaman, C.H., Palcic, M.M. and Kagan, H.M. (1993) *J. Biol. Chem.*, **268**,11573-11579.

33. Steinebach, V., Groen, B.W., Wijmenga, S.S., Niessen, W.M.A., Jongejan, J.A. and Duine, J.A. (1995) *Anal. Biochem.*, **230**, 159-168.

34. Laemmli, U.K. (1970) *Nature (London)*, **277**, 680.

35. Paz, M.A., Fluckiger, R., Boak, A., Kagan, H.M. and Gallop, P.M. (1991) *J. Biol. Chem.*, **266**, 689-692.

36. Tabor, C. W., Tabor, H. and Rosenthal, S. M. (1954) *J. Biol. Chem.* **208,** 645-661.

37. Palcic, M.M. and Janes, S.M. (1995) in *Methods in Enzymology 258*, Klinman, J.P. (Ed.) pp. 34-38 Academic Press, New York, NY.

38. Klinman, J.P. and Mu, D. (1994) *Annu. Rev. Biochem.*, **63**, 299- 344.

39. McIntire, W.S. and Hartmann, C. (1993) in *Principles and Applications of Quinoproteins,* Davidson, V.L. (Ed) pp. 97-109 Macel Dekker, Inc., New York, NY.

40. Cai, D. and Klinman, J. P. (1994) *Biochemistry*, **33**, 7647-7653.

41. Brown, D.E., McGuirl, M.A., Dooley, D.M., Janes, S.M., Mu, D. and Klinman, J.P. (1991) *J. Biol. Chem.*, **266**, 4049-4051.

42. Dooley, D.M., Freeman, H.C., Guss, J.M., Harvey, I., Kumar, V., McGuirl, M.A. and Zubak, V.M., (1996) Personal Communication.

43. Klinman, J.P. (1995) Personal communication.

44. Williamson, P.R., Moog, R.S., Dooley, D.M. and Kagan, H.M. (1986) *J. Biol. Chem.*, **261**, 16302-16305.

45. Choi, Y.-H., Matsuzaki, R., Fukui, T., Shimizu, E., Yorifuji, T., Sato,H., Ozaki, Y. and Tanizawa, K. (1995) *J. Biol. Chem.*, **270**, 4712-4720.

46. McIntire, W.S., Bates, J.L., Brown, D.E. and Dooley, D.M. (1991) *Biochemistry*, **30**, 125-133.

47. Loccoz, P.M., Nakamura, N., Steinbach, V., Duine, J.A., Mure, M., Klinman, J.P. and Loehr, J.S. (1995) *Biochemistry*, **34**, 7020-7026.

48. Becker, E. (1991) *J. Phys. Chem.*, **95**, 2818-2823.

49. Parsons M.R., Convery M.A., Wilmot C.M., Yadav K.D.S., Blakely V., Corner A.S., Phillips S.E.V., McPherson M.J. and Knowles P.F. (1995) *Structure* , **3**, 1171-1184.

50. Janes, S.M. and Klinman, J.P. (1995) in *Methods in Enzymology vol. 258*, Klinman, J.P. (Ed.) pp. 20-34 Academic Press, New York, NY.

Chapter Five
General Conclusions

5.1 Literature Relevance and Research Objectives

The amine oxidases comprise a large and ubiquitous family of oxidoreductases. Two large (multienzyme) classes are the flavin-dependent monoamine oxidases [EC 1.4.3.4] and the topaquinone-containing copper amine oxidases [EC 1.4.3.6]. Lysyl oxidase is the only member of its class [EC 1.4.3.13] and is somewhat similar to the copper amine oxidases. The monoamine oxidases have been the focus of intense pharmacological research because inhibitors of these enzymes are therapeutically efficacious in Parkinson's disease and depression. Copper amine oxidases have received less attention pharmacologically, but perhaps more attention from a physical-chemical and enzymological viewpoint. This is illustrated by a Chemical Abstract Service (CAS) computer database search on February 8, 1996, covering the period 1967-1996, that revealed 1102 research publications concerning amine oxidases, with 741 articles that did not relate to monoamine oxidases. This database search does not reflect the publications associated with the pharmacological literature.

The bacterial copper amine oxidases have a well-defined role, providing carbon and/or nitrogen for growth of the organism. Eukaryotic copper amine oxidases have poorly defined roles. This is, in part, due to the broad substrate specificity of these enzymes and to the fact that amine oxidases isolated from different species, but identical tissue sources, display different substrate selectivities. Additionally, several enzymes, such as the semicarbazide-sensitive amine oxidases, are neither definitively characterized as copper-containing nor topaquinone-containing. Both copper and topaquinone are important cofactors

required during enzymatic catalysis by the copper amine oxidases. The lack of information concerning several of the amine oxidase enzymes may reflect the difficulty in obtaining sufficient amounts of pure protein for physical-chemical characterization. The homodimeric glycoprotein nature of the eukaryotic copper amine oxidases seems universal, but only one X-ray crystal structure and very few amino acid sequences have been reported. Thus, it has been difficult to establish definitive relationships among the different amine oxidases.

In contrast, the stereochemical classification of copper amine oxidase reactions can provide specific information relative to active site mechanistic interactions and configuration. Thus, one of the major goals of this thesis research was to establish further the stereochemical relationships of the copper amine oxidases. Copper amine oxidases isolated from similar tissue sources (e.g., bovine, porcine, equine, ovine and leporine plasma) have been shown previously to belong to different stereochemical classes (i.e., *pro*-R and net nonstereospecific for hydrogen abstraction from C1 of alkyl amines). Furthermore, the stereochemical specificity of the amine oxidases is correlated with hydrogen exchange reactions at C2 of the corresponding product aryl and alkyl aldehydes. It is envisaged that these stereochemical classifications reflect genuine differences in the enzymes' active site configurations and that this may, in the future, be shown to be correlated with specific amino acid sequences (i.e., gene products).

Some copper amine oxidase enzymes have previously been shown to remove only the *pro*-S hydrogen of benzylamine, irrespective of their arlyalkylamine stereochemical specificity. Thus, another significant objective of this research was to evaluate the stereochemical specificity of several copper amine oxidases for hydrogen abstraction from benzylamine. In contrast to the observed aryl and alkyl amine stereochemical heterogeneity, the extensive nature of *pro*-S

specific hydrogen abstraction from benzylamine for several eukaryotic and bacterial copper amine oxidases was established in this thesis work.

As previously stated, the essential redox cofactor in several amine oxidases has not been definitively characterized as topaquinone. The tissue-bound semicarbazide-sensitive amine oxidases were considered to contain a redox cofactor similar to, but distinct from, topaquinone, based on stereochemical data and visible absorbance spectroscopy of derivatized enzymes. Therefore, the primary objective of this thesis was to determine unequivocally the molecular structure of the redox cofactor in these enzymes and to obtain active site amino acid sequence information in proximity to the cofactor. Somewhat surprisingly, the redox cofactor of porcine and bovine aorta semicarbazide-sensitive amine oxidases was shown to be topaquinone. This is the first report defining the molecular structure of a redox cofactor for a non-flavin, membrane-bound amine oxidase.

5.2 Research Results

Chapters two, three and four of this thesis relate to the investigation of a specific research objective. The specific research findings are outlined below in a point-form chapter summary format.

Chapter 2

- Chirally deuterated R- and S-[*methylene*-^{2}H]benzylamine were synthesized by a combined chemical-enzymatic procedure and the enantiomeric purities of these amine oxidase substrates were evaluated by high-field ^{1}H NMR of the (1S)-(-)-Camphanamide diastereomers.

- Bovine, leporine and ovine plasma amine oxidases (nonstereospecific for C1 of alkyl amine), porcine and equine plasma amine oxidases (*pro*-R for C1 of alkyl amine), and pea seedling amine oxidase (*pro*-S for C1 of alkyl amine) were shown to be strictly *pro*-S specific for hydrogen abstraction from benzylamine.

Chapter 3

- Product benzyl alcohols, derived from the alcohol dehydrogenase coupled incubations of deuterobenzylamine with amine oxidases, were examined for deuterium content by the triply redundant ^{1}H NMR analysis protocol described in Chapter 2. The salient feature of this protocol was the unequivocal determination of the fate of deuterium derived from chirally deuterated benzylamine by analysis of micromolar quantities of the product benzyl alcohols in an impure reaction mixture extract.

- *Arthrobacter globiformis* histamine oxidase and phenethylamine oxidase, *Escherichia coli* amine oxidase and *Klebsiella oxytoca* amine oxidase were shown to be *pro*-S specific for hydrogen abstraction from benzylamine and tyramine. Furthermore, no hydrogen exchange was observed at C2 of the product *p*-hydroxyphenylacetaldehydes for any of the bacterial copper amine oxidases.

Chapter 4

- Bovine and porcine aorta semicarbazide-sensitive amine oxidases were derivatized with *p*-nitrophenylhydrazine and characterized by visible absorbance and resonance Raman spectroscopy.

- *p*-Nitrophenylhydrazine adducts of cofactor-containing peptides were released by proteolysis, purified by sequential reverse-phase HPLC and analyzed by visible absorbance spectroscopy and mass spectrometry.

- The tissue-bound aorta enzymes were shown to contain topaquinone as the essential redox cofactor, based on the above analyses. These results demonstrate that the semicarbazide-sensitive amine oxidases can be classified with the copper amine oxidases (EC 1.4.3.6). It is anticipated that the Enzyme Commission may proceed with re-classification of these enzymes at its' next meeting.

Thus, the research outlined in this thesis extends the scientific knowledge concerning the molecular mechanisms of these fascinating and extraordinary proteinaceous catalysts, collectively designated as the Copper Amine Oxidases.

5.3 Future Research

Much remains to be studied concerning the copper amine oxidases and their physiological roles within the organisms in which they are found. As more amino acid, or cDNA, sequences become available it may be possible to determine the degree of evolutionary relatedness among the various amine oxidases. Indeed, since

most organisms contain copper amine oxidases then systematic comparisons of gene nucleotide homology might be useful for standardization of the "evolutionary clock".

Site-directed mutagenesis, enzymology and X-ray crystallography should elucidate the detailed molecular transformations that occur at the active site during catalysis. The oxidative half-reaction, which is only poorly understood, requires particular attention, as does the putative role of copper in mediating electron transfer. The interesting inter-subunit connection between the active sites in the functional homodimer and the large number of secondary structural domains not associated with the active site suggest that additional functions or non-substrate molecular interactions (e.g., regulators?) remain to be discovered. This might be investigated by heterologous expression of truncated or point mutants to address structure-function relationships.

Selective inhibitors for each type of amine oxidase (soluble or tissue-bound) may provide insight into the physiological function of these enzymes in xenobiotic amine toxicology or maintenance of normal physiology. Additionally, the high degree of glycosylation of the eukaryotic amine oxidases may be important for the physiological function or targeting of the enzymes. Enzymatic or chemical deglycosylation/modification may be useful for probing such functions. From a mechanistic enzymology viewpoint, the molecular orbital and conformational transitions that occur during the catalytic cycle can be investigated with quantum chemical computational methods.

Although many interesting areas of fundamental and applied amine oxidase research remain, the continuous reduction in research budgets is a significant hurdle. Increasingly, only projects with direct and rapid results significant to human welfare are funded. Despite this, many accomplished scientists continue to provide interesting and valuable information concerning the amine oxidases.

Appendix I

Visible absorbance spectrum of *p*-nitrophenylhydrazine derivatized rabbit plasma amine oxidase at pH 7.0 (—) and in 2.8 M KOH (---).

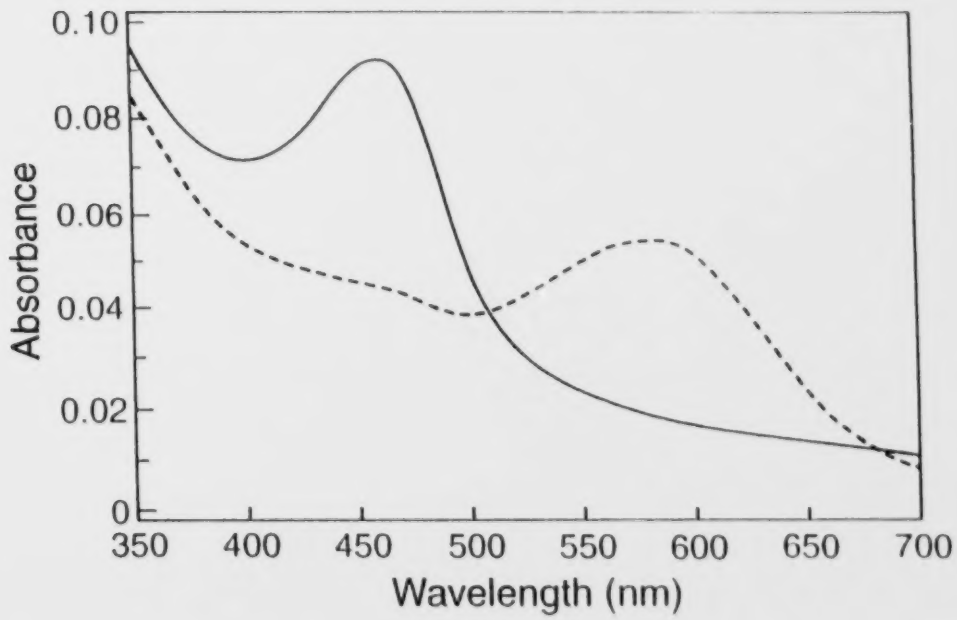

Appendix II

Partial 500 MHz ^{1}H NMR spectra of benzyl alcohols, benzylic proton region, derived from coupled incubations of plasma amine oxidases and S-[*methylene*-^{2}H]benzylamine (left panels) and R-[*methylene*-^{2}H]benzylamine (right panels).

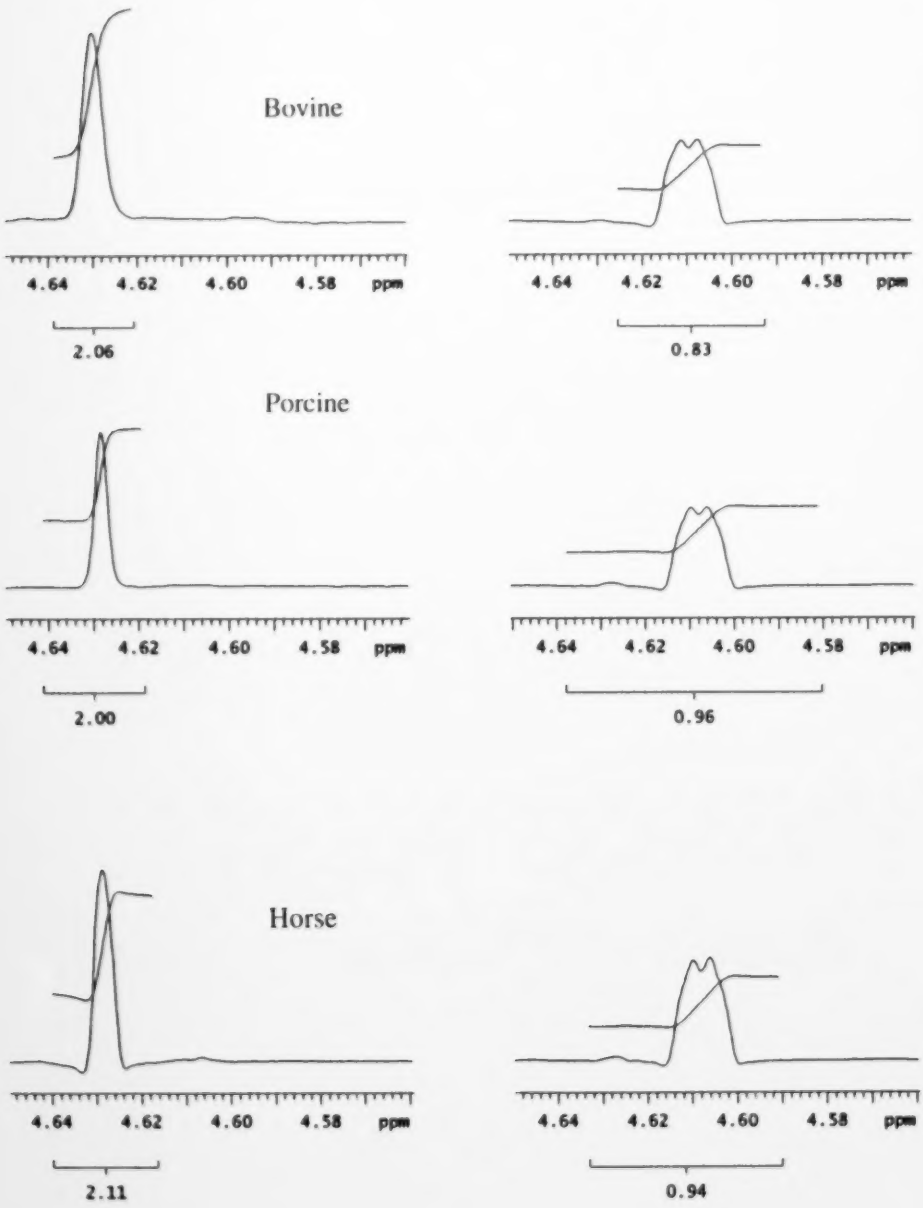

Appendix III

Partial 500 MHz ^{1}H NMR spectra of benzyl alcohols derived from coupled incubations of bacterial amine oxidases and R-[*methylene*-^{2}H]benzylamine.

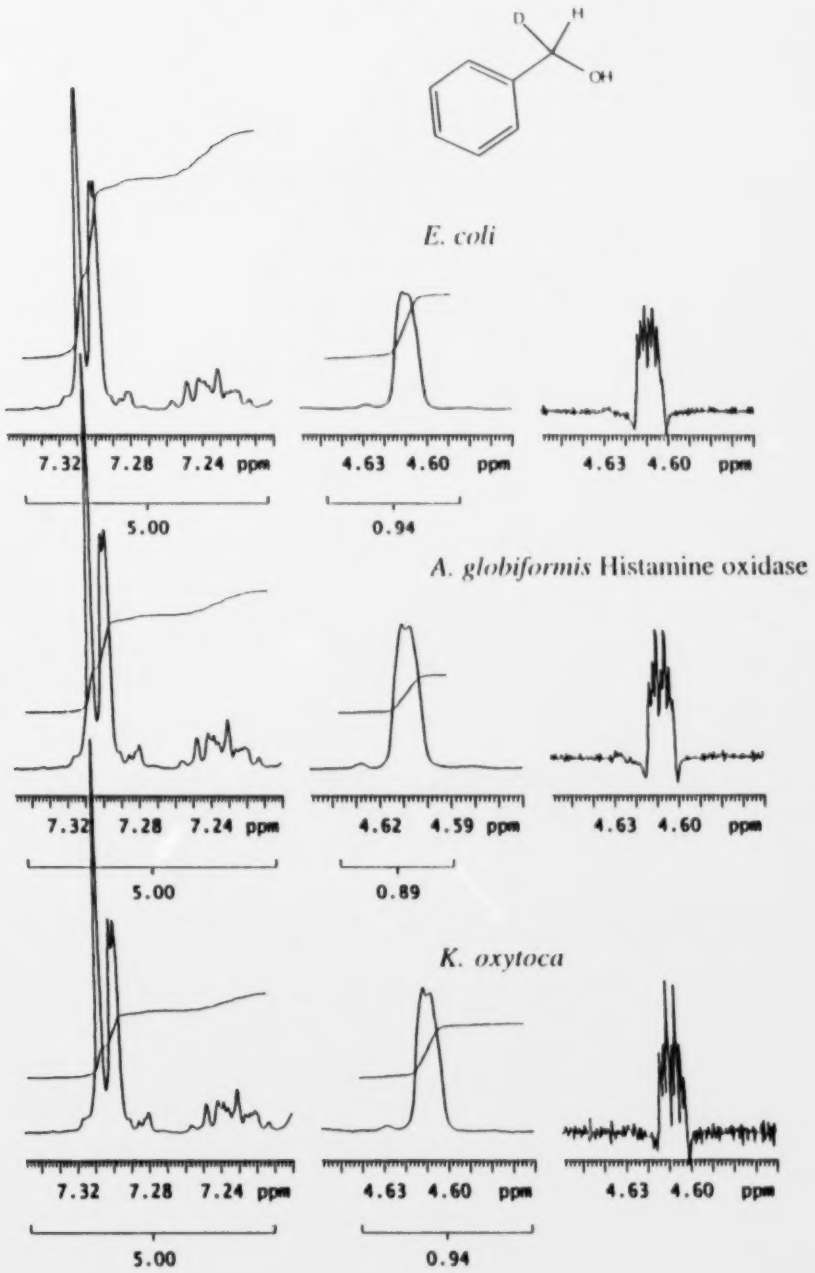

Appendix IV

Partial 500 MHz ^{1}H NMR spectra of benzyl alcohols derived from coupled incubations of bacterial amine oxidases and S-[*methylene*-^{2}H]benzylamine.

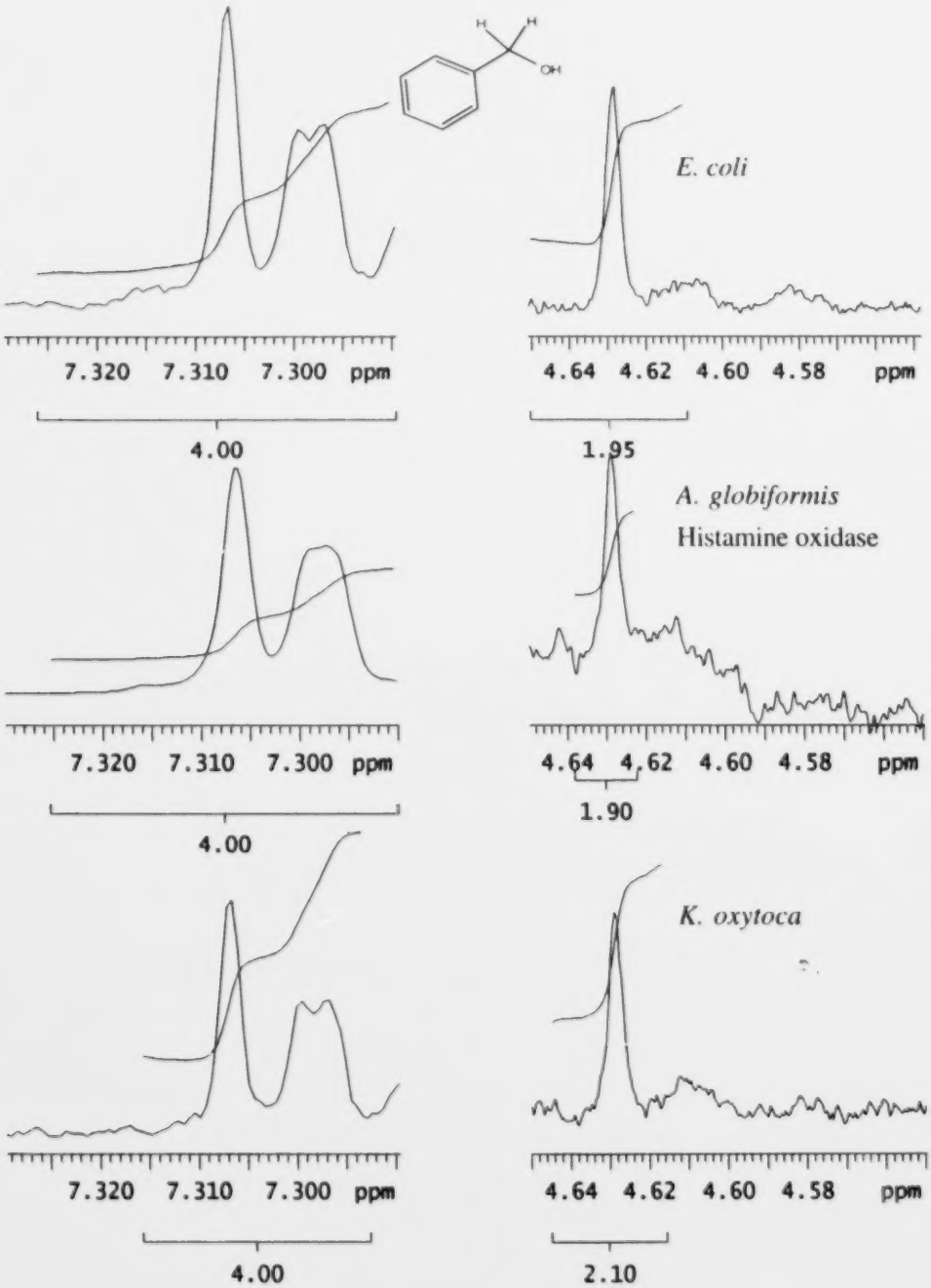

Appendix V

Partial 500 MHz ^{1}H NMR spectra of *p*-hydroxyphenethyl alcohols derived from coupled incubations of bacterial amine oxidases and [1(S)-^{2}H]tyramine and [1(R)-^{2}H]tyramine.

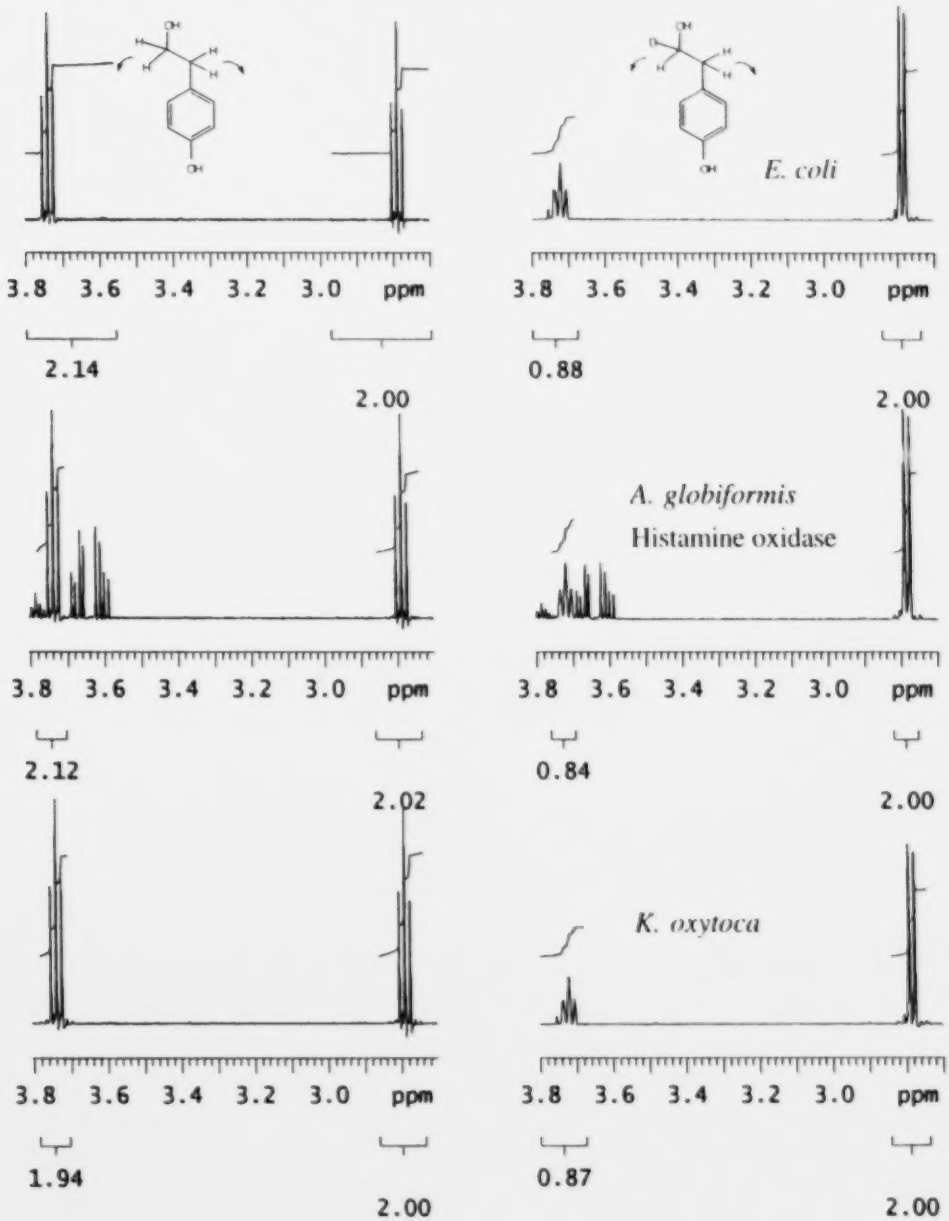

Appendix VI
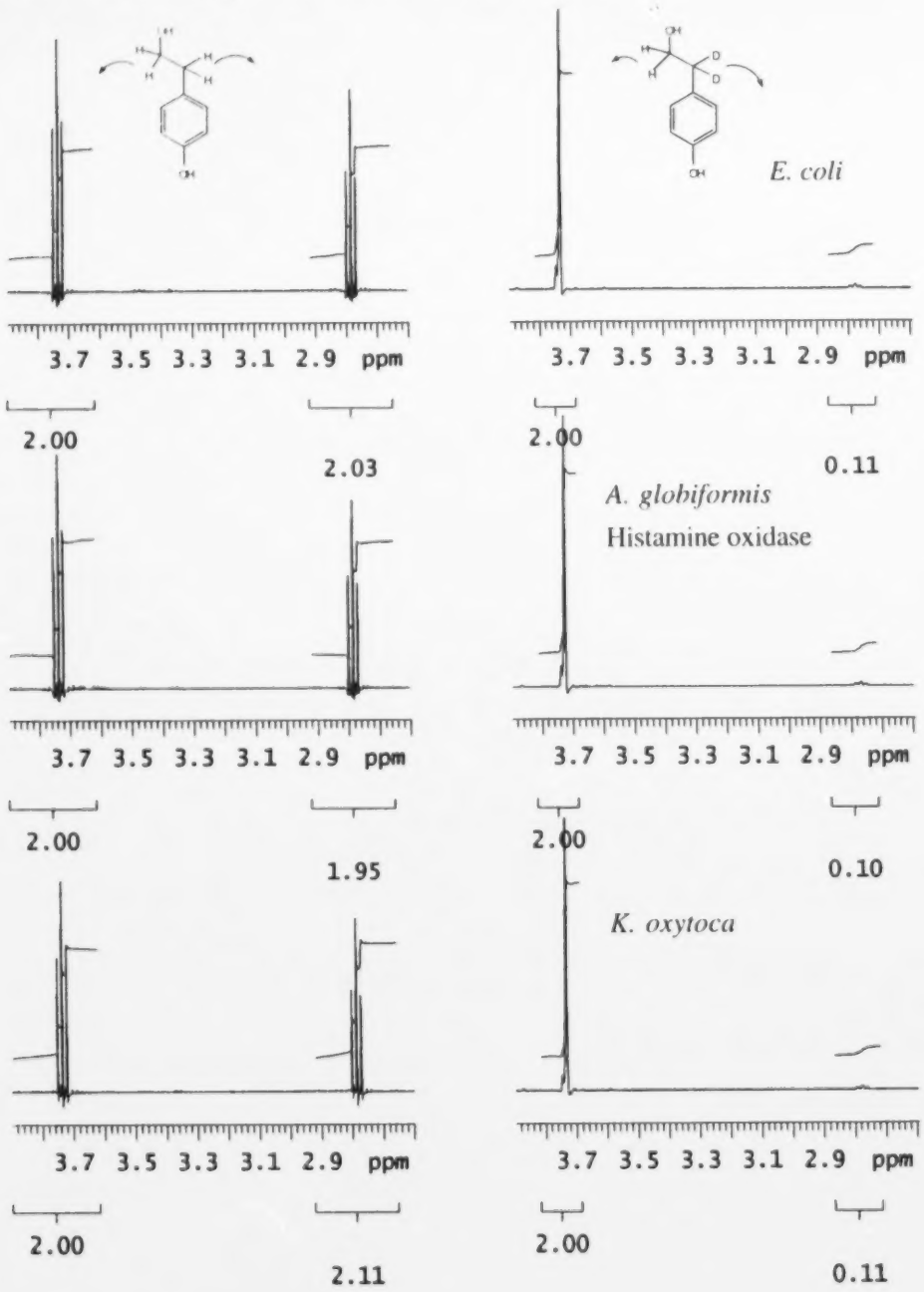
Partial 500 MHz ^{1}H NMR spectra of *p*-hydroxyphenethyl alcohols derived from coupled incubations of bacterial amine oxidases with tyramine in deuterated buffer (left) and [2,2-^{2}H]tyramine in protiated buffer (right).